PNC TN9410 91-196

Investigation on Applicability of Turbulence Models to Low Reynolds Number Flows

July, 1991

OARAI ENGINEERING CENTER

POWER REACTOR AND NUCLEAR FUEL DEVELOPMENT CORPORATION

動力炉・核燃料開発事業団（Power Reactor and Nuclear Fuel Development Corporation）

PNC TN9410 91-196
July, 1991

Investigation on Applicability of Turbulence Models to Low Reynolds Number Flows*

Jae Ho Kim** and Toshiharu Muramatsu***

Abstract

There are many arguments on the empirical constants of the turbulence models because their original values are selected on the basis of the dimensional analysis. Especially, the particular model form of the generation - destruction terms in the transport equation for the turbulent kinetic energy dissipation rate ε has been treated as a source of the arguments. Having recognized the cause for sensitivities of calculations on the relevant constants, this study could be performed to evaluate the applicability of the turbulence models adopted in AQUA to relatively slow flows through analyses of a typical thermal cavity problem and the 7th IAHR benchmark problem featuring many aspects of the phenomena predicted during the natural circulation decay heat removals in the FBR reactor vessel.

Despite the level of handled turbulence models, such as the standard k & ε two-equation model and the algebraic stress / flux model, the calculation results are fairly sensitive to the variations of the pertinent model constants representing an approximate vorticity budget of turbulence. However, given some controlled experimental results of the 7th IAHR benchmark problem, these characteristics were tested numerically to match the calculation results with the experiments.

---

* STA Researcher Exchange Program on the Nuclear Power Industry,

** Mechanical Engineering Department-Nuclear, Korea Power Engineering Company, 87 Samsung Dong, Kangnam Gu, SEOUL, KOREA, (Telex) KOPEN K22562, (FAX) 82-2-540-4184, (Phone) 540-7701

*** Reactor Engineering Section, Safety Engineering Division, OEC, PNC

RESEARCH SUBJECT: Heat Transfer and Fluid Dynamics

"Numerical analysis of three dimensional heat transfer behavior and experimental analysis using analytical codes"

RESEARCH PERIOD: JAN 15 to JUL 13, 1991

ASSIGNED SECTION:

Reactor Engineering Section,
Safety Engineering Division,
Oarai Engineering Center,
Power Reactor and Nuclear Fuel Development Corporation

TITLE, DIVISION, AND ORGANIZATION:

Engineer, Mechanical Engineering Department - Nuclear,
Korea Power Engineering Company, Inc.

FIRST AND FAMILY NAME: Jae Ho Kim

SIGNATURE:

CONTENTS

TABLES

FIGURES

1. FOREWORD

The researcher exchange program covering the nuclear power technology has held between Japan and Asian countries, which is sponspored by the Science and Technology Agency (STA) of Japanese government. As a participant of that program, I have taken a research subject in the Power Reactor and Nuclear Fuel Development Corporation (PNC) from January 15 to July 13, 1991.

During the past six months, a subject relating to the heat transfer and fluid dynamics was handled in the Reactor Engineering Section of Safety Engineering Division included in the Oarai Engineering Center (OEC). The details of work are related to the use of a multi-dimensional single phase thermohydraulic computer code called AQUA (Advanced simulation using Quadratic Upstream difference Algorithm). The AQUA has already been developed and used successfully by the PNC to simulate various thermohydraulic phenomena especially occurring in the Liquid Metal Fast Breeder Reactor (LMFBR) internals. In connection with the designated STA research theme 6.1, "Numerical analysis of three-dimensional heat transfer behavior and experimental analysis using analytical codes", I could take a chance to cope some practical approaches on turbulence flows as well as basic numerical issues on the field of heat transfer and fluid dynamics.

With regard to the proper usages and developments of the AQUA, I could find out that it was the time to improve the accuracy of calculations and to refine the turbulence models. After obtaining some technical backgrounds incorporated in AQUA, this study could be performed to treat a specific item on turbulence models which are required to close the governing mean flow equations. This report will describe the results of this specific technical activities.

In addition to the specific technical works, I think that it was also important to know some basic information for the future nuclear power plants in Japan. It was great experiences for me to look over a systematic approach having been conducted by the PNC through JOYO, MONJU, and the scheduled demonstratonal FBR power plants.

While staying in Japan and taking the research work, I received many kinds of support from everyone. In particular, I wish to thank my adviser Mr. T. Muramatsu, group leader Mr. A. Yamaguchi, and section manager Mr. S. Sugawara for their guidance and help of the research

work. My thanks are also due to Mr. H. Miyakoshi, and Mr. M. Murata, who have worked together in the same room. Also I would like to thank Mr. Y. Mimoto, the manager of the PNC international house located in Oarai.

2. ABSTRACT

There are many arguments on the empirical constants of the turbulence models because their original values are selected on the basis of the dimensional analysis. Especially, the particular model form of the generation - destruction terms in the transport equation for the turbulent kinetic energy dissipation rate ε has been treated as a source of the arguments. Having recognized the cause for sensitivities of calculations on the relevant constants, this study could be performed to evaluate the applicability of the turbulence models adopted in AQUA to relatively slow flows through analyses of a typical thermal cavity problem and the 7th IAHR benchmark problem featuring many aspects of the phenomena predicted during the natural circulation decay heat removals in the FBR reactor vessel.

Despite the level of handled turbulence models, such as the standard k & ε two-equation model and the algebraic stress/flux model, the calculation results are fairly sensitive to the variations of the pertinent model constants representing an approximate vorticity budget of turbulence. However, given some controlled experimental results of the 7th IAHR benchmark problem, these characteristics were tested numerically to match the calculation results with the experiments.

3. RESEARCH SCHEDULE

A. Master of AQUA numerics by "Numerical heat transfer and fluid flow" and computer handling. (JAN 21 to FEB 28)

B. Master of AQUA input scheme by some sample problems. (FEB 4 to FEB 22)

C. Calculation of the thermal cavity problem with laminar and turbulence model. (FEB 25 to MAR 15)

D. Comparison with the reference solutions indicated in "Application of a k & ε turbulence model to an enclosed buoyancy driven recirculation flow". (MAR 18 to MAR 29)

E. Investigation of the 7th IAHR benchmark problem. (APR 1 to APR 12)

F. Calculation of the IAHR benchmark problem with turbulence models. (APR 15 to MAY 31)

G. Tour to MONJU and FUGEN sites. (JUN 24 to JUN 26)

H. Arrangement of calculated results and documentation of activity. (JUN 3 to JUL 12)

4. DETAILS

4.1 Introduction

A computer code AQUA has been developed and used successfully in order to simulate multi-dimensional single phase thermohydraulic phenomena in arbitrary geometries. With regard to the development of the AQUA it is the time to refine the turbulence models adopted in the code (See Table 1). There are two turbulence models in the AQUA having some different levels of complexity. One is the standard k & ε two-equation model proposed first by Launder and Spalding and the other is the algebraic stress/flux model suggested by W. Rodi. Actually both models are included in the so-called the k & ε two-equation turbulence models. However in order to tell the difference between the two, a k & ε two-equation model having the algebraic stress and flux relations will simply be called as the algebraic stress/flux model in this report and the other will be called as the k & ε two-equation model.

The present study was undertaken to apply these turbulence models to relatively slow flows through analyses of a typical thermal cavity problem and the 7th IAHR benchmark problem. In the case of a thermal cavity problem, a numerical study is performed of the turbulent two-dimensional air flow featuring an enclosed buoyancy driven recirculating flow. This problem is extensively based on the work of Marie-Pierre Fraikin, Jean J. Portier, and Christian J. Fraikin which shows a numerical application of the k & ε two-equation model to the transition region.

Recent interests in LMFBR thermohydraulic design and safety evaluations have required a need for highly accurate computations of relatively slow flows in complicated geometries. The 7th IAHR benchmark problem detailed in section 4.4 was prepared to approach the above subject with extensive experiments. Given some control results of the experiments, this study is to apply turbulence models already adopted in AQUA to the benchmark problem featuring many aspects of the phenomena predicted during the natural circulation decay heat removals in the FBR reactor vessel. In this problem, it is important to see the thermal stratification and plenum-core thermohydraulic interactions in which the flow and temperature fieleds are governed by buoyance driven flow.

Also, a sensitivity study could be handled to check the effect of the model constants on the results of calculations. Among the empirical model constants on the two turbulence models in AQUA, there are three common constants, C_1, C_2, and C_3, in the transport equation for turbulent kinetic energy dissipation rate. In connection with the modeling process, C_1 and C_3 are multiplied to the generation of vorticity due to self-stretching action of turbulence and buoyance, while C_2 is multiplied to the viscous destruction. It should be mentioned here that the calculations are fairly sensitive to the variation of these model constants.

Table 1 Development of AQUA

YEAR	SUBJECTS
1983	COMMIX-1A from ANL
1984	Implementation of the k & ε two-equation model
1985	Modification for Poisson Solvers, Implementation of DRACS model
1986	Higher order difference schemes implementation, Mass transport model addition
1987	Development of Adaptive control system
1988	Development of the algebraic stress/flux model
1989	Development of the algebraic stress/flux model
1990	Refinement of the turbulence models
1991	Refinement of the turbulence models

4.2 Analytical Models

Most flows occurring in nature and in engineering application are turbulent. However, it is not feasible to prepare a description of the turbulent flow at all points in time and space. It is the time-mean behavior of these flows that is usually of practical interest. Therefore, the equations for unsteady laminar flow are converted into the time-averaged equations for turbulent flow by an averaging operation in which it is assumed that there are rapid fluctuations about the mean value. The additional terms arising from this operation are the so-called Reynolds (or turbulent) stresses, turbulent heat flux, and etc.

So in connection with the time-averaged equations for turbulent flow, it should be said that the task of a turbulence model is to express these fluxes in terms of the mean properties of the flow.

After the proper modeling, the result is that numerically the time-averaged equations for turbulent flow have the same appearance as the equations for laminar flow, but the laminar exchange coefficients such as viscosity and diffusivity are replaced by effective exchange coefficients.

4.2.1 The k & ε two-equation model

The k & ε two-equation model employs the transport equations for turbulent kinetic energy k and its dissipation rate ε in order to calculate the velocity and length scales of turbulence. This turbulence model was established using the concept of the isotropic turbulent viscosity and diffusivity to express the turbulent stresses and fluxes. Rigorously the concept of isotropy is of limited realism in complex flows and in particular in turbulence exposed to directional influences like gravity. However it is the most popular model in turbulence and its predicative capabilities for non-buoyant shear layer flows and also for confined recirculating flows are well established.

The transport equations for turbulent kinetic energy and its dissipation rate used in AQUA are written as follows:

$$\frac{\partial}{\partial t}(\rho k) + \frac{\partial}{\partial x_i}(\rho U_i k) = \frac{\partial}{\partial x_i}\left(\frac{\mu_{eff}}{\sigma_k}\frac{\partial k}{\partial x_i}\right) + P + G - \rho\varepsilon$$

$$\frac{\partial}{\partial t}(\rho \varepsilon) + \frac{\partial}{\partial x_i}(\rho U_i \varepsilon) = \frac{\partial}{\partial x_i}\left(\frac{\mu_{eff}}{\sigma_\varepsilon}\frac{\partial \varepsilon}{\partial x_i}\right)$$

$$+ C_1\frac{\varepsilon}{k}(P + G)\left(1 - C_3\frac{G}{P+G}\right) - C_2\frac{\varepsilon^2}{k}$$

with

$$P = \mu_t\frac{\partial U_i}{\partial x_j}\left(\frac{\partial U_j}{\partial x_i} + \frac{\partial U_i}{\partial x_j}\right), \quad G = g_i\beta\frac{\mu_t}{Pr_t}\frac{\partial T}{\partial x_i}$$

$$\mu_{eff} = \mu_l + \mu_t$$

$$\mu_t = \rho\, C_\mu\, k^2/\varepsilon$$

In the above modeling, the constants are as follows:

σ_k	σ_ε	C_1	C_2	C_3	C_μ	Pr_t
1.0	1.3	1.44	1.92	0.70	0.09	0.9

4.2.2 The algebraic stress/flux model

To relieve some difficulties arising from the assumption of isotropic turbulent viscosity and diffusivity on the k & ε two-equation model, the algebraic stress/flux model has been adopted and used in AQUA.

Among the turbulence models, the original stress/flux models can be used as guidance to remove some of the restrictions imposed on the simpler models. The derivation of exact transport equations for the individual turbulent stresses and fluxes is the first step to make a turbulence model having non-isotropic turbulent viscosity and diffusivity relations. After some modeling processes, these equations can be rearranged to the form of the original stress/flux model. However it is not feasible to treat this original model on the computer because it would contain at least 10 partial differential equations in three dimensional situation. The algebraic stress/flux model adopted in AQUA is based on an approximation proposed by Rodi converting these partial differential equations into algebraic expressions. Theoretically, this model is superior than the k & ε two-equation model because it can account for the directional effects due to body forces and walls. Also this model can provide some information about the temperature fluctuations, which are indicated as a major shortcoming of the k & ε two equation model.

The following equations make up a part of the closed form of this model in AQUA.

$$\frac{\partial}{\partial t}(\rho k) + \frac{\partial}{\partial x_i}(\rho U_i k) = P + G - \rho\varepsilon$$

$$+ \frac{\partial}{\partial x_m}[C_s \frac{k}{\varepsilon}(\overline{u_i'u_n'}\frac{\partial}{\partial x_n}\overline{u_i'u_n'} + \overline{u_m'u_n'}\frac{\partial k}{\partial x_n})]$$

$$\frac{\partial}{\partial t}(\rho\varepsilon) + \frac{\partial}{\partial x_i}(\rho U_i \varepsilon) = C_1 \frac{\varepsilon}{k}(P+G)(1-C_3 \frac{G}{P+G}) - C_2\rho \frac{\varepsilon^2}{k}$$

$$+ \frac{\partial}{\partial x_m}(C_D \frac{k}{\varepsilon}\overline{u_m'u_n'}\frac{\partial \varepsilon}{\partial x_n})$$

$$\frac{\partial}{\partial t}(\rho\overline{\theta'^2}) + \frac{\partial}{\partial x_i}(\rho U_i\overline{\theta'^2}) = -2\,\rho\,\overline{u'_1\theta'}\frac{\partial T}{\partial x_1} - 2C_{z1}\,\frac{k}{\varepsilon}\,\rho\overline{\theta'^2}$$

$$+ \frac{\partial}{\partial x_i}(C_z\,\rho\,\frac{k^2}{\varepsilon}\,\frac{\partial\overline{\theta'^2}}{\partial x_j})$$

In contrast to the k & ε two-equation model, the P and G of the above equations can be obtained by the following prescriptions.

$$P = -\,\rho\,\overline{u_i'u_1'}\frac{\partial U_i}{\partial x_1} \qquad G = -\,\beta\,g_i\,\rho\,\overline{u_i'\theta'}$$

C_s	C_1	C_2	C_3	C_D	C_{z1}	C_z
0.11	1.44	1.90	0.70	0.15	0.62	0.13

Also to account for the different production or destruction process acting on the stress and flux components, and to a certain extent for the transport of these components, the algebraic relations shown on below have been adopted in AQUA.

For the turbulent stresses,

$$-\overline{u_i'u_j'} = \frac{k}{C_{R1}\varepsilon}\,\frac{(C_{R2}-1)P_{ij}+(C_{R3}-1)P_{ij,b}-2\delta_{ij}[C_{R2}P+C_{R3}G+(C_{R1}-1)\varepsilon]\,/3}{1 + [(P+G)/\varepsilon-1]\,/\,C_{R1}}$$

with

$$P_{ij} = -\,(\overline{u_i'u_j'}\frac{\partial U_j}{\partial X1} + \overline{u_j'u_i'}\frac{\partial U_j}{\partial X1})$$

$$P_{ij,b} = -\,\beta\,(g_i\,\overline{u_j'\theta'} + g_i\,\overline{u_i'\theta'})$$

δ_{ij}: Kronecker delta

$C_{R1} = 2.3, \quad C_{R2} = 0.5, \quad C_{R3} = 0.4$

and for turbulent heat flux

$$-\overline{u_i'\theta'} = \frac{k}{C_{T1}\varepsilon}\,\frac{-P_{i,T} - (1+C_{T3})\beta g_i\overline{\theta'^2} - C_{T2}\,\overline{u_m'\theta'}\,(\partial U_i/\partial X_m)}{1 + [(P+G)/\varepsilon-1]\,/\,C_{T1}}$$

with

$$P_{i,T} = -\,(\overline{u_i'u_j'}\frac{\partial T}{\partial X1} + \overline{u_j'\theta'}\frac{\partial U_i}{\partial X1})$$

$C_{T1} = 3.20, \quad C_{T2} = 0.50, \quad C_{T3} = 0.50$

4.2.3 Model constants

There are many considerations for the model constants of turbulence models. To show the cause for the various consideratons, it is appropriate to introduce a kind of arguments existing on a model constants of the k & ε two-equation model. A constant, $C_\mu = 0.09$, was chosen on the basis of experiments in flows in which the production P and dissipation ε of the turbulence energy were in approximate balance. Following the energy budgets of the transport equation for the turbulent kinetic energy k in a steady, homogeneous, pure shear flow, this balance could be achieved. However it should be noted that in most shear flows production and dissipation do not balance, though they are nearly always of the same order of magnitude. So, for thin shear layers, there is a suggestion to use a functional relations modifying the values of C_μ depending the ratio of the production and the dissipation.

Anyway, the value of C_μ, σ_k and σ_ε in the k & ε two-equation model can be considered as relevant values because it is possible to find out many works using that value with a reasonable degree of success. The most important ones are the three constants C_1, C_2, and C_3 on the dissipation rate equation appearing in both of the k & ε two-equation model and the algebraic stress/flux model. Even though there are also another model constants on the algebraic stress/flux model, this study will not cope with those constants.

Following the closed forms of the k & ε two-equation model and the algebraic stress/flux model in AQUA, the constant C_3 showing the effect of buoyance have already been adjusted by introducing a part of Rodi's suggestion with some prescription.

However, it is better to look over some arguments on the effect of buoyancy. In connection with an exact transport equation for the dissipation rate ε, the terms expressing the generation of vorticity due to the self-stretching action of turbulence and the viscous destruction can be written as below for non-buoyant flows.

(Generation due to vortex stretching)
- (Viscous destruction)

$$= (C_1 \frac{P}{\varepsilon} - C_2)\frac{\varepsilon^2}{k} \qquad (1)$$

In buoyant flows, a buoyancy contribution has to be added, and it is possible to rewrite the above expression as follows:

(Generation due to vortex stretching)
+ (Buoyancy contribution)
- (Viscous destruction)

$$= (C_1 \frac{P}{\varepsilon} + C_3'' \frac{G}{\varepsilon} - C_2)\frac{\varepsilon^2}{k} \qquad (2)$$

Following the work of M.P. Fraikin, J.J. Portier, and C.J. Frikin, C_3'' on (2) should have a different value at each point, close to 1.44 near the vertical and to 0.4 near the horizontal boundary layers. So its value was chosen as a mean value between the above two extremes in the reference work of the thermal cavity problem detailed in section 4.3.

There is also an another form of consideration. Rodi suggests to replace P/ε in (1) by

$$\frac{P+G}{\varepsilon}(1 + C_3 R_f)$$

where R_f is the flux Richardson number.

Usually R_f is defined as minus the ratio of buoyancy production of turbulent kinetic energy to stress production, $-G/P$. With this definition of Richardson number, C_3 should be close to zero for vertical buoyant shear layers and close to unity for horizontal layers. $C_3 = 0$ and $C_3'' = 1.44$ imply that the buoyancy term is multiplied with the same constants as the stress production while $C_3 = 1$ and $C_3'' = 0.4$ imply that there is no buoyancy term in the dissipation equation. This controversy has to do with the definition of the flux Richardson number to which C_3 is a multiplier.

To resolve this controversy, Rodi also suggests to replace in the R_f definition the buoyancy production G of the total turbulent kinetic energy by the buoyancy production G_v^2 of only the lateral energy component v^2 and to write $R_f = - G_v^2/2(P+G)$. In horizontal shear layer, where v is in the direction of gravity, all buoyancy production goes into the component v^2 so that $G_v^2 = 2G$ and $R_f = -G/(P+G)$; the source term in the dissipation equation reads in this case $C1\varepsilon[P + (1-C_3)G]/k$. In vertical layers the lateral component is perpendicular to the gravity vector and receives no buoyancy contribution so that $G_{v2}^2 = 0$

and also $R_f = 0$; in this case the source term in the dissipation equation is $C1\varepsilon[P+G]/k$, which means that the buoyancy production is multiplied with the same constant as the shear production P.

With respect to the above arguments, it may be easy to find out that a part of Rodi's suggestion has been incorporated in AQUA. Actually AQUA has been established using the modified definition of the flux Richardson number within the horizontal shear layers.

In addition to the above, the key considerations of this study is also on the balance of the vorticity budgets to be expressed by the model constants of C_1 and C_2. The previous sensitivity study for these model constants indicates that these values are also important on the turbulent quantities.

4.2.4 Numerical solution schemes

In AQUA, there are two algorithms called SIMPLEST-ANL and MICE (Modified Implicit Continuous Fluid Eulerian) respectively.

The MICE is based on the ICE technique developed at Los Alamos National Laboratory. The solution sequence incorporated in the MICE is semi-implicit because the old values of all variables, except pressure in the momentum equation and mass fluxes in the continuity and energy equations, are assumed to prevail throughout the time step period, except at time $t + \Delta t$. Only under this algorithm, AQUA uses two higher order difference schemes, the QUICK (Quadratic Upstream Interpolation for Convective Kinematics) and the QUICK-FRAM (Filtering Remedy and Methodology), to obtain accurate solutions of buoyancy dominated flow. Therefore this MICE algorithm could be taken to achieve accurate solutions. However, this algorithm has time step size limitations because of the semi-implicit nature of the formulation.

On the other hand, the SIMPLEST-ANL in AQUA, was suggested by the Argonne National Laboratory on the basis of a modification to the SIMPLE/SIMPLER procedure developed at Imperial College in England. It is a fully-implicit algorithm using the first order upwind scheme, so it relieves many of the time-step size limitations, permitting use of larger time-step sizes. I think that it is better to say again that the SIMPLEST-ANL is a fully-implicit algorithm even though the original name of SIMPLE stands for Semi-Implicit Method for Pressure-Linked Equations.

The MICE and the SIMPLEST-ANL algorithms both have advantages and

limitations and it is possible to use of either one of these two algorithms. Further, the option has been used usually in such a manner that a user can switch from one algorithm to another at any time during simulations. Generally it is beneficial to use the SIMPLEST-ANL at the first stage of analysis, and at the next stages it may be preferable to use the MICE with higher order difference schemes for the accurate solutions.

4.3 Thermal Cavity Problem

A typical thermal cavity problem could be taken to familiarize me with AQUA. Also this problem has its own interests and could be treated as a vehicle of the whole study. The reference solutions of this problem have been obtained from the work of Marie-Pierre Fraikin, Jean J. Portier, and Christian J. Fraikin. Covering the Grashof number range of 10^7 to 10^8, this work implies that, even though the k & ε two-equation model cannot be expected to predict perfectly the transition region considered, the calculation results seem physically very good for an enclosed buoyancy driven recirculating air flow. In order to handle that implication, this study would use the same definition of the reference work.

4.3.1 Description of the problem

A cavity shown on Fig. 1 has been used in the reference work with air as working fluid. This cavity has the constant temperature conditions on the vertical walls and the linear distribution of temperature on the horizontal walls. The mean motion was assumed to be two-dimensional which means that the movement in the third direction is supposed to be equal to zero in the mean.

To describe the reference work, it is better to write a model equation having the value of $C_3'' = 0.7$ as follows.

$$\frac{\partial}{\partial t}(\rho\varepsilon) + \frac{\partial}{\partial X_i}(\rho U_i \varepsilon) = \frac{\partial}{\partial X_i}\left(\frac{\mu_{eff}}{\sigma_\varepsilon}\frac{\partial \varepsilon}{\partial X_i}\right)$$

$$+ \frac{\varepsilon}{k}(C_1 P + C_3'' G) - C_2 \frac{\varepsilon^2}{k}$$

As mentioned in section 4.2.3, this is a simple equation that can account for the effects of buoyancy on the turbulent length scale

without the concept of the flux Richardson number.

Table 2 shows the results of sensitivity study having been taken for the base model constants C_1, C_2, and C_3". From this table, it is easy to find out some drastic changes on the maximum turbulent viscosity with the variations of those constants. But there are little changes on the maximum velocity and the mean Nusselt number along the hot wall. On this table, an improved form of the ε - equation proposed by Rodi also results in the case of C_3" = 1.44 + X, where a linear combination of C_3" between the value of horizontal (C_3" = 0.4) and that of vertical (C_3" = 1.44) boundary layers has been taken. Therefore, in this case, C_3" has a different value at each point.

When interpreting those results, it may be helpful to remind the corresponding model equation of AQUA with the definition of the flux Richardson number only suitable in the horizontal boundary shear layers.

Table 2 Extracted results of sensitivity study, Gr = 5.0E7

	NuH_{mean}	v^*_{max}	u^*_{max}	$\mu^*_{t max}$	
Base	21.56	1014.27	685.54	4.23 A	7.9 B
C_1=1.15 (-20%)	+6.6%	+0.2%	-8.4%	+76.8%	+13.9%
C_1=1.73 (+20%)	-6.8%	+0.3%	+7.4%	-58.2%	-18.0%
C_2=1.54 (-20%)	-7.3%	-0.3%	+6.8%	NA	-37.1%
C_2=2.30 (+20%)	+5.4%	+0.8%	-8.9%	+66.9%	+32.9%
C_3"=0.40	+1.5%	+0.1%	+0.4%	-3.5%	+45.6%
C_3"=1.44	-2.8%	-2.1%	-8.7%	+2.6%	-67.8%
C_3"=1.44+X (Rodi's)	+2.0%	-0.3%	-1.3%	+12.8%	+41.8%

A. Occurs in the upper part of the vertical boundary layer

B. Occurs in the left lower corner

X = (0.7 - 1.44) $ABS(U_{mean})/SQRT(U^2 + V^2)$

Figs. 2 and 3 show the turbulent viscosity diagrams of the reference work to indicate the various levels of turbulence with Grashof number. Figs. 4 and 5 show velocity profiles at the middle of the left

wall and local Nusselt numbers along the hot wall. The following dimensionless variables may be used to see the figures and table.

$$x^* = \frac{x}{L} \qquad y^* = \frac{y}{H} \qquad u^* = \frac{H}{\nu} u \qquad v^* = \frac{L}{\nu} v \qquad \mu_t^* = \frac{\mu_t}{\mu}$$

$$Gr = 8g\beta(T_H - T_C)L^3/\nu^2$$

$$Nu(y) = \frac{2L}{T_H - T_C} \frac{T_H - T(y)}{x_1} \text{ at } x = -L \text{ along the hot wall}$$

In addition to the above mentioned reference results, a correlation NuH_{mean} - Gr as

$$NuH_{mean} = 0.162\ Gr^{0.275} \text{ for } 6.06E6 < Gr < 1.0E8$$

could be found out with some comparisons of another works.

By the way, I think, it is better to mention additionally that the reference work was establshed using the so-called "the vorticity and the stream function method" which has some attractive features. Based on this method, the reference work solves equations for the stream function and the vorticity instead of dealing with the continuity equation and two momentum equations in two dimensions. It means that, in two dimensions, the elimination of pressure terms from two momentum equations by cross differentiation leads to a vorticity transport equation. With the definition of a stream function, this equation composes the basis of the above method. Thus it can relieve numerically the difficulty associated with the determination of pressure.

The pressure field is indirectly specified via the continuity equation. So when the correct pressure field is substituted into the momentum equations, the resulting velocity field satisfies the continuity equation. If we attempt a direct solution of the whole set of the discretization equations resulting from the momentum and continuity equations, this indirect specification of pressure can be tackled conveniently. However it is well known that numerically the direct method is not economical. When the AQUA was developing, the subject relating to this problem also handled extensively from the comparisons of various matrix solvers. As a result of the above subject, nowadays it is almost fixed to use the ICCG (Incomplete Choleski Conjugate Gradient) method. Anyway it is still possible in AQUA to select different methods, such as the PSOR (Point Successive Over Relaxation) and a kind of direct method.

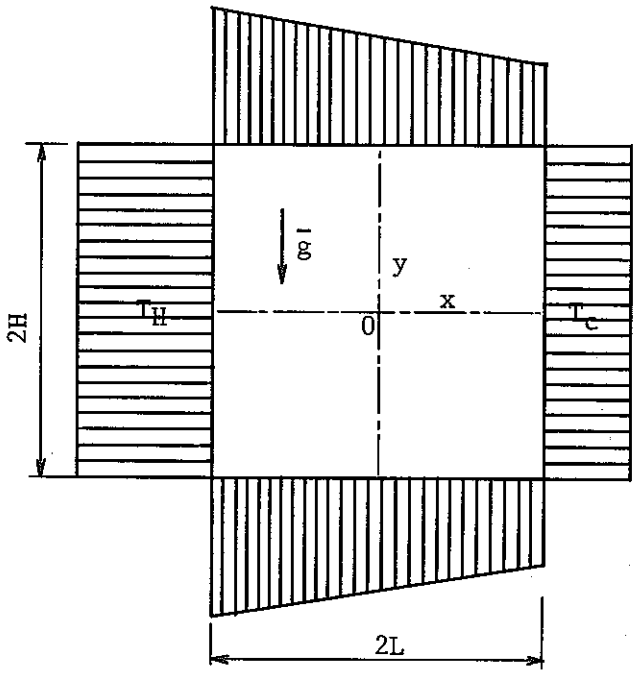

Fig. 1 A typical thermal cavity

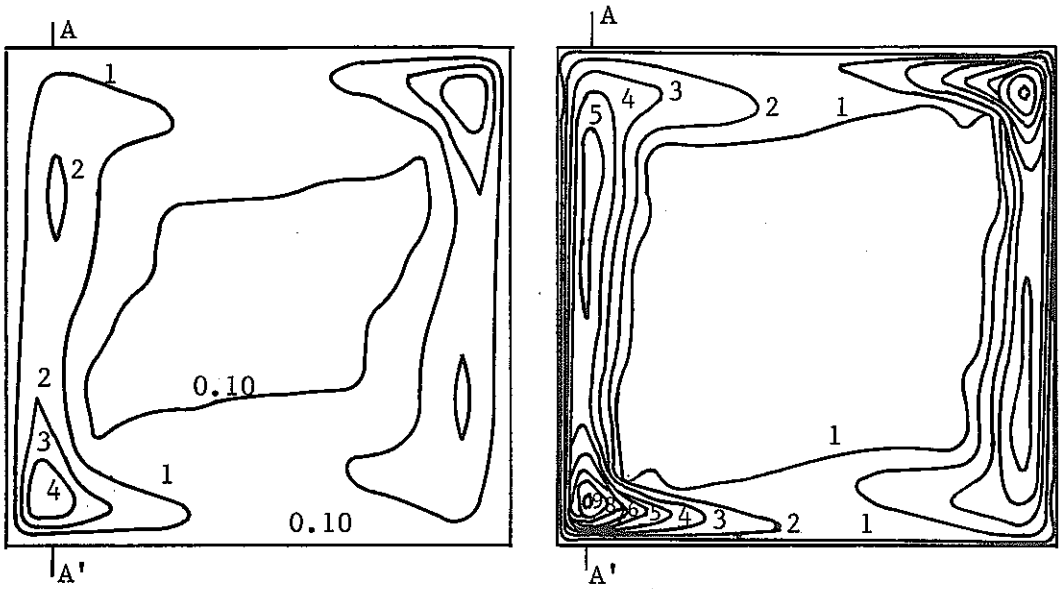

(a) Gr 1.0E7 (b) Gr 1.0E8

Fig. 2 Iso-μ_t diagrams of the cavity

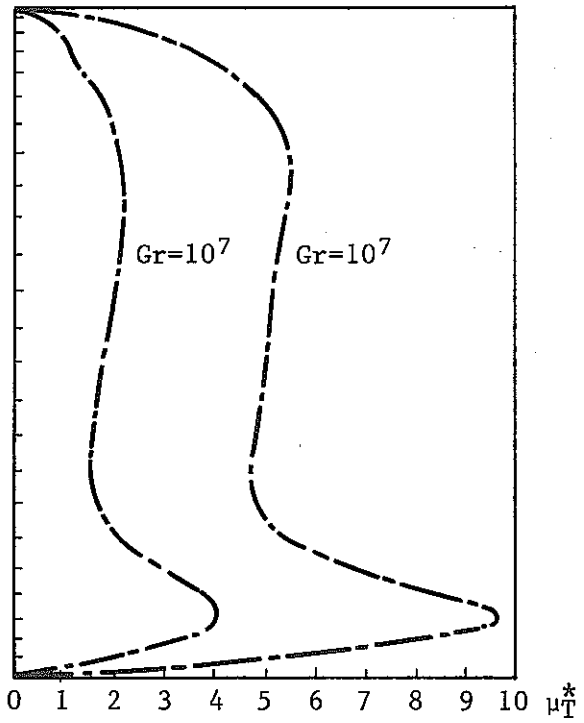

Fig. 3 Turbulent viscosity profiles along the A-A section of the figure 2

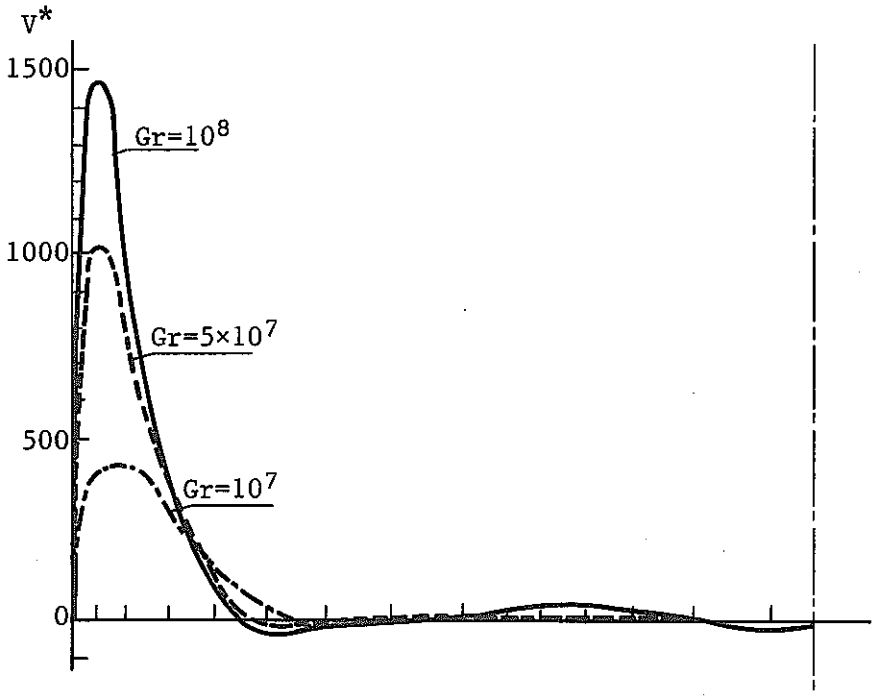

Fig. 4 Velocity profiles at the middle of the left wall for a half cavity

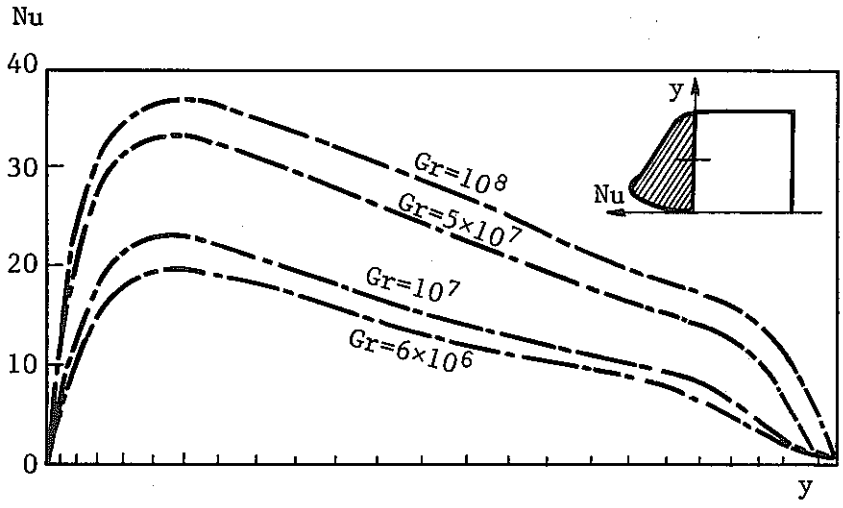

Fig. 5 Local nusselt numbers along the hot wall

4.3.2 Calculations and results

The purpose of this calculation is to make a comparison to results of the reference work. Therefore an irregular grid shown on Fig. 6 has been selected to have the same relative mesh arrangement of the reference work. With the following conditions, the results shown on Table 3 and Figs. 7, 8, 9, 10 have been obtained to correspond the reference results. Additionally, Fig. 11 shows various levels of the turbulent viscosity with modified model constants at Gr 5.0E7. With regard to the Fig. 7 and Fig. 11, the iso-lines of turbulent viscosity was calculated using a logarithmic formula, Iso-μ_t = $\log_{10}(\mu_t * 1.0E10)$.

Coordinate:	X - Z, Two Dimension
Mesh Arrangement:	25 * 25, Total 625 meshes
Numerical Method:	SIMPLEST-ANL with UPWIND scheme
Boundary Conditions:	No slip for velocity on walls and constant temperatures

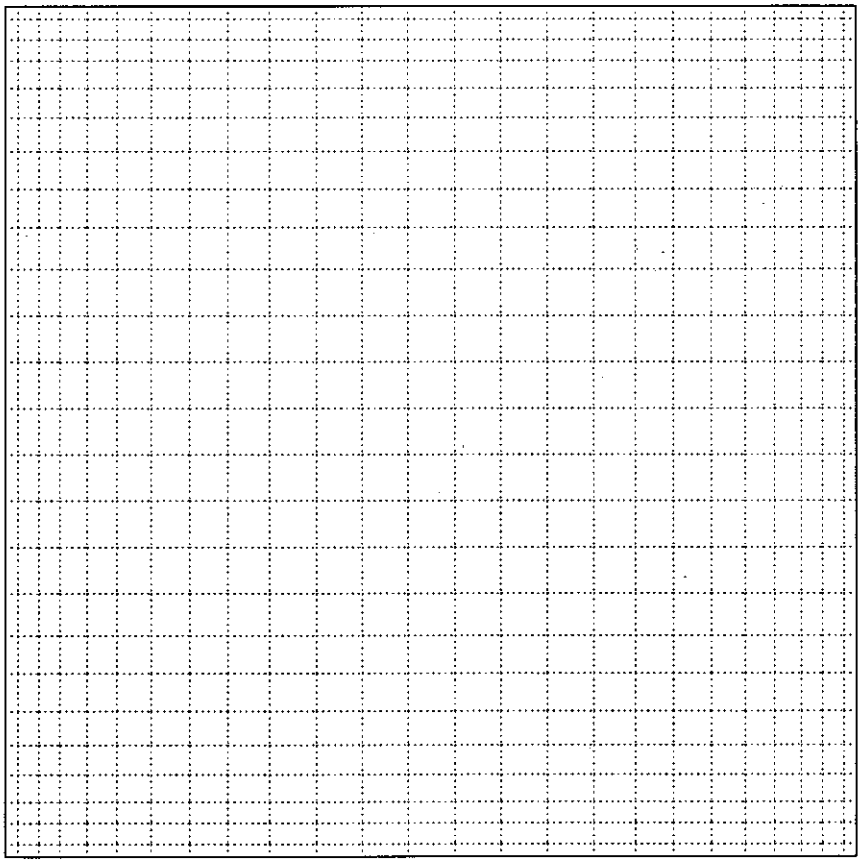

Fig. 6 Mesh arrangements of the thermal cavity problem

Table 3 Results of sensitivity study on AQUA, Gr = 5.0E7

	NuH_{mean}	v*	u*	μ_t
X coordinates	NA	i = 2	i = 7	i = 4
Z coordinates	NA	k = 14	k = 24	k = 4
Base	8.103	1104.8	733.3	3.4
C_1=1.15, C_3=0.4	+1.3%	-2.5%	-3.6%	+37.0%
C_1=1.73, C_3=0.6	-0.8%	+1.5%	+2.8%	-20.9%
C_2=1.54, C_3=0.5	-2.9%	+3.4%	+4.4%	-71.8%
C_2=2.30, C_3=0.5	+3.5%	-3.8%	-3.6%	+99.2%
C_3=0.70 (Default)	+0.4%	-0.1%	+0.9%	+36.9%
C_3=0.00	-1.0%	0.0%	-2.0%	-51.6%

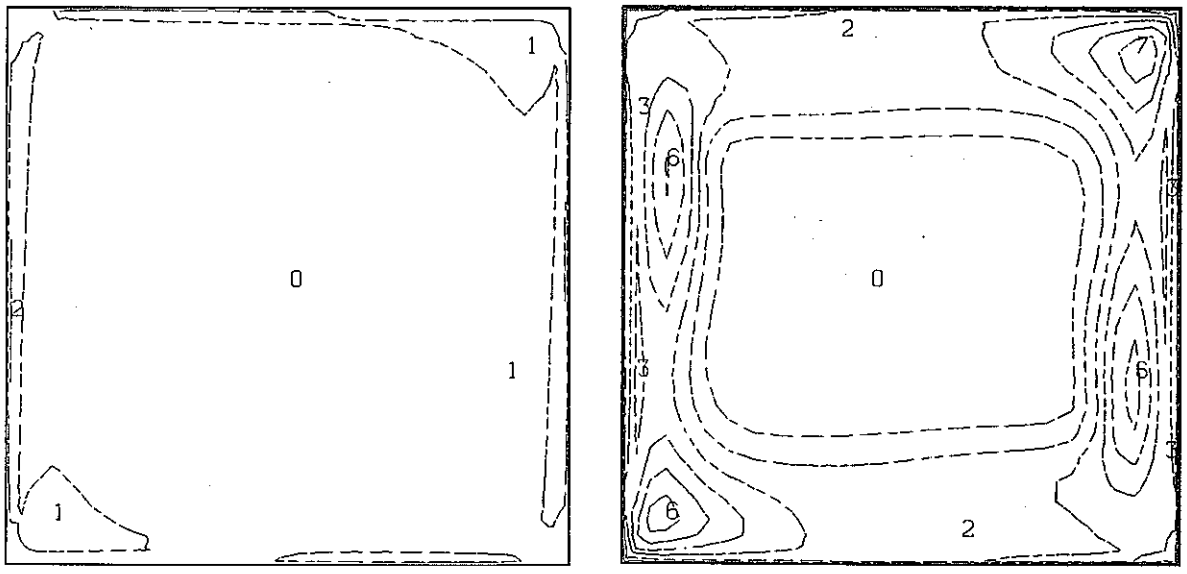

(a) Gr 1.0E7 (b) Gr 1.0E8

Fig. 7 Calculated Iso-μ_t diagrams of the cavity

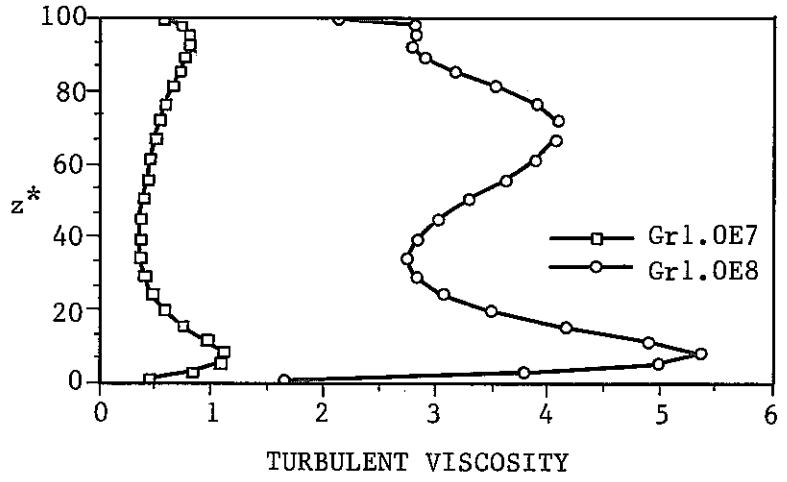

Fig. 8 Calculated turbulent viscosity profiles at section A-A

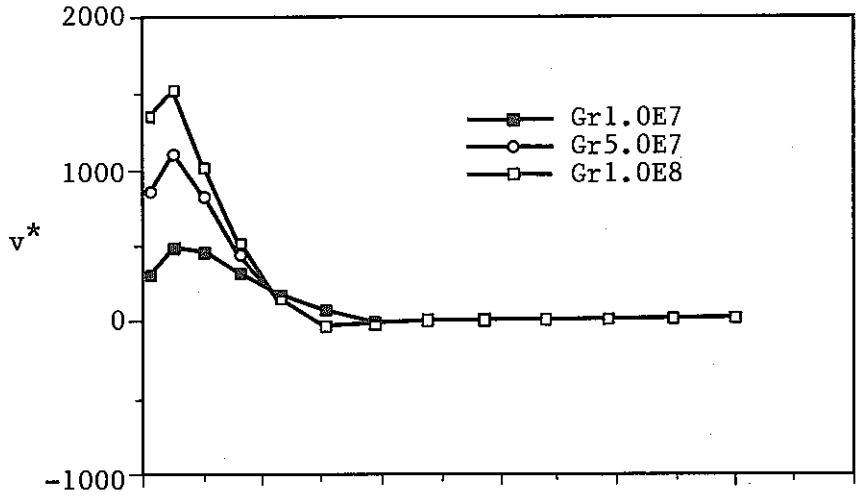

Fig. 9 Calculated velocity profiles at the middle of the left wall for a half cavity

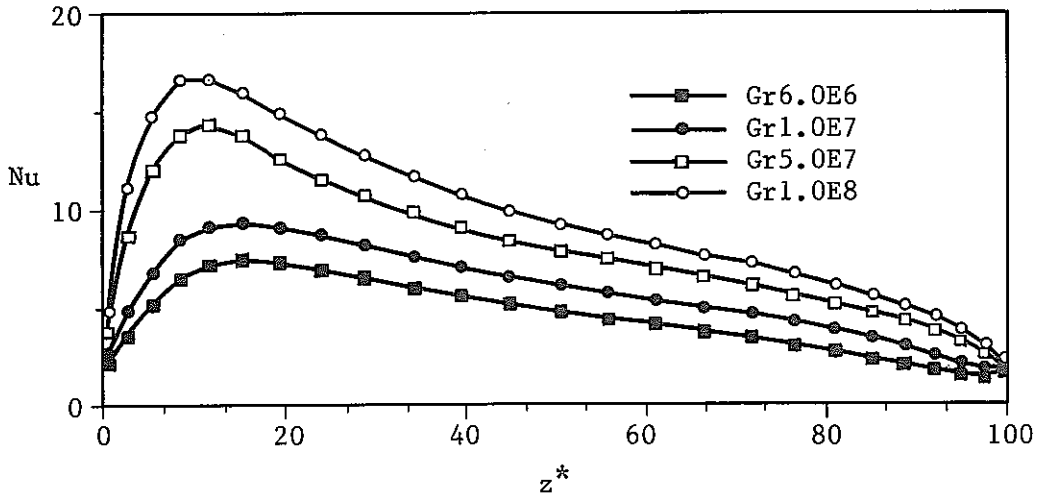

Fig. 10 Calculated local nusselt numbers along the hot wall

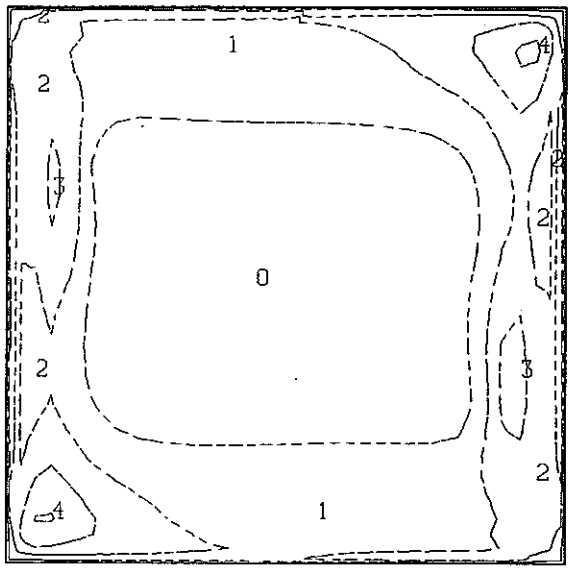

(a) BASE C_3 = 0.5

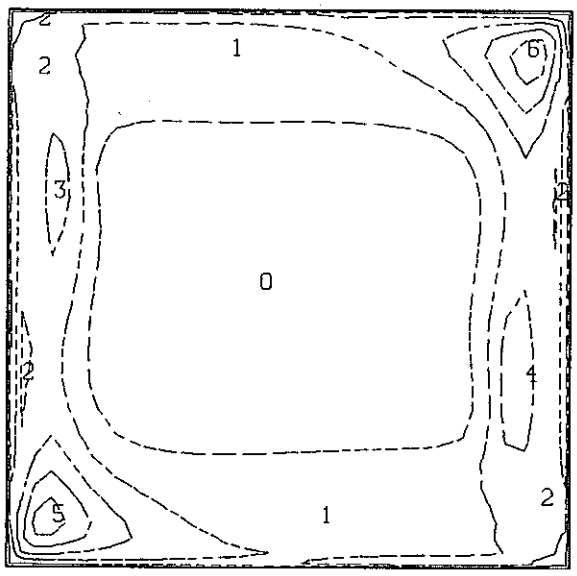

(b) AQUA default C_3 = 0.7

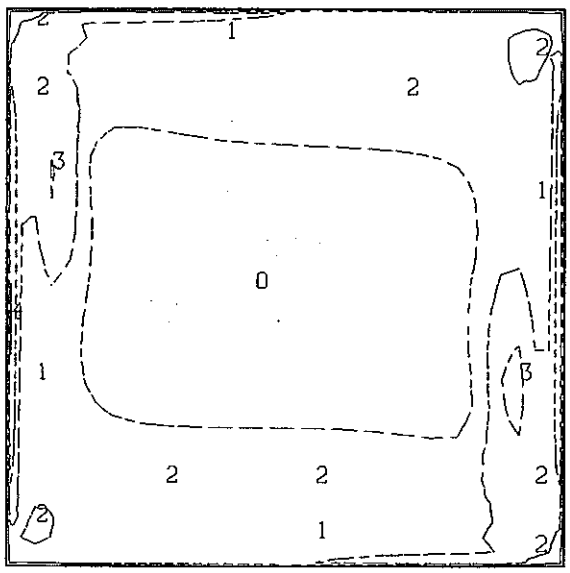

(c) C_3 = 0.0

Fig. 11 Variation of turbulent viscosity with modified model constants at Gr 5.0E7 (continued)

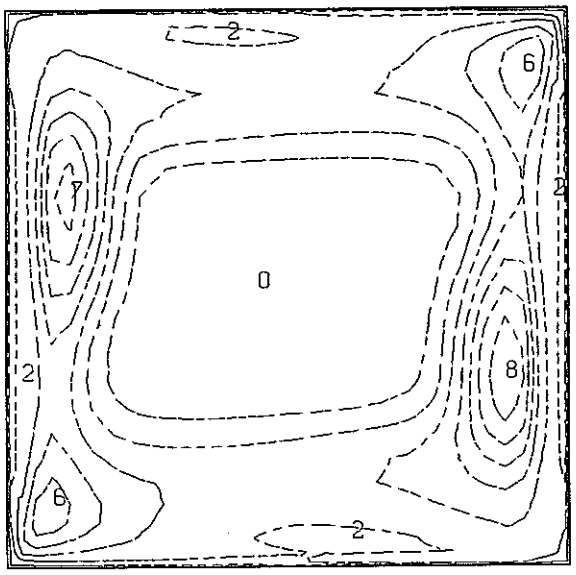

(d) C_1 = 1.15, C_3 = 0.4

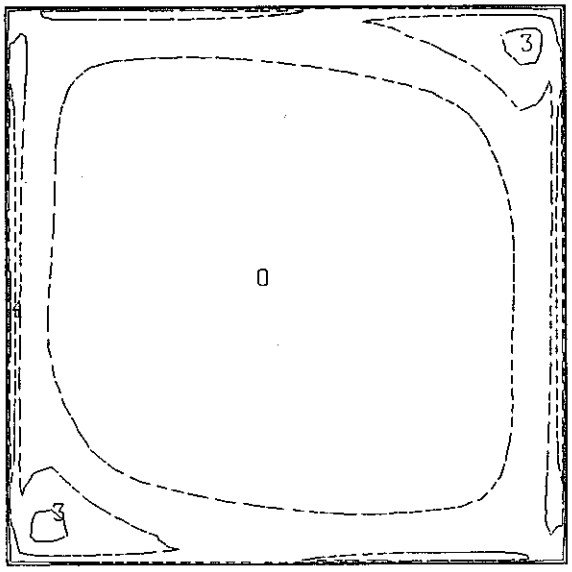

(e) C_1 = 1.73, C_3 = 0.6

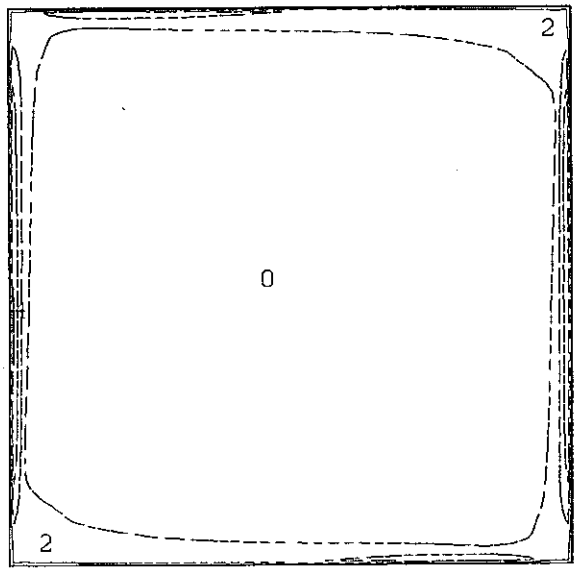

(f) C_2 = 1.54, C_3 = 0.5

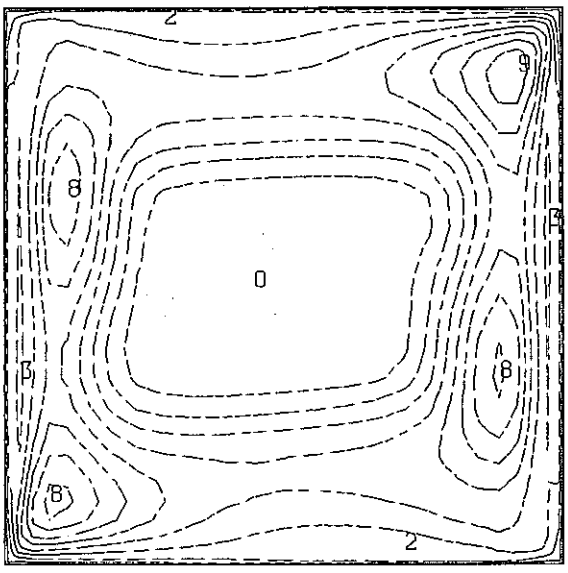

(g) C_2 = 2.30, C_3 = 0.5

Fig. 11 Variation of turbulent viscosity with modified model constants at Gr 5.0E7

4.4 The 7th IAHR Benchmark Problem

This benchmark problem has been prepared for the 7th Meeting of the IAHR Working group on Advanced Nuclear Reactors Thermal Hydraulics, which is to be held in Kernforschungszentrum Karlsruhe GmbH, FRG, August 27-29, 1991. Given some control results of extensive experiment, a numerical study could be performed to see the applicability of the turbulence models in AQUA. In this problem, it is important to see the thermal stratification and plenum-core thermohydraulic interactions in which the flow and temperature fields are governed by buoyancy driven flow.

4.4.1 Control results of the experiment

Fig. 12 shows the experiment test section representing a reactor core by a simple inlet channel, hot plenum and cold wall. The inclined ceiling of the plenum section was provided intentionally for checking adequate boundary treatment in computational procedure. The test section is a slab geometry model 150 mm in depth with water as a working fluid.

Hot fluid is supplied to the plenum from the inlet channel and flows through the plenum toward the outlet with heat loss on the cold wall. According to the experiment, it is important to note a large clockwise recirculating flow in the plenum and a stratified flow at the bottom of the plenum. The cold fluid flow toward the exit of the inlet channel interacts and mixes with the hot fluid flowing upward in the vicinity of the exit of the inlet channel. It was also reported that, under certain conditions, the cold fluid flow could penetrate into low the inlet channel.

Following the experiment, the calculation cases are selected as shown on Table 4 from the combination of the inlet flow temperature, inlet flow rate to the test section, and the heat flux on the cold wall. Also this table shows a measured temperature at the bottom of the traverse line P4. The mean motion is assumed to be two dimensional. It can be also assumed that no heat transfer has happened on the surrounding walls except the cold wall.

Actually, the test uses sufficiently long inlet channel with a flow straightener at the lower part of that channel to make nearly fully developed turbulent flow field in the channel. The measured

profile of velocity component V_z is provided at z = -200 mm as shown on Fig. 13. In addition to the above, there are also measured temperature profiles along the traverse line P1 for the case 1 and case 4 as shown on Fig. 14.

The measured velocity profile at z = -200 was used as boundary conditions on this study even though the original requirements for this benchmark problem recommended not to use the measured velocity profile as boundary conditions except for the case 4. The requirements indicate that the development of velocity along the inlet channel is closely related to the thermal siphon phenomena, which means cold fluid flow penetration to the inlet channel due to the balance of the inertia forces and the buoyance forces. Thus the results of this study may have some lack of capabilities on the above phenomena.

Table 4 Calculation cases for the 7th IAHR benchmark problem

	CASE1	CASE2	CASE3	CASE4
Inlet Temperature (Deg C)	48.9	49.0	49.1	49.1
Average Inlet Velocity (cm/s)	4.15	5.16	6.34	11.4
Outlet Boundary Pressure	Constant (P = 1.0132E5 Pa)			
Cold Wall Temperature (Deg C)	14.8	14.4	14.5	15.4
Heat Flux on the Cold Wall (W/m^2)	-2.13E4	-2.24E4	-2.34E4	-2.40E4
Measured Temperature at the bottom of the line P4 (Deg C)	37.0	36.7	36.4	38.5

4.4.2 Calculations and results

The object of this calculation is to match the results of calculation with some given control results of the experiment using the modified model constants on the turbulence model.

As the first step of this calculation, two mesh arrangements shown on Figs. 15 and 16 have been tackled on this problem. Of these arrangements, the origin point of test z = 0 mm corresponds to the grid coordinates z' = 200 mm and z" = 500 mm for Fig. 15 and Fig. 16 respectively. The mesh arrangement shown on Fig. 15 has total 2468 calculaition cells with relative large changes between meshes having some fine grids near the walls, while the other shown on Fig. 16 has 3157 cells with smooth changes between meshes. Fig. 17 shows the comparison of the calculation results with isothermal diagrams inside the plenum and the temperature profile along the traverse line P1 for the case 1 between two mesh arrangements. With respect to the control results of the experiment, it may be said that the mesh arrangement having 2468 cells produces more reasonable results, especially on the temperature profiles near walls. Therefore the mesh arrangement shown on Fig. 15 has been selected on this study, even though it might make the problem of time step size limitations more strictly with the implementation of MICE.

Fig. 18 indicates how the turbulence model can be used for wall flows. Theoretically, the model constants of the k & ε two-equation model are based on extensive examination of free flow. Thus in the case of the free slip boundary conditions, the flow inside the plenum can be represented by only large scale of turbulence length, such as the Fig. 18(b). Therefore it is important to implement the no slip boundary conditions in AQUA on the walls with the logarithmic law of the wall to account for the effects of viscous layer on the turbulence length scale.

On all calculation results, the calculated average inlet velocities at z = -200 mm shown on Table 5 have been used even though this is not the proper treatments of inlet boundary conditions.

Based on the SIMPLEST-ANL algorithm with first order difference scheme, Tables 6 and 7 show the results of sensitivity study with modified model constants of the k & ε two-equation model.

Overall calculation results having been based on the default values of AQUA are prepared as Fig. 19 through Fig. 32 for the k & ε two-equation model and the algebraic stress/flux model. Another calculation results shown on Fig. 33 through Fig. 39 with the value of C1 = 1.656 could also be prepared to show some agreements to the experiment. The MICE method with the default values of model constants has

been tested for the case 1 as shown on Fig. 40. A transient calculation has also been conducted for the case 1 using the previous results of tne MICE method as shown on Fig. 41. When preparing figures, the values of turbulent quantities are converted using a formula $\phi = \log_{10}$ (values * AMULT) with AMULT = 1.0E8 for turbulent kinetic energy k and its dissipation rate ε and AMULT = 1.0E7 for turbulent viscosity μ_t.

Table 5 Calculated average inlet velocity (unit: cm/sec)

	CASE 1	CASE 2	CASE 3	CASE 4
Reference	4.15	5.16	6.34	11.4
Calculated	4.19	5.23	6.41	11.4

Table 6 Temperatures at the bottom of the traverse line P4 with the modified model constants (Unit: dec G)

	CASE 1	CASE 2	CASE 3	CASE 4
Reference	37.0	36.7	36.4	38.5
Default	40.7480	41.0314	40.8306	42.8237
C_1=1.150	42.5507	-	-	-
C_1=1.584	38.9304	39.0498	39.3562	41.4705
C_1=1.656	38.3361	37.6011	37.6666	39.8606
C_1=1.730	38.1062	-	-	-
C_2=1.540	35.5401	-	-	-
C_2=1.728	38.4967	38.5932	38.8533	40.4907
C_2=2.300	42.4474	-	-	-
C_3=0.000	40.8404	41.1764	41.0158	43.0121

Table 7 X direction velocities at x = 187.5 mm, z = 25.0 mm with the modified model constants (unit: cm/sec)

	CASE 1	CASE 2	CASE 3	CASE 4
Reference(*)	-0.90	-	-	-0.65
Default	-0.5239	-0.4736	-0.4814	-0.5041
C_1=1.150	-0.8392	-	-	-
C_1=1.584	-0.6553	-0.5465	-0.4587	-0.3445
C_1=1.656	-0.8030	-0.6149	-0.5198	-0.3822
C_1=1.730	-1.1407	-	-	-
C_2=1.540	-0.8640	-	-	-
C_2=1.728	-0.6701	-0.5578	-0.4810	-0.3783
C_2=2.300	-0.5538	-	-	-
C_3=0.000	-0.5081	-0.4838	-0.4805	-0.4256

(*) Estimated value

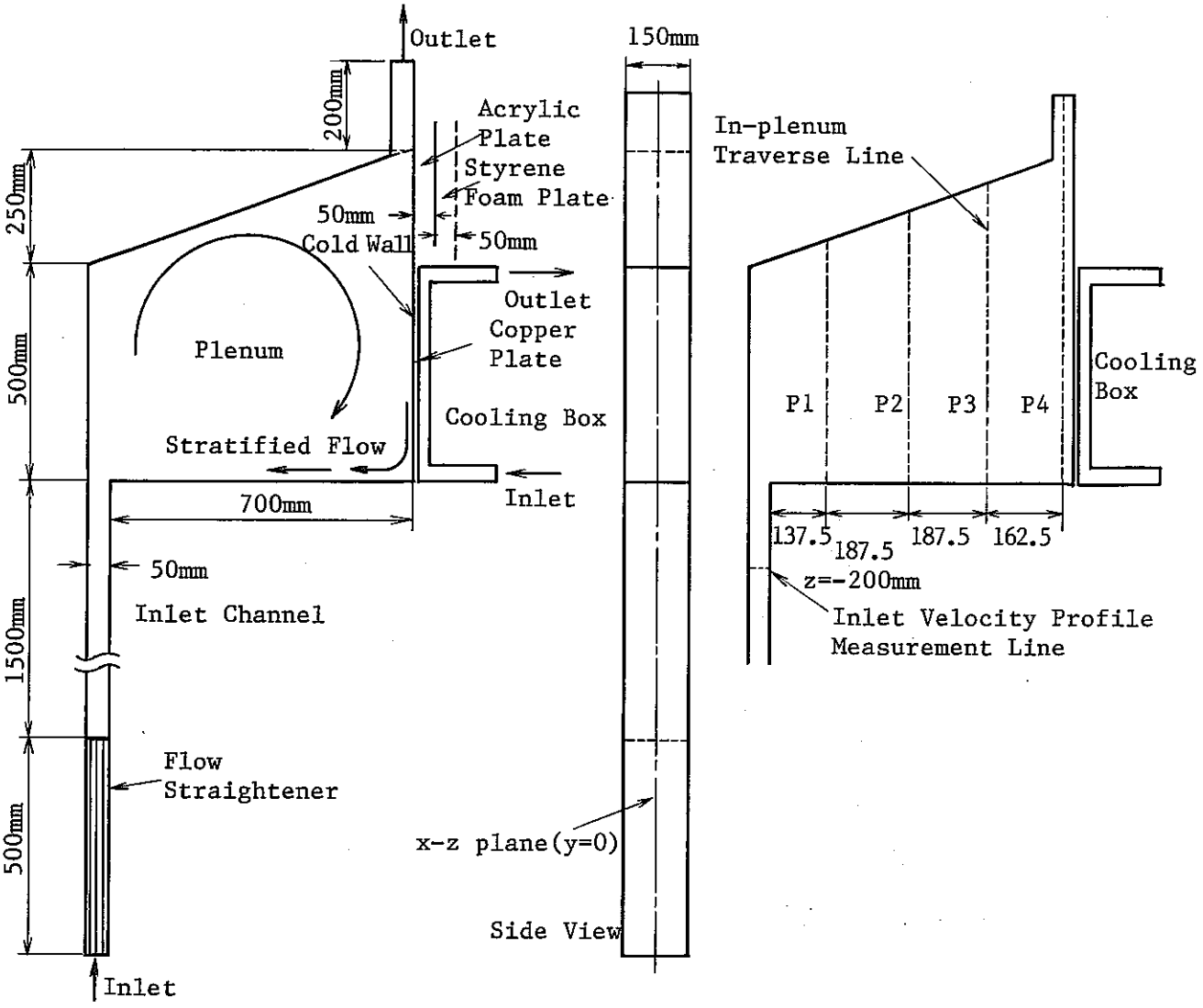

Fig. 12 Test section of the 7th IAHR benchmark problem

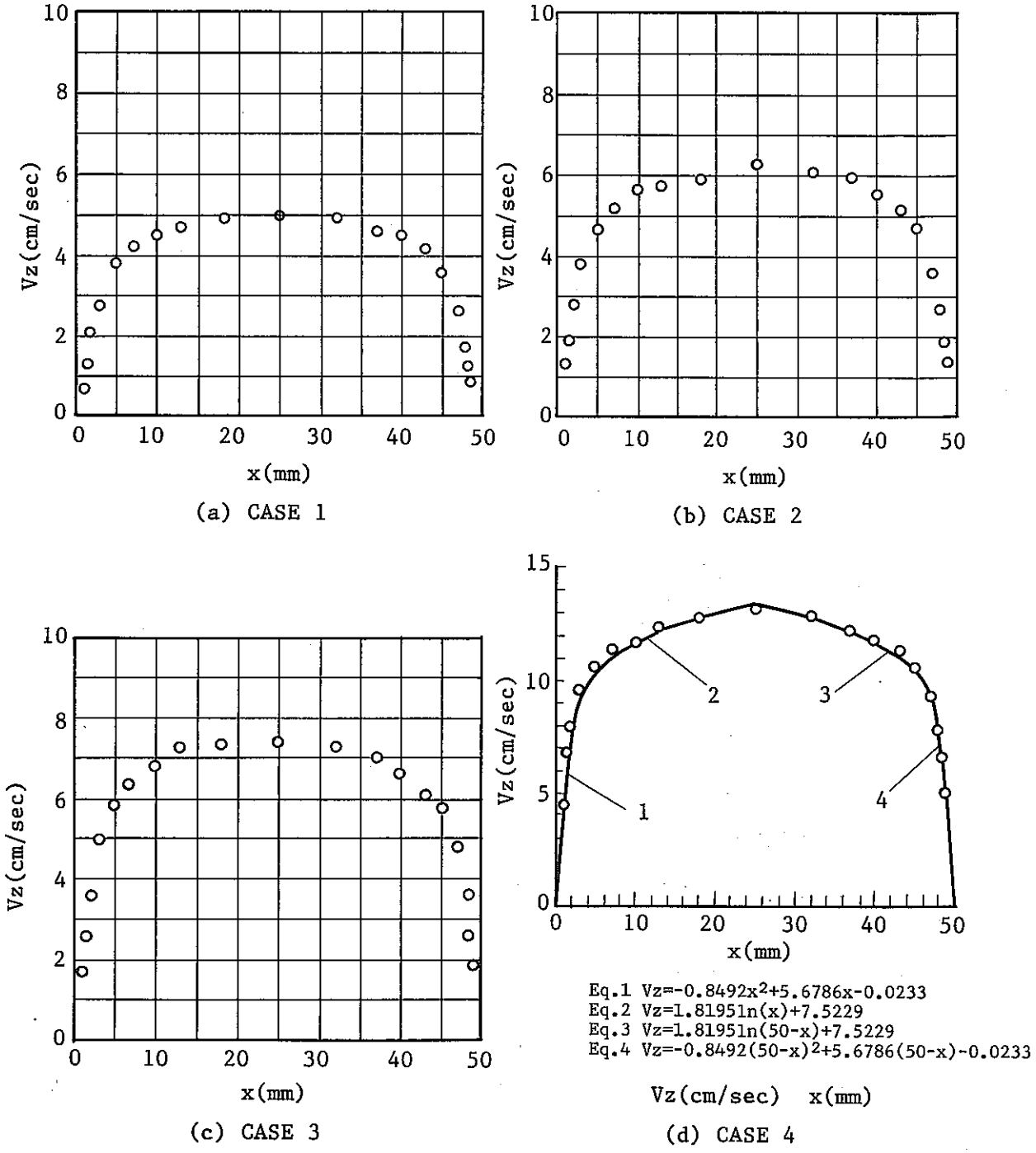

Fig. 13 Measured inlet velocity profiles at z = -200 mm

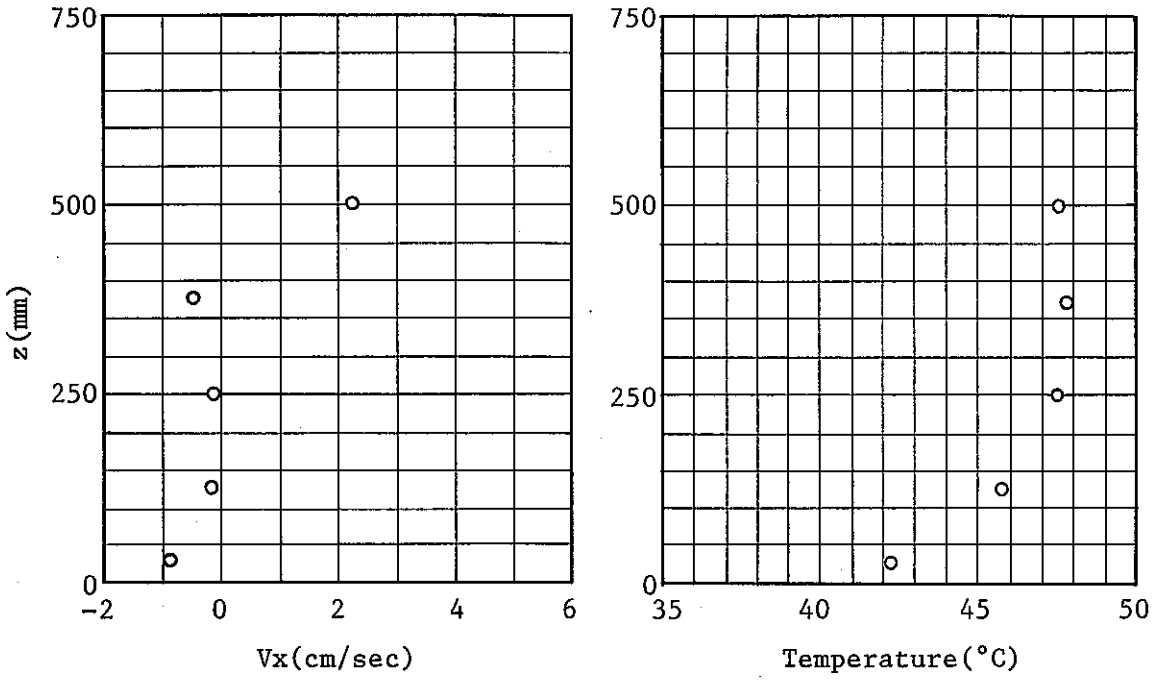

(a) CASE 1

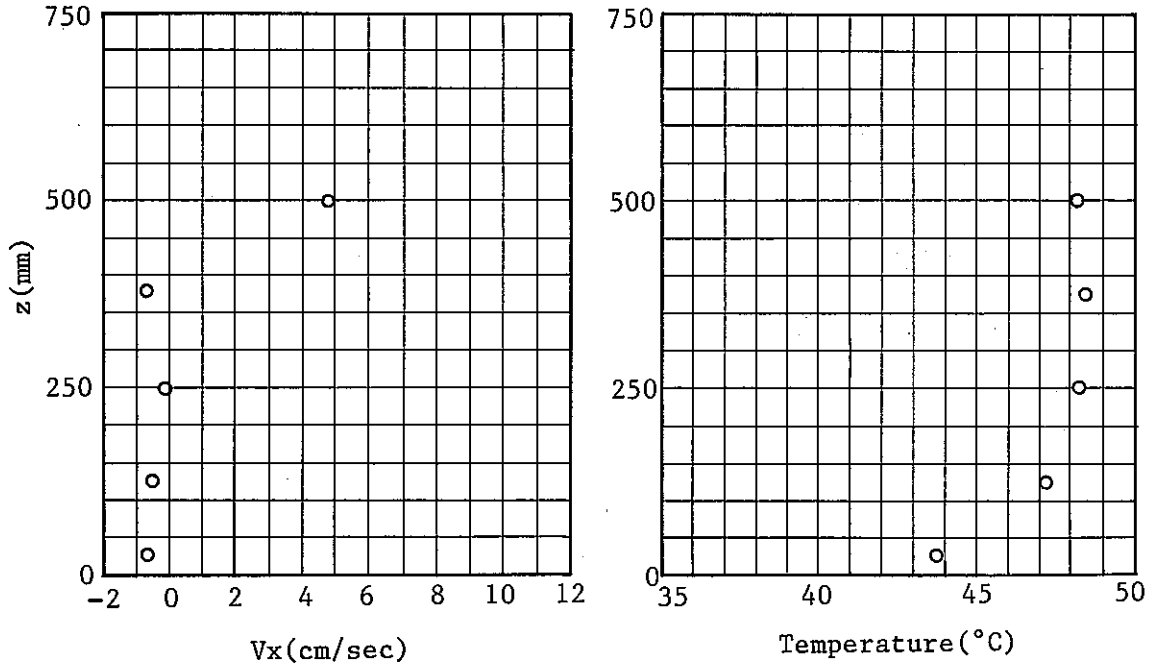

(b) CASE 4

Fig. 14 Control results on the traverse line P1

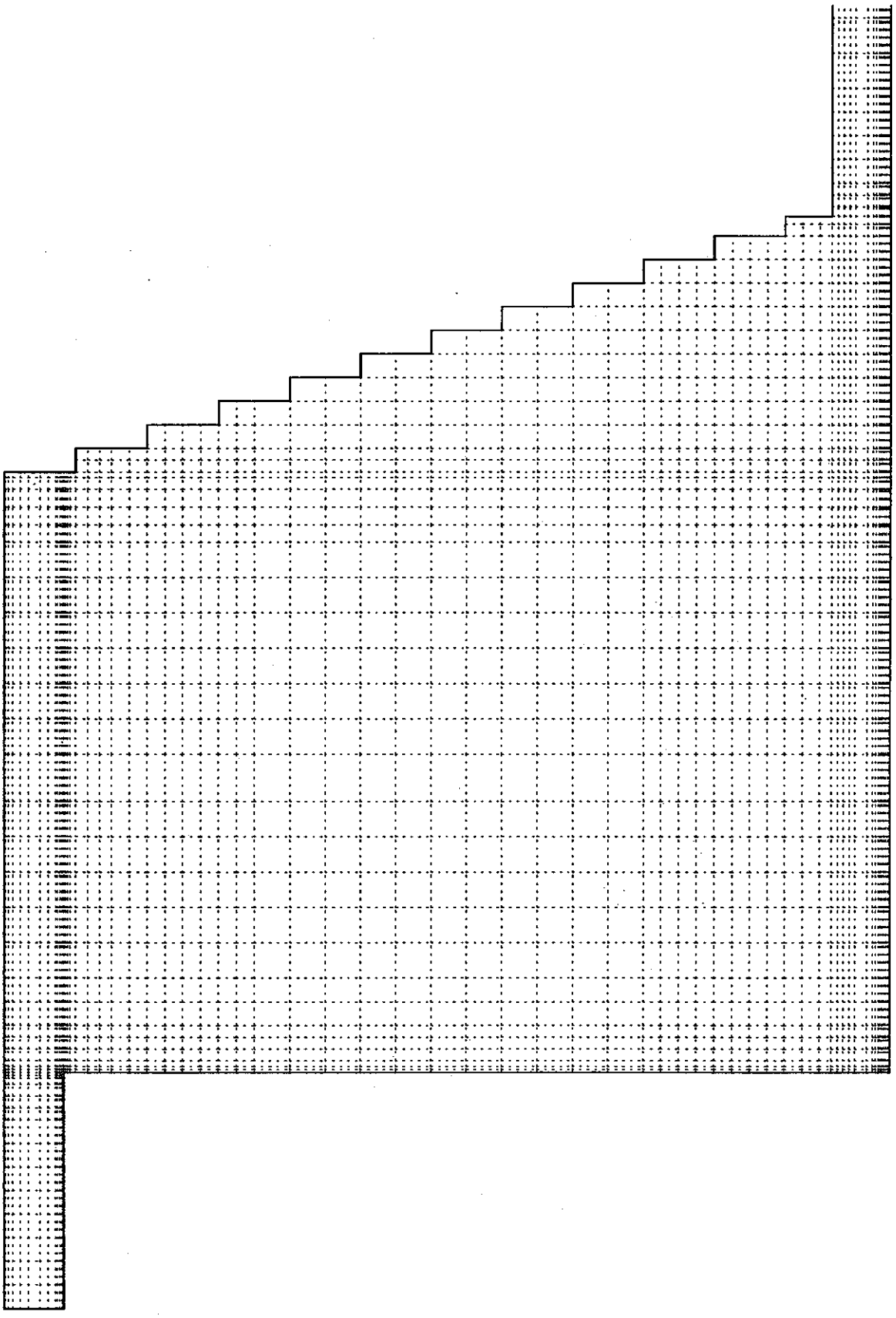

Fig. 15 Mesh arrangements with 2468 calculation cells

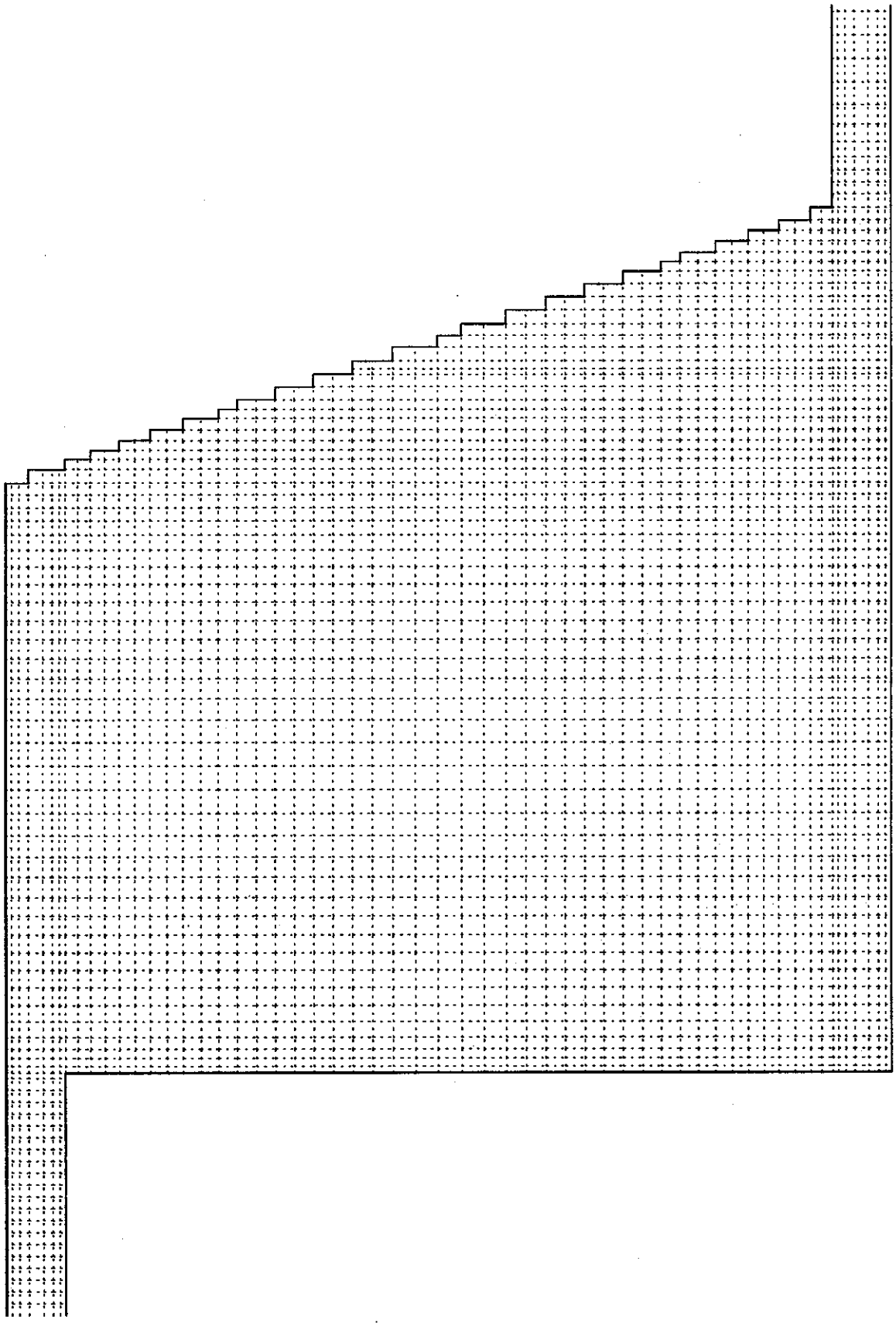

Fig. 16 Mesh arrangements with 3157 calculation cells

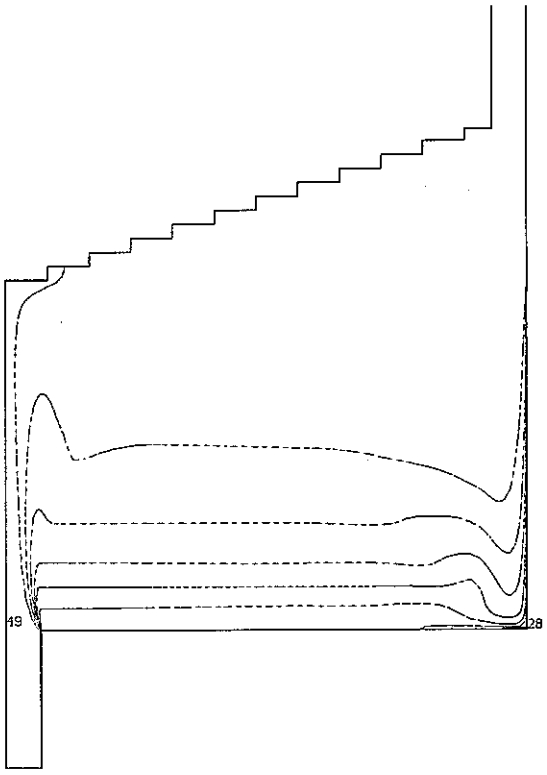

TIME: 9567.0 SEC. J = 1

(a) Iso-temperature
2468 cells

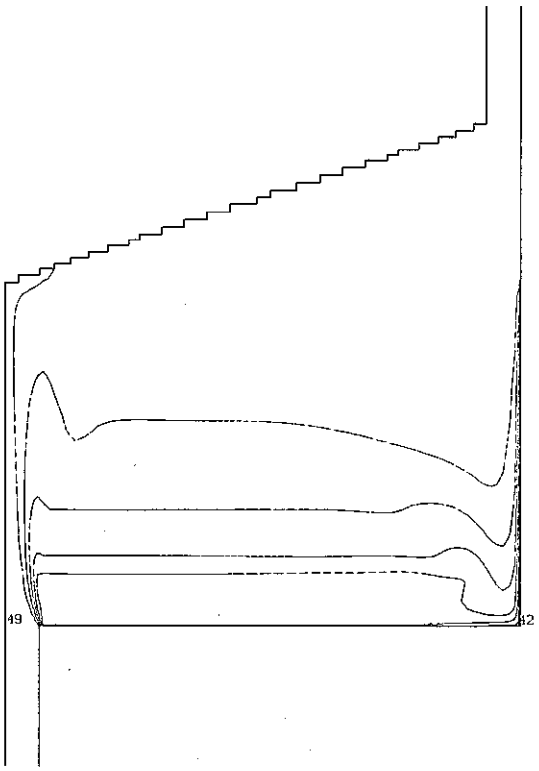

TIME: 9973.0 SEC. J = 1

(b) Iso-temperature
3157 cells

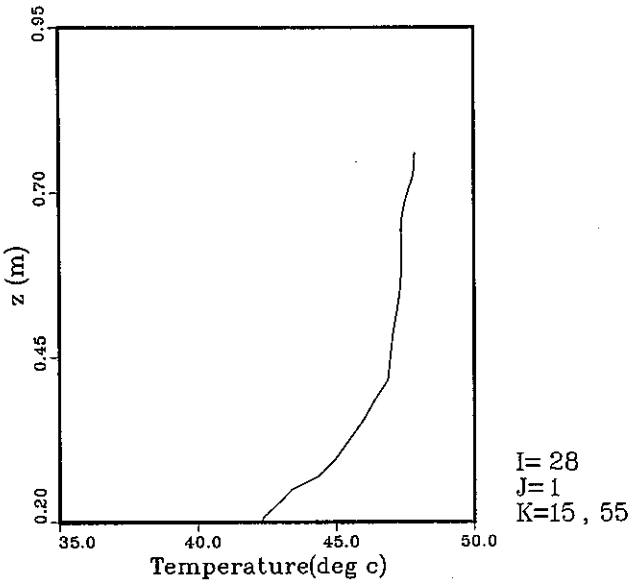

(c) Temp. distribution
on P1,2468 cells

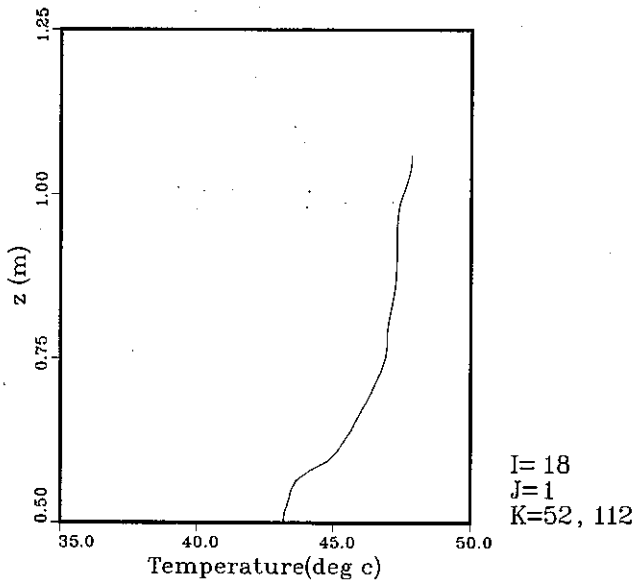

(d) Temp. distribution
on P1,3157 cells

Fig. 17 Cell number 2468 vs 3157 results for case 1

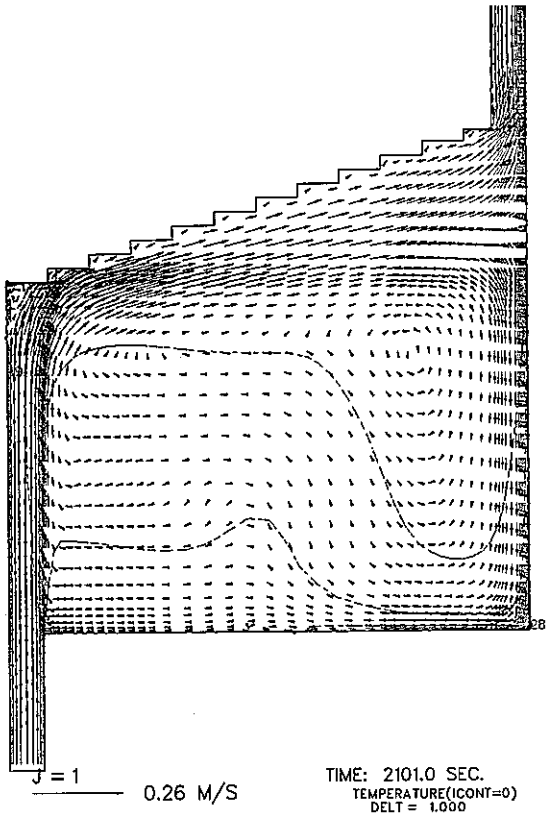

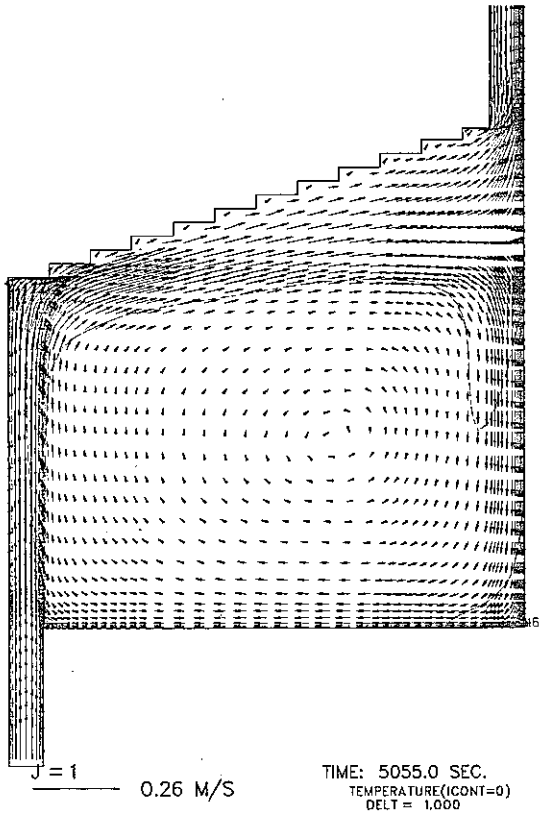

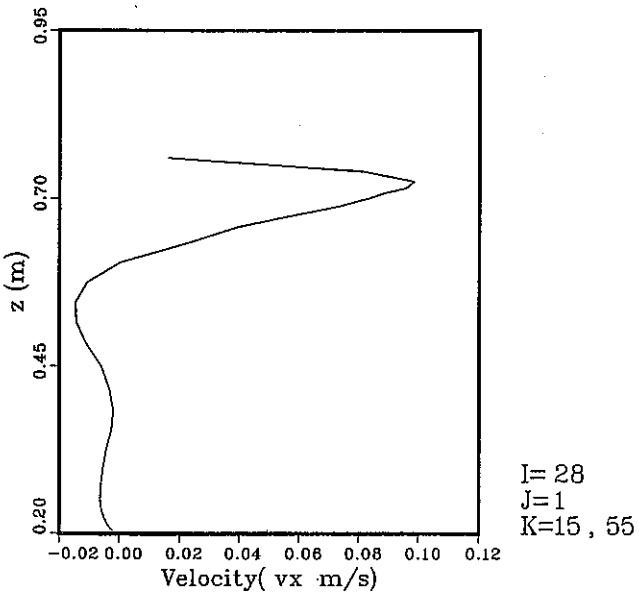

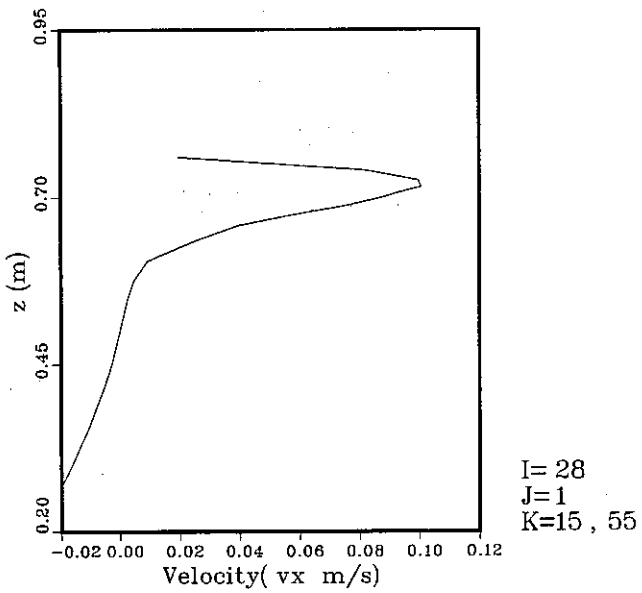

(a) No slip

(b) Free slip

Fig. 18 No slip vs free slip results for case 4

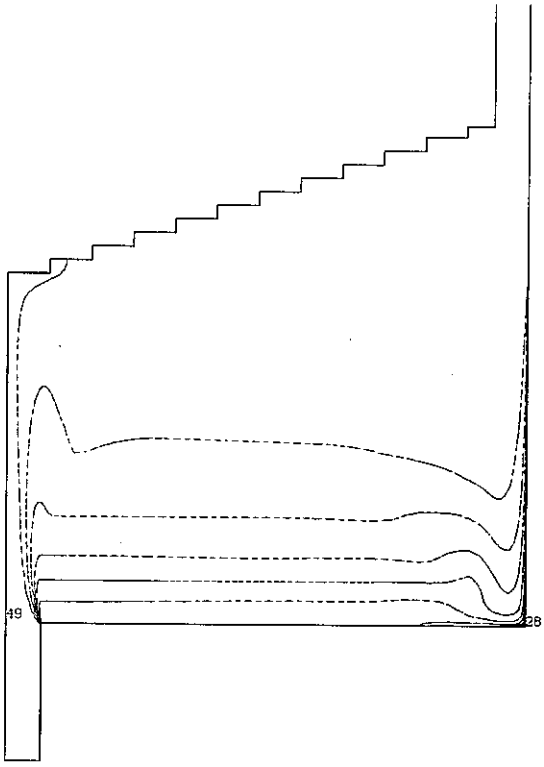

TIME: 9567.0 SEC. J = 1

(a) CASE 1

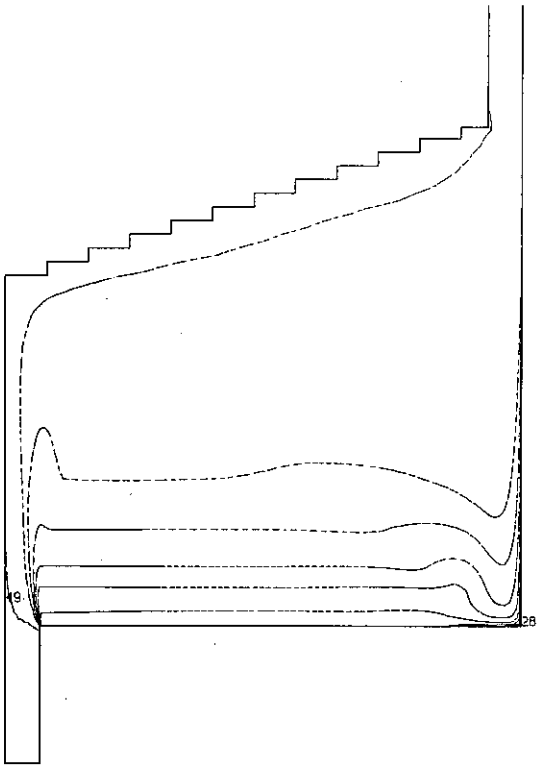

TIME: 8077.0 SEC. J = 1

(b) CASE 2

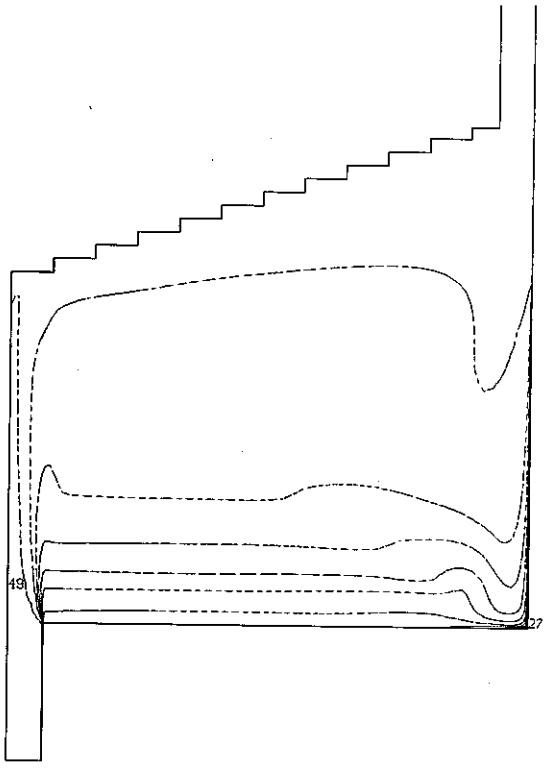

TIME: 4688.0 SEC. J = 1

(c) CASE 3

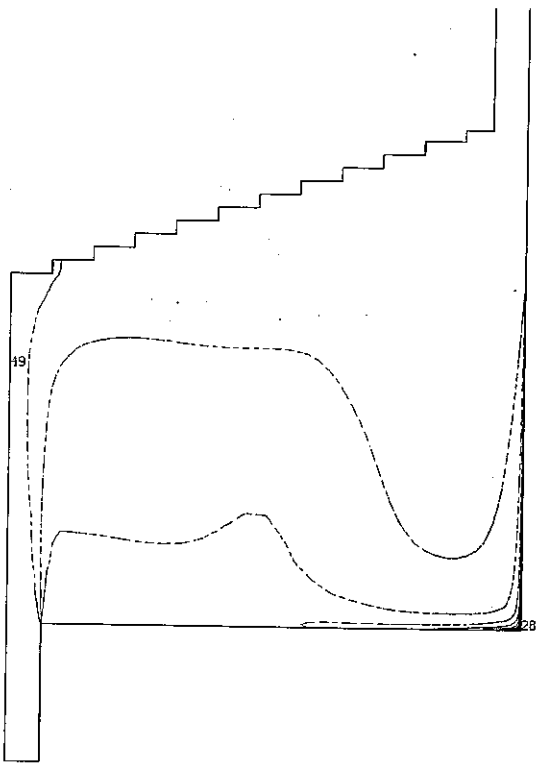

TIME: 2101.0 SEC. J = 1

(d) CASE 4

Fig. 19 Iso-temperature diagrams with default constants of the k & ε two-equation model

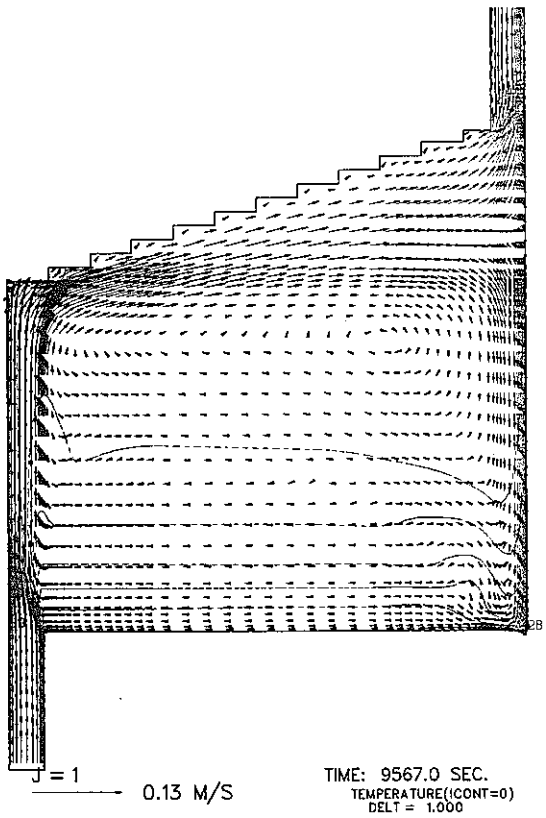

(a) CASE 1

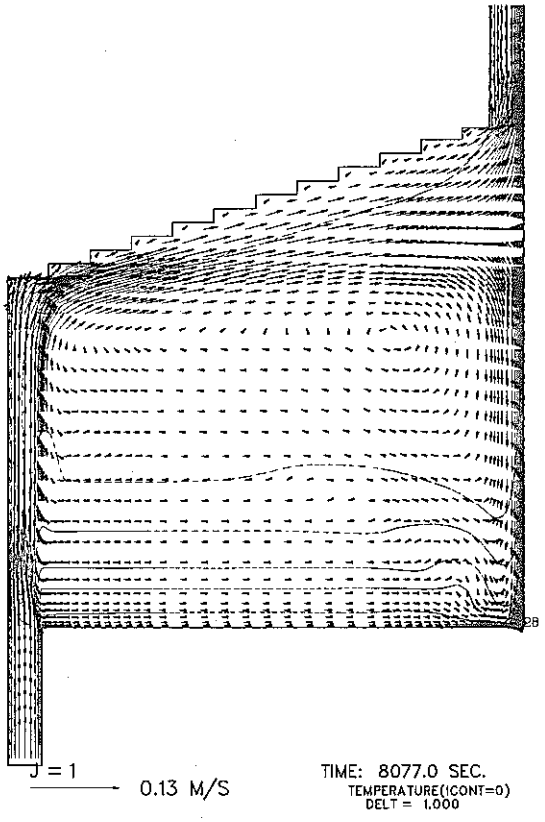

(b) CASE 2

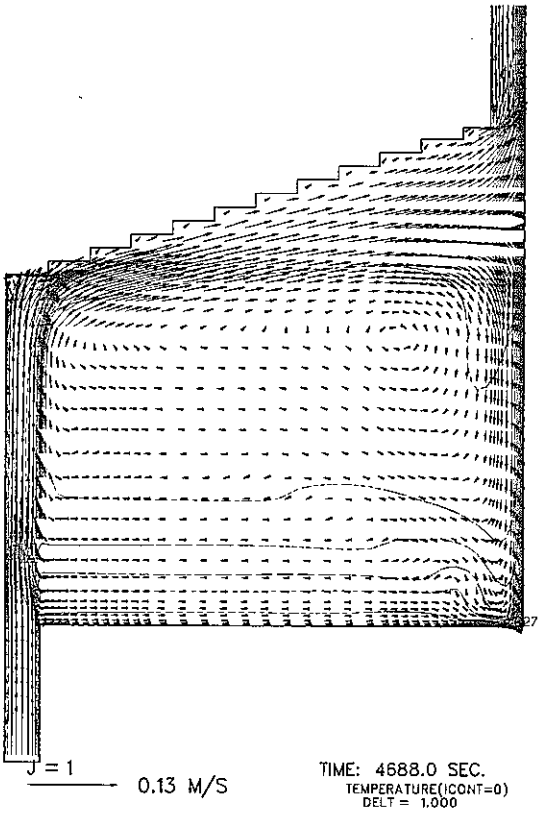

(c) CASE 3

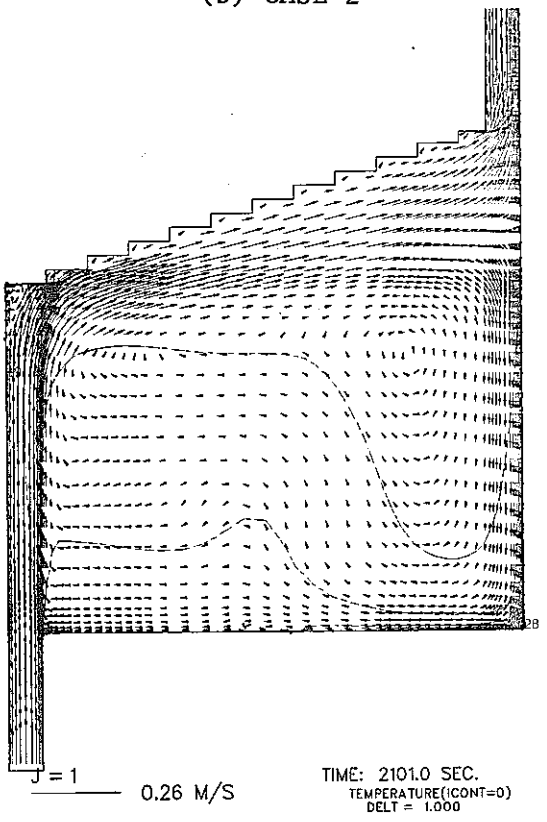

(d) CASE 4

Fig. 20 Iso-vector diagrams with default constants of the k & ε two-equation model

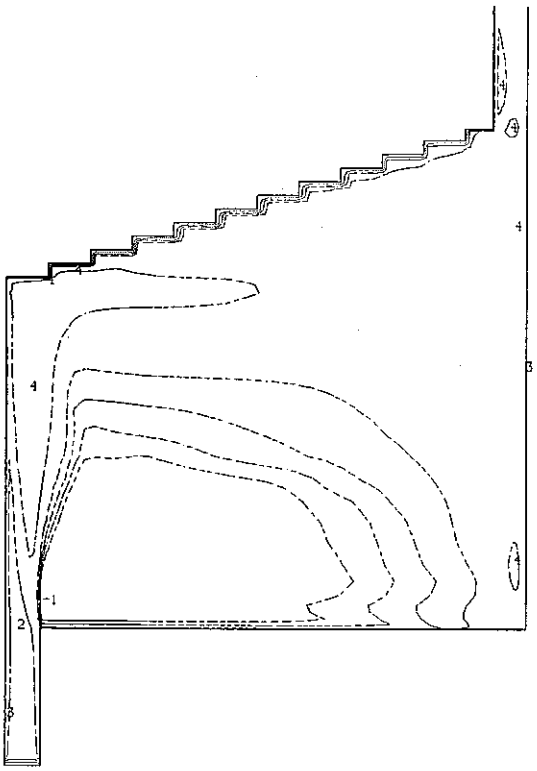

TIME: 9567.0 SEC. J = 1

(a) CASE 1

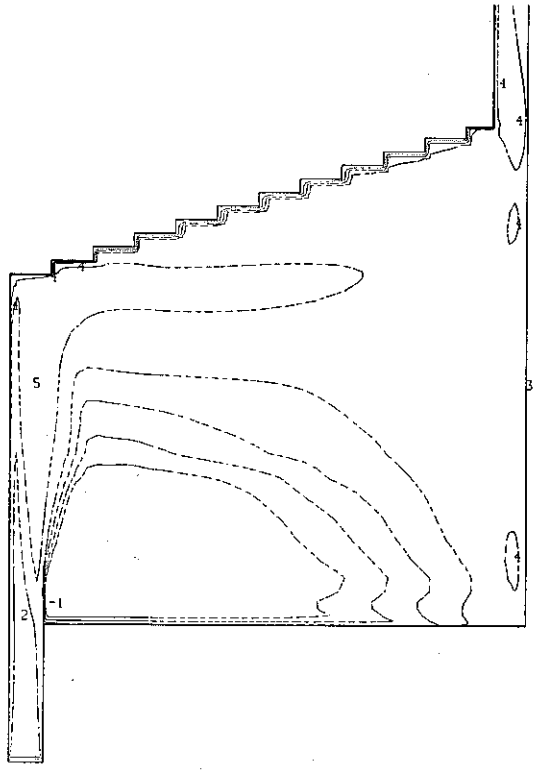

TIME: 8077.0 SEC. J = 1

(b) CASE 2

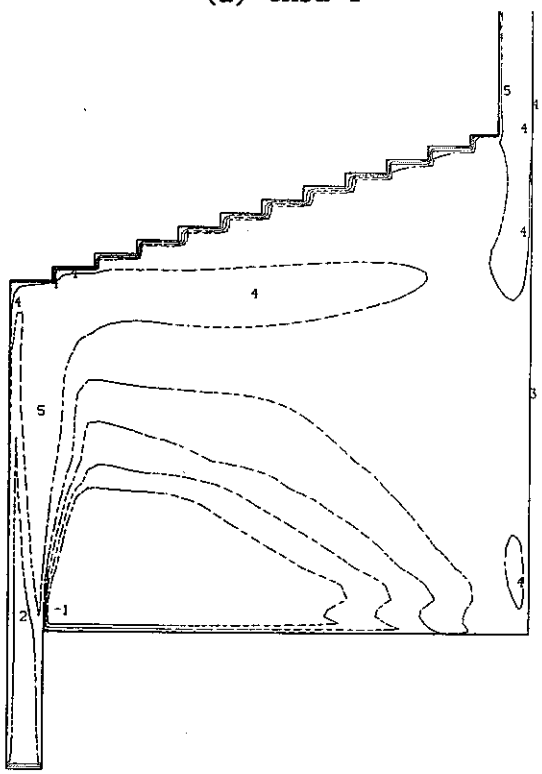

TIME: 4688.0 SEC. J = 1

(c) CASE 3

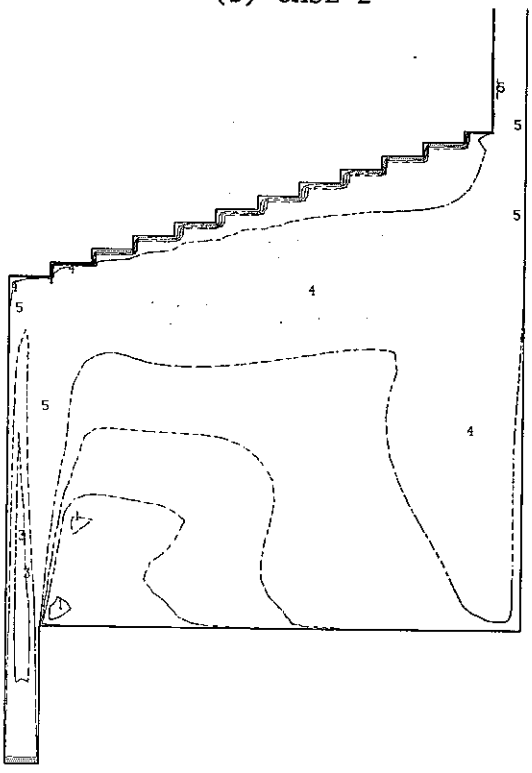

TIME: 2101.0 SEC. J = 1

(d) CASE 4

Fig. 21 Iso-k diagrams with default constants of the k & ε two-equation model

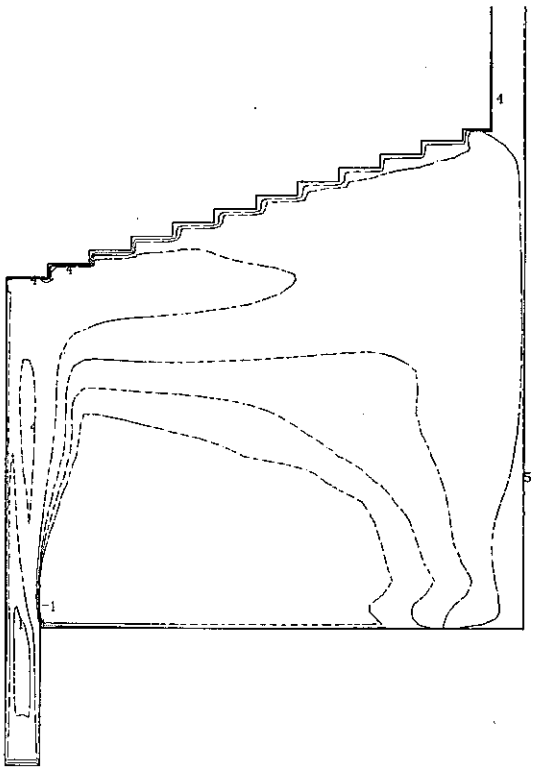

TIME: 9567.0 SEC. J = 1

(a) CASE 1

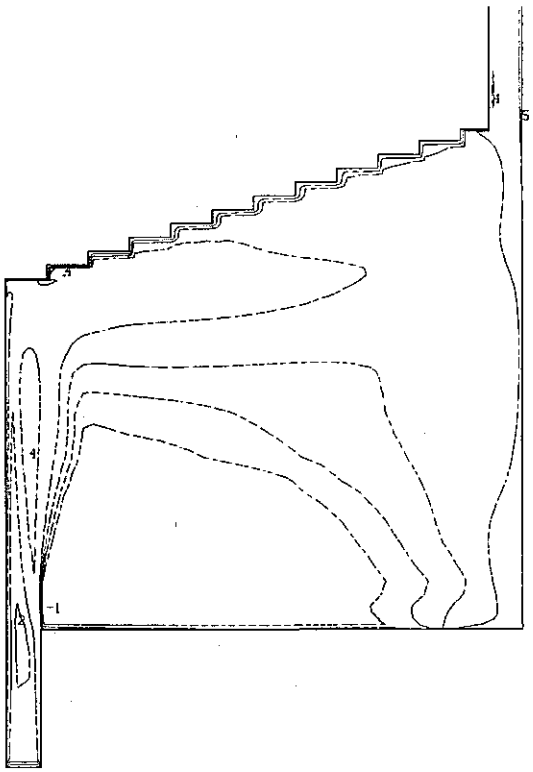

TIME: 8077.0 SEC. J = 1

(b) CASE 2

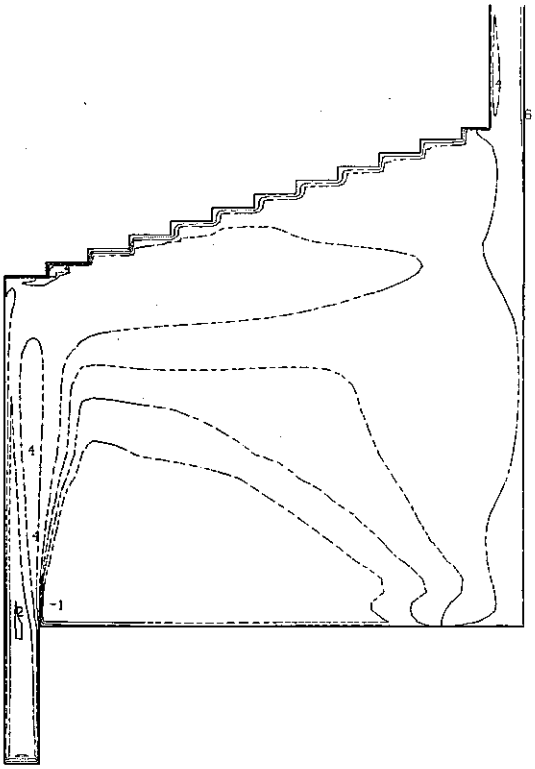

TIME: 4688.0 SEC. J = 1

(c) CASE 3

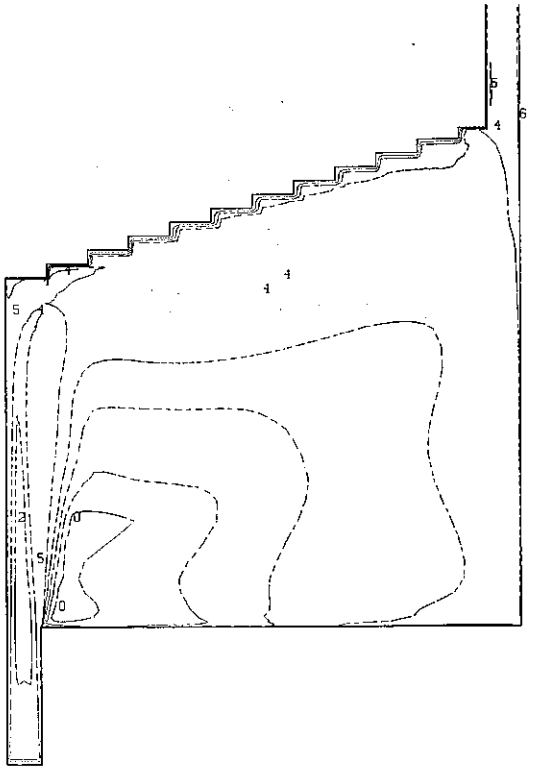

TIME: 2101.0 SEC. J = 1

(d) CASE 4

Fig. 22 Iso-ε diagrams with default constants of the k & ε two-equation model

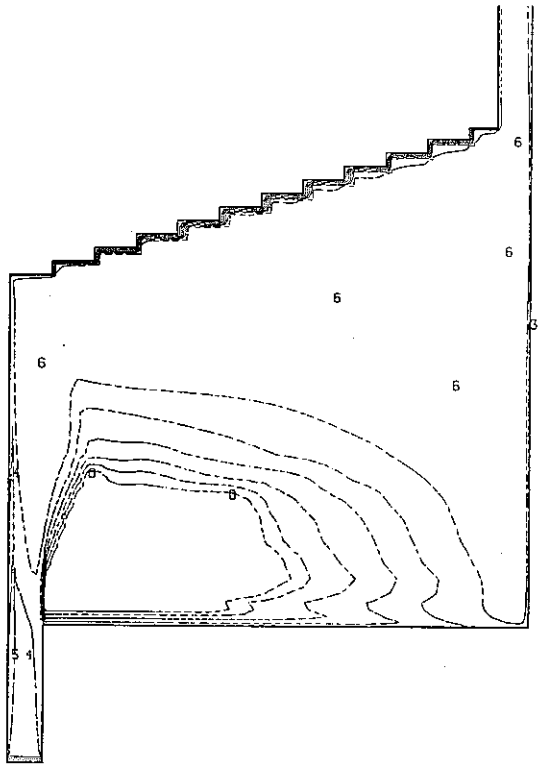

TIME: 9567.0 SEC. J = 1

(a) CASE 1

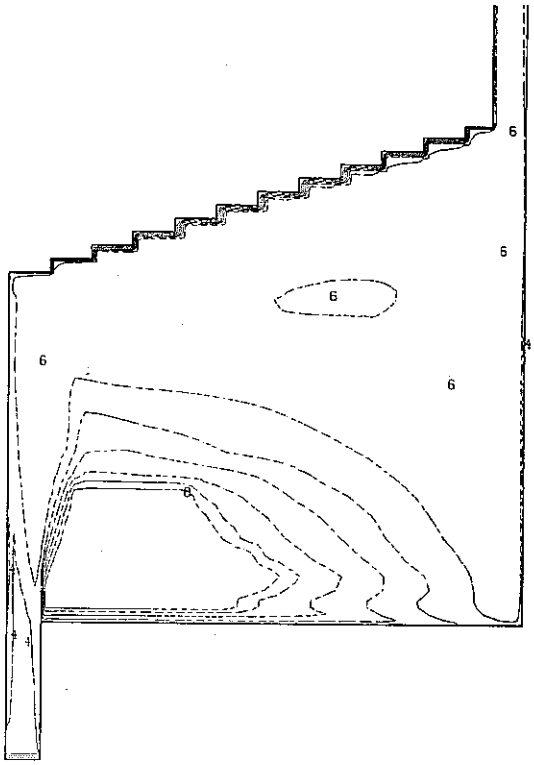

TIME: 8077.0 SEC. J = 1

(b) CASE 2

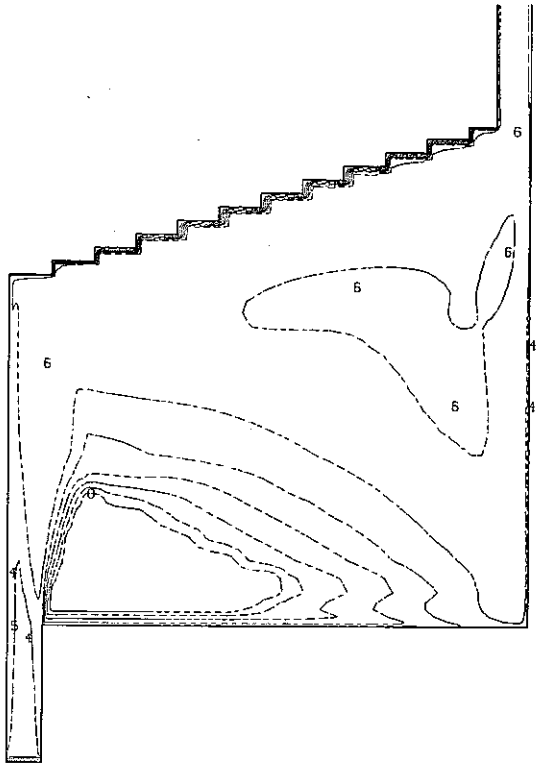

TIME: 4688.0 SEC. J = 1

(c) CASE 3

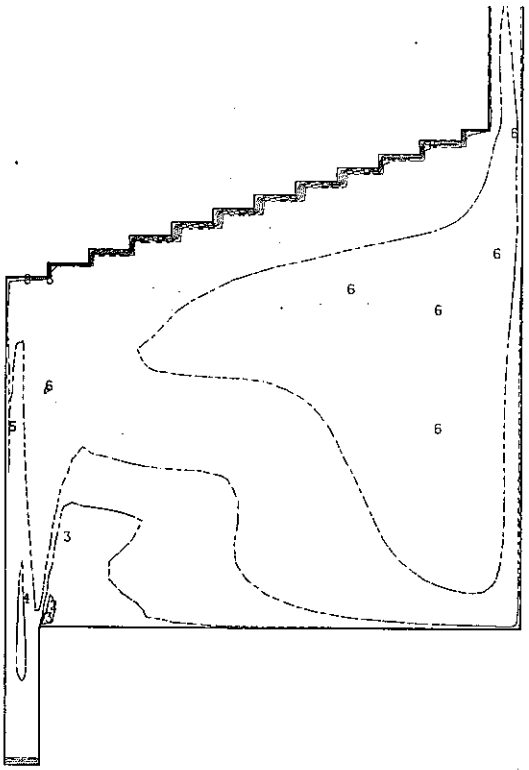

TIME: 2101.0 SEC. J = 1

(d) CASE 4

Fig. 23 Iso-μ_t diagrams with default constants of the k & ε two-equation model

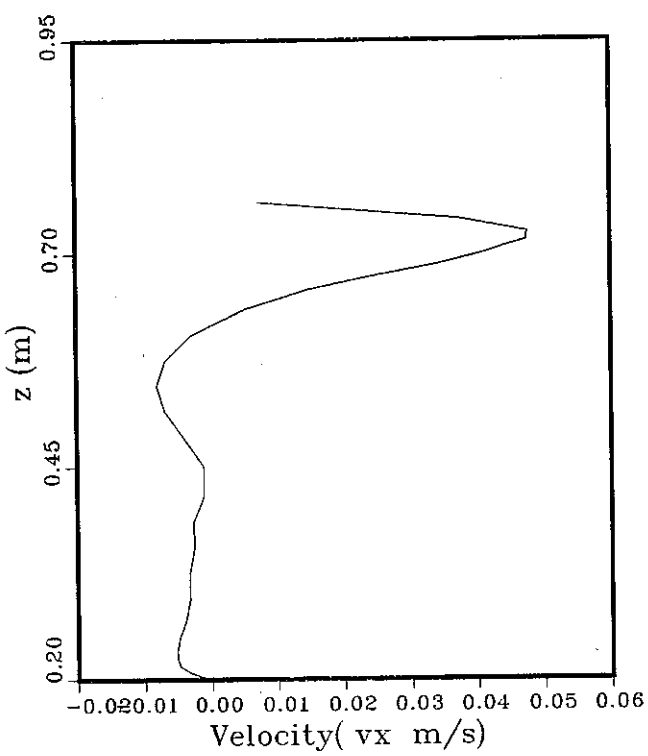

(a) CASE 1

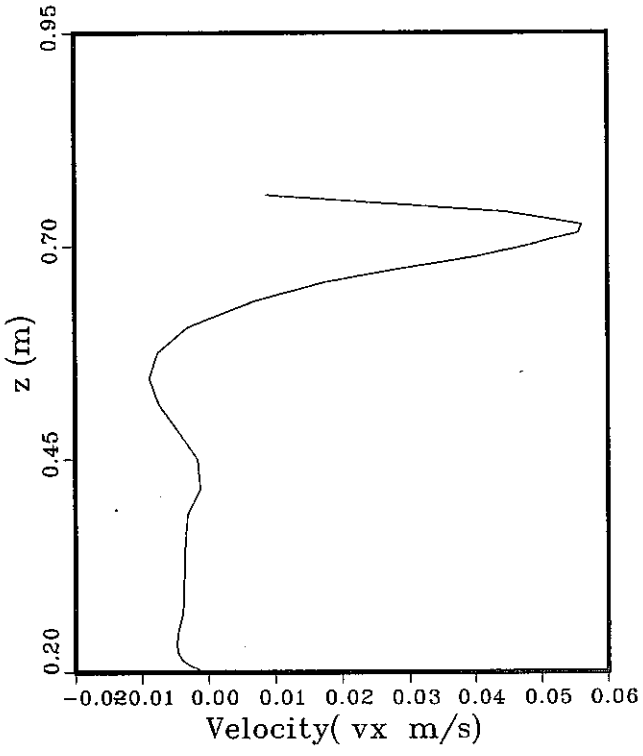

(b) CASE 2

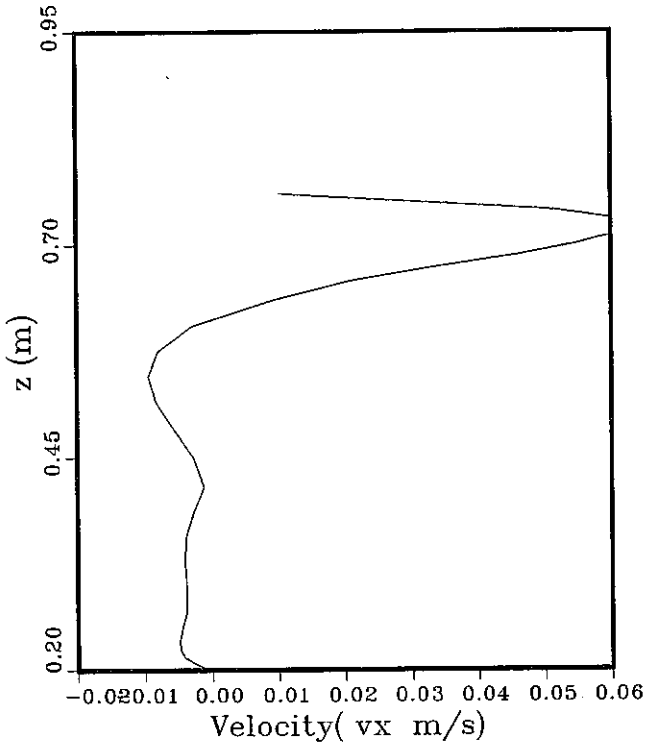

(c) CASE 3

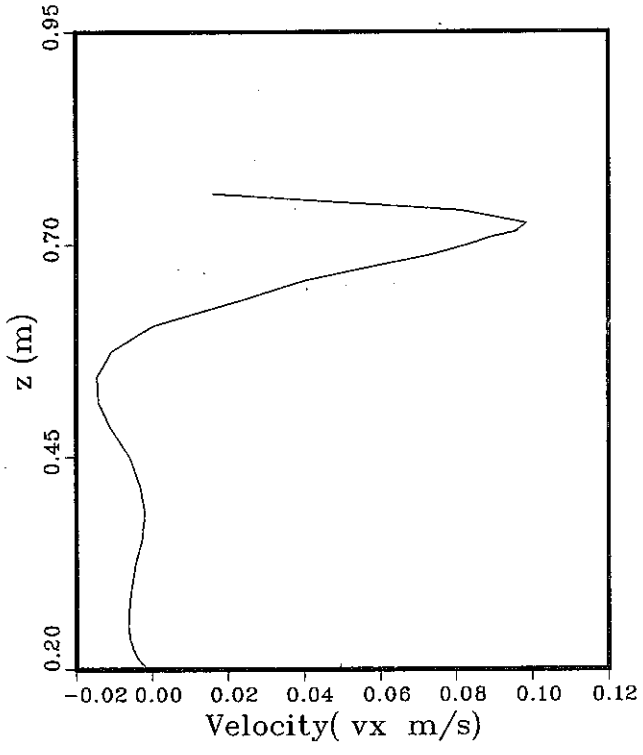

(d) CASE 4

Fig. 24 Velocity distribution on P1 with default constants of the k & ε two-equation model

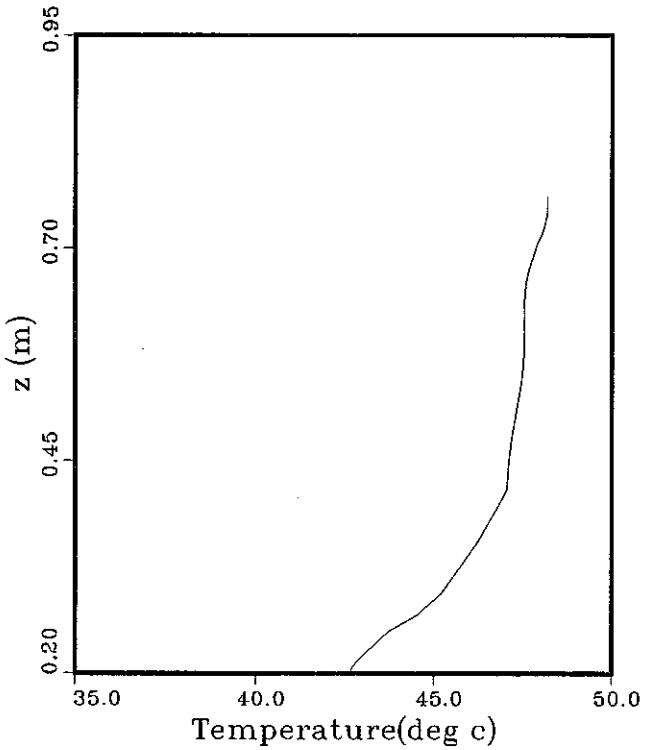

(a) CASE 1

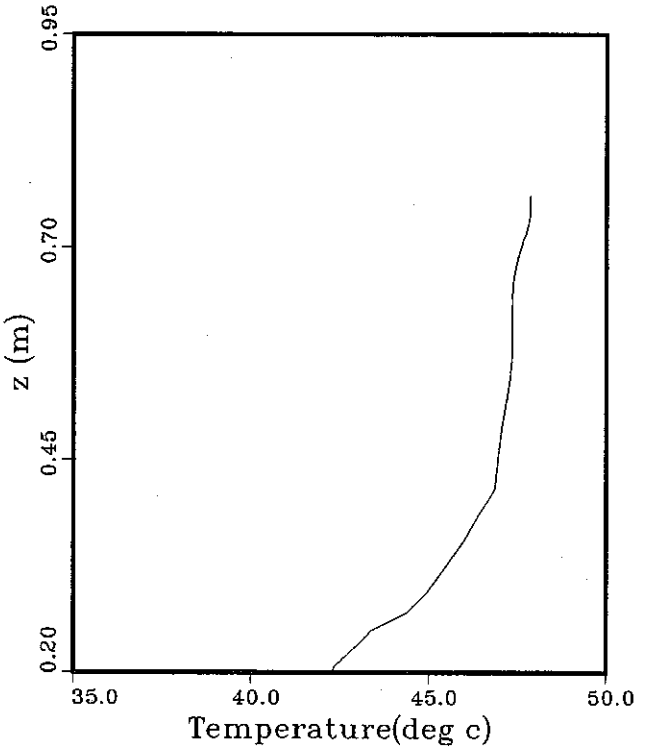

(b) CASE 2

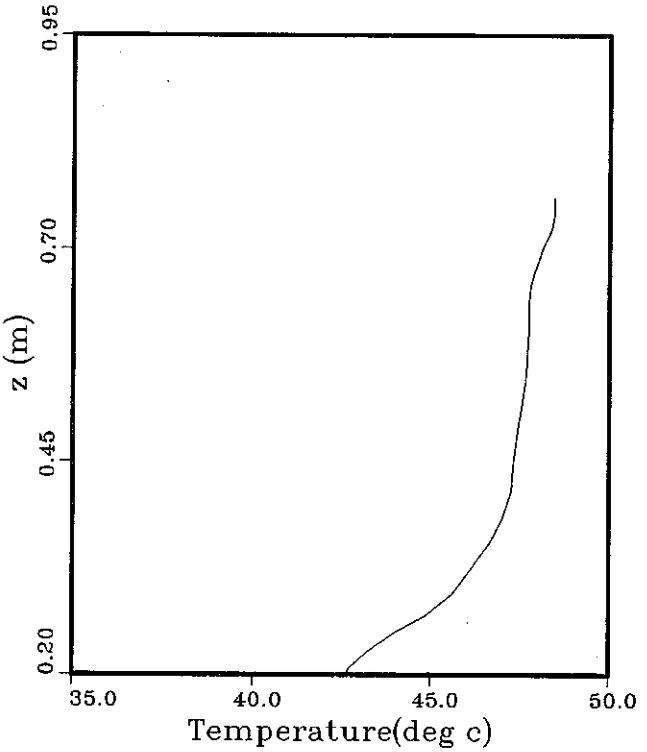

(c) CASE 3

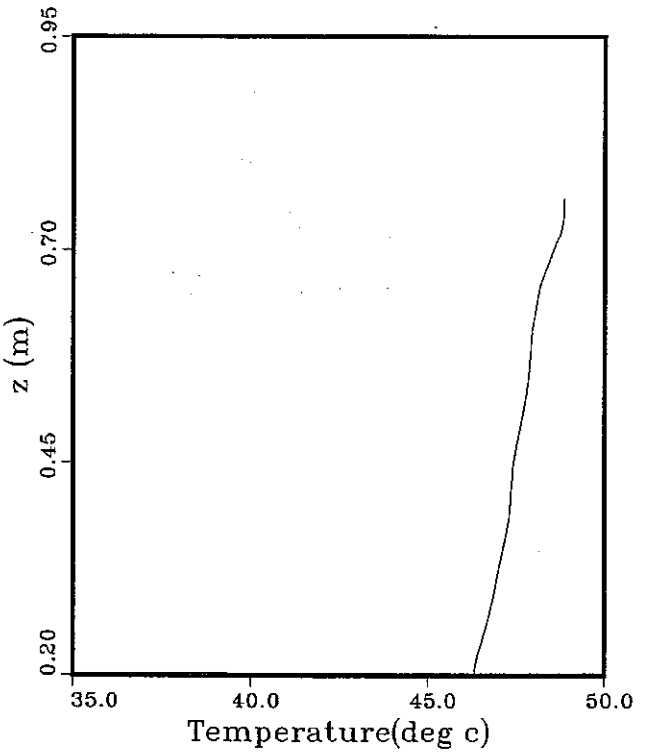

(d) CASE 4

Fig. 25 Temperature distribution on P1 with default constants of the k & ε two-equation model

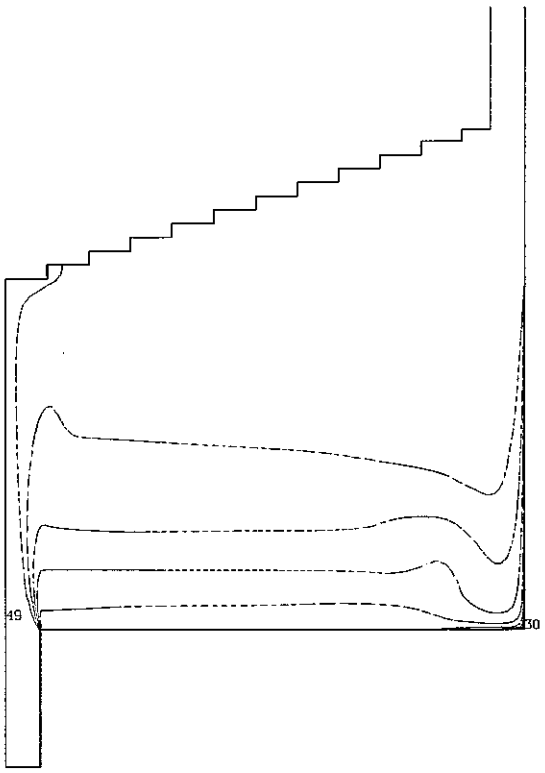

TIME: 7871.0 SEC. J = 1

(a) CASE 1

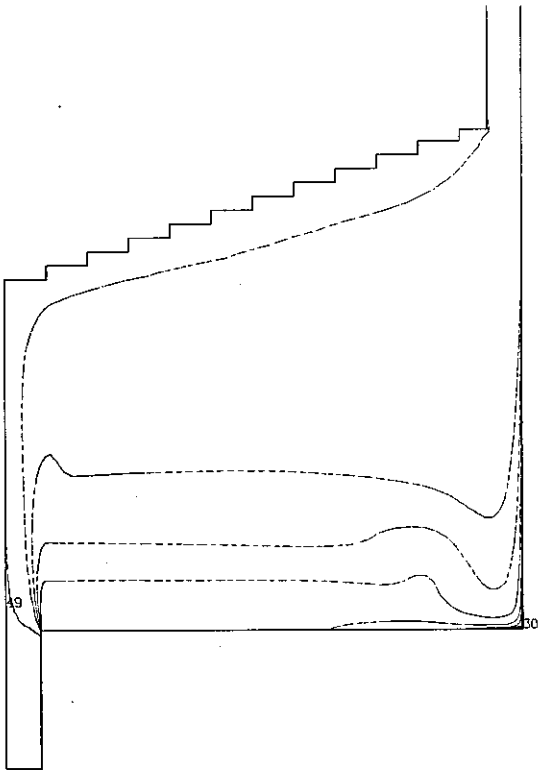

TIME: 7948.0 SEC. J = 1

(b) CASE 2

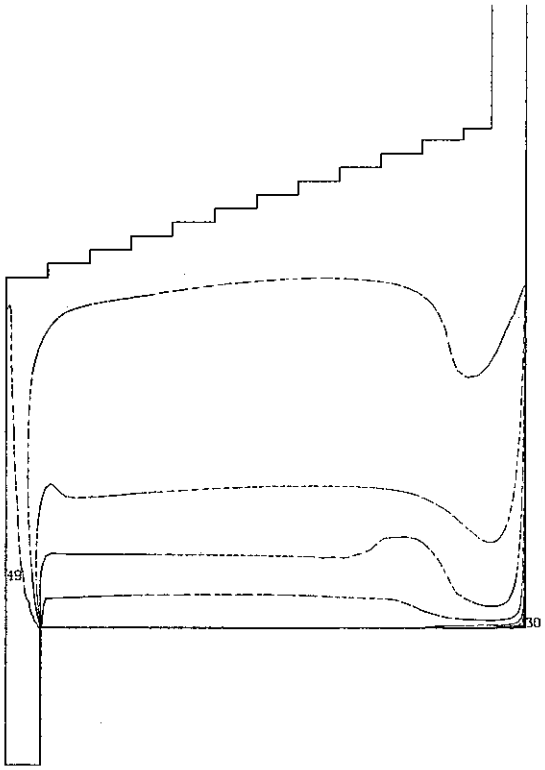

TIME: 4360.0 SEC. J = 1

(c) CASE 3

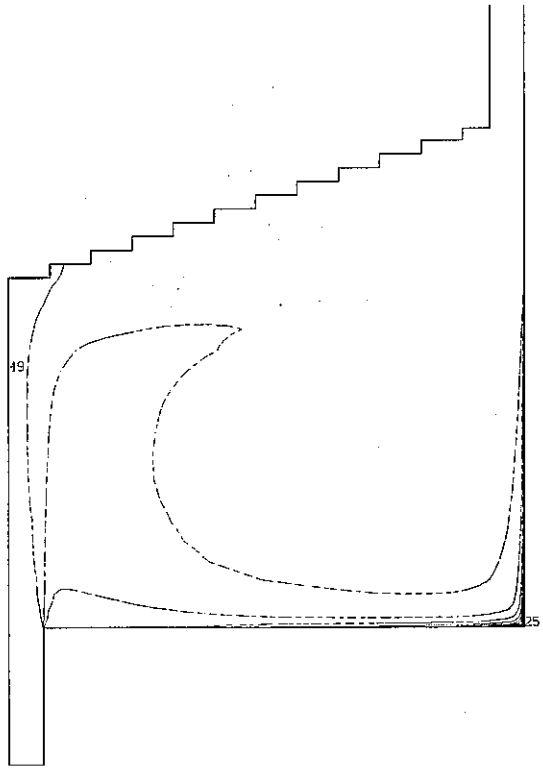

TIME: 6328.0 SEC. J = 1

(d) CASE 4

Fig. 26 Iso-temperature diagrams with default constants of the algebraic stress / flux model

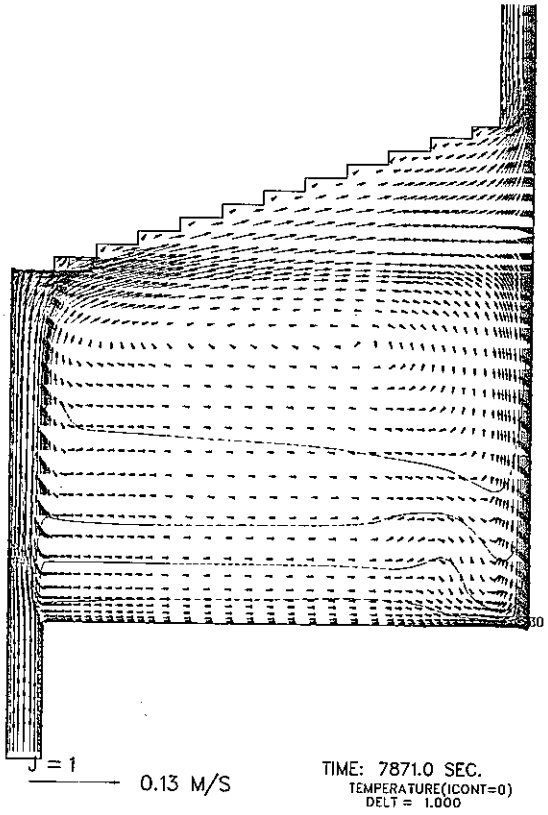

(a) CASE 1

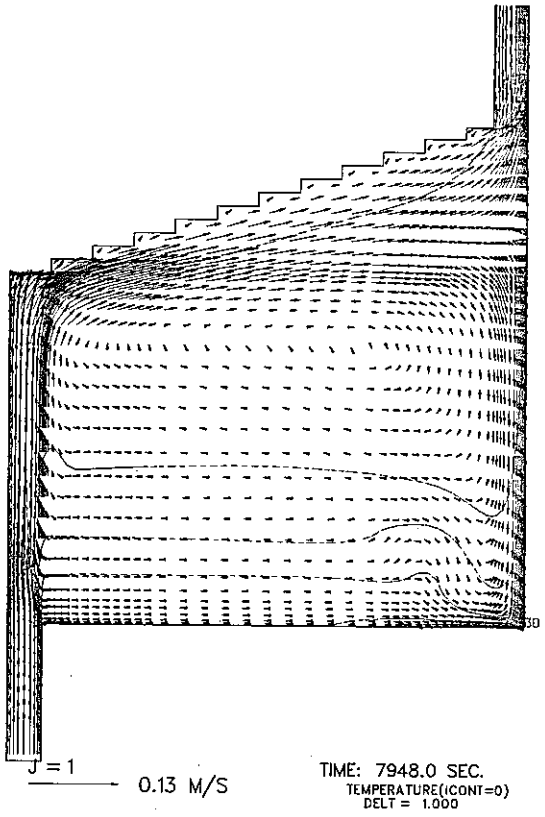

(b) CASE 2

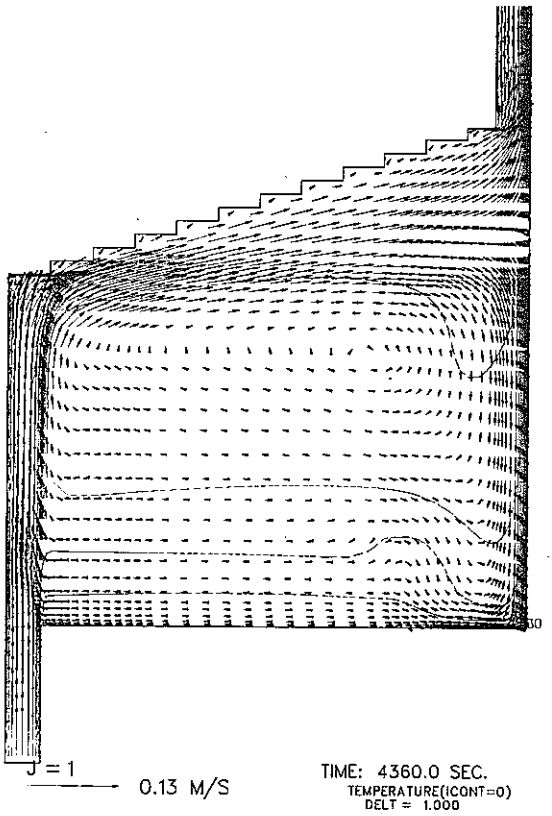

(c) CASE 3

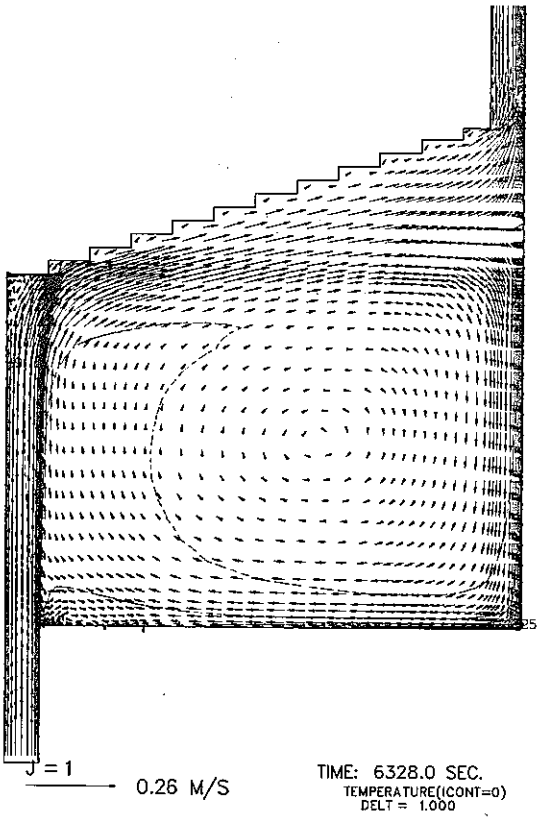

(d) CASE 4

Fig. 27 Iso-vector diagrams with default constants of the algebraic stress / flux model

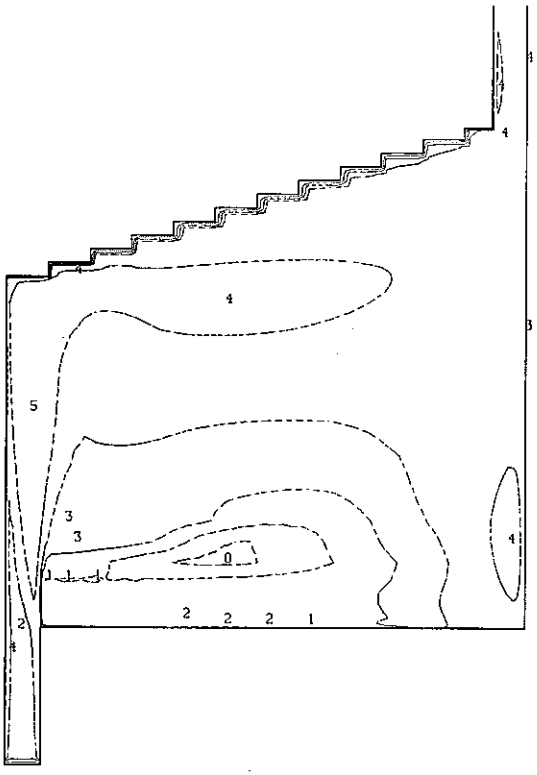

TIME: 7871.0 SEC. J = 1

(a) CASE 1

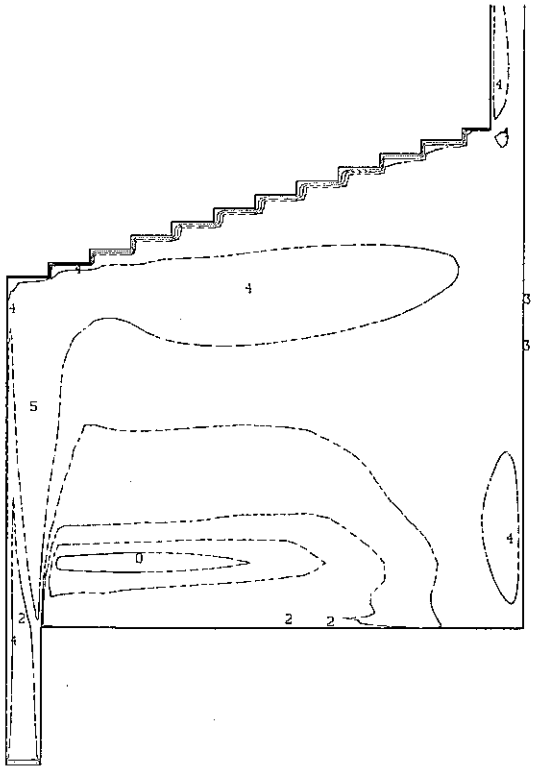

TIME: 7948.0 SEC. J = 1

(b) CASE 2

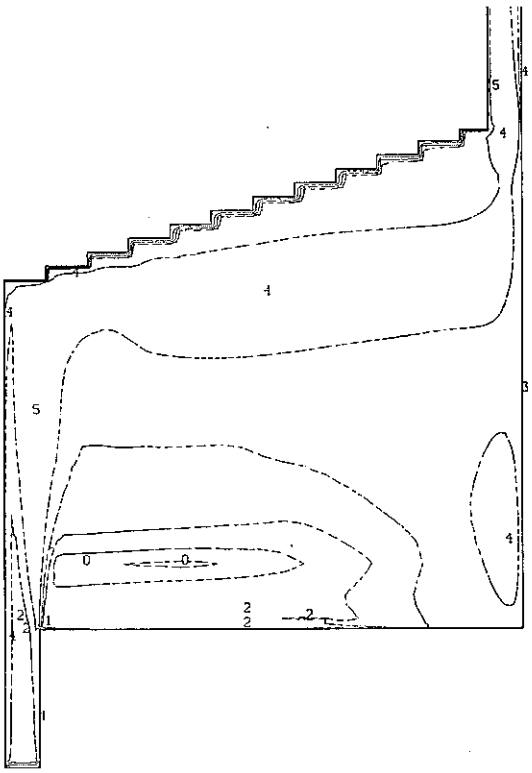

TIME: 4360.0 SEC. J = 1

(c) CASE 3

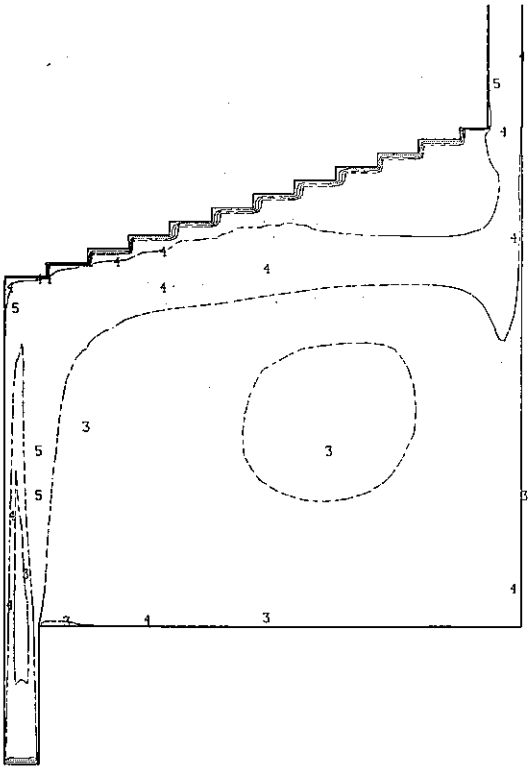

TIME: 6328.0 SEC. J = 1

(d) CASE 4

Fig. 28 Iso-k diagrams with default constants of the algebraic stress / flux model

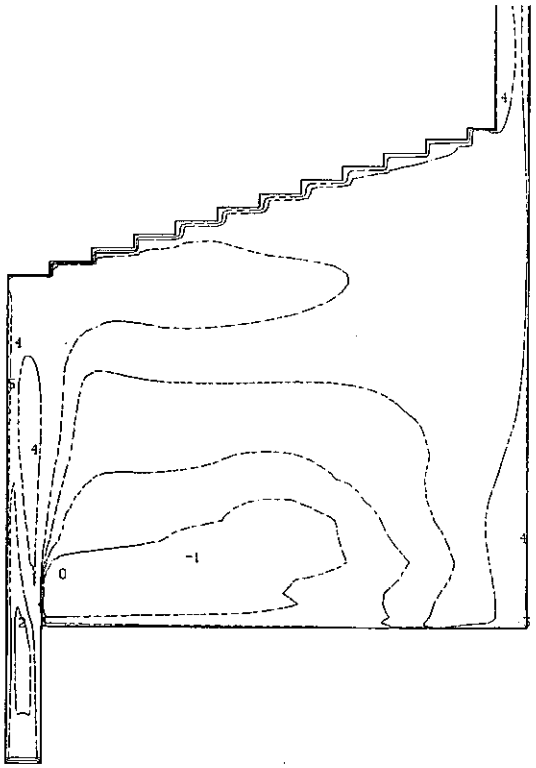

TIME: 7871.0 SEC. J = 1

(a) CASE 1

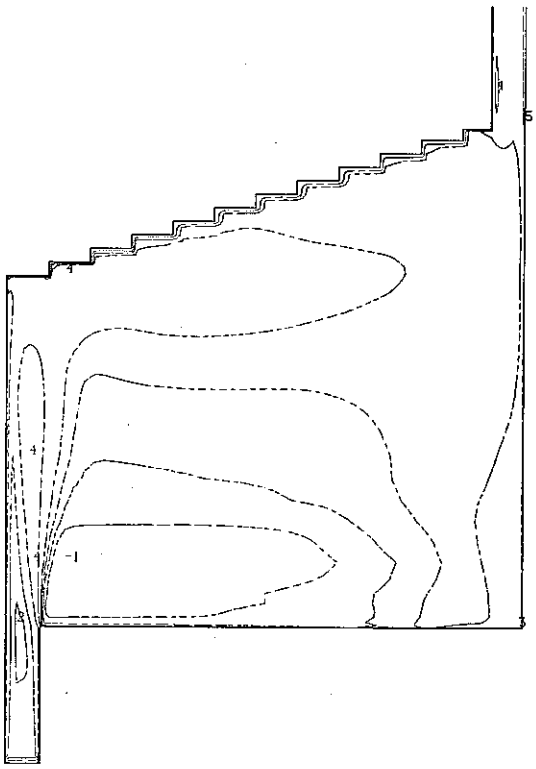

TIME: 7948.0 SEC. J = 1

(b) CASE 2

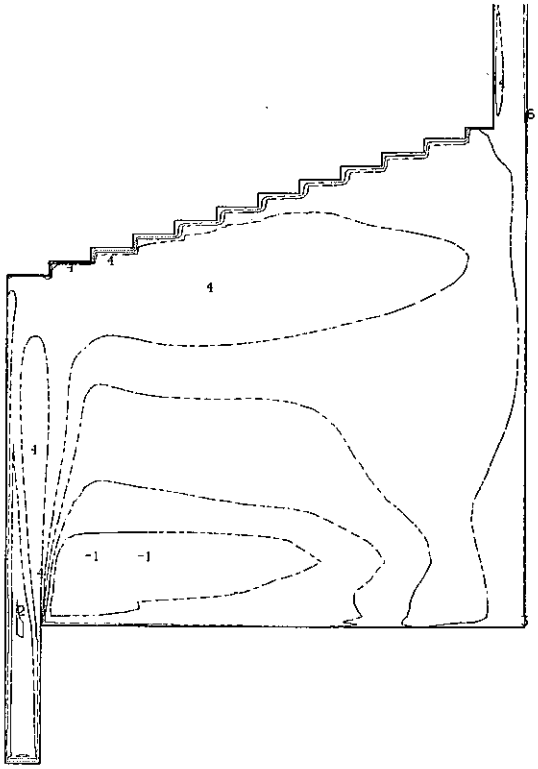

TIME: 4360.0 SEC. J = 1

(c) CASE 3

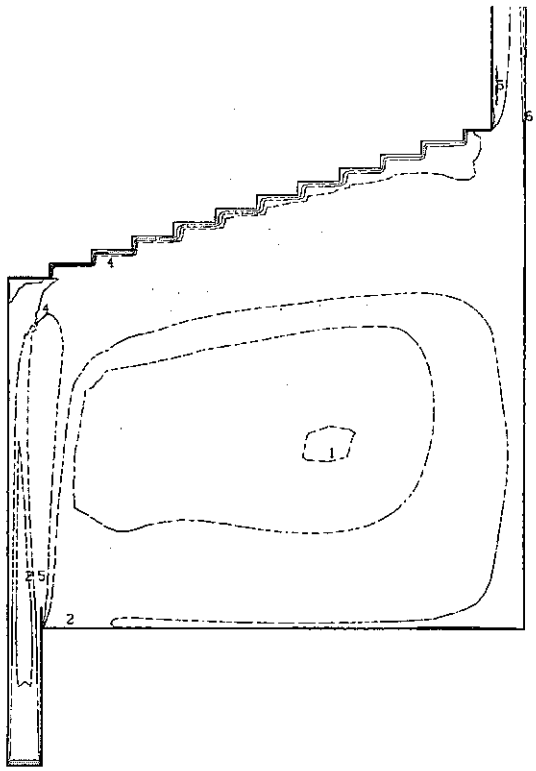

TIME: 6328.0 SEC. J = 1

(d) CASE 4

Fig. 29 Iso-ε diagrams with default constants of the algebraic stress / flux model

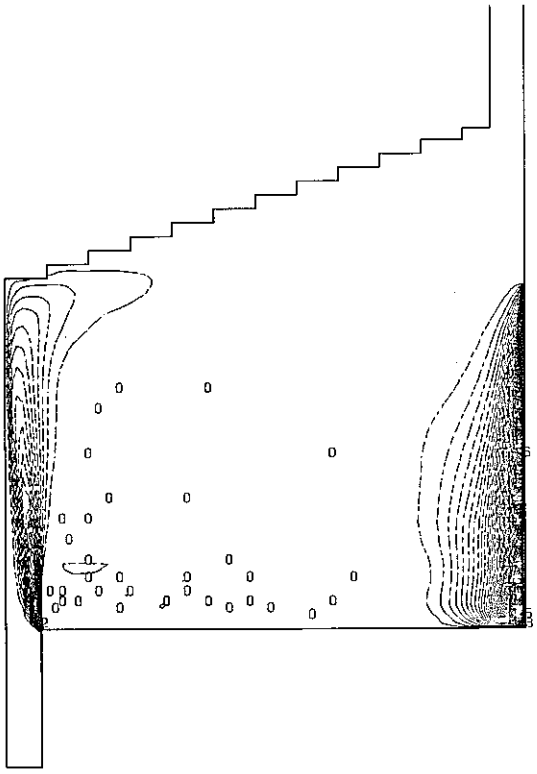

TIME: 7871.0 SEC. J = 1

(a) CASE 1

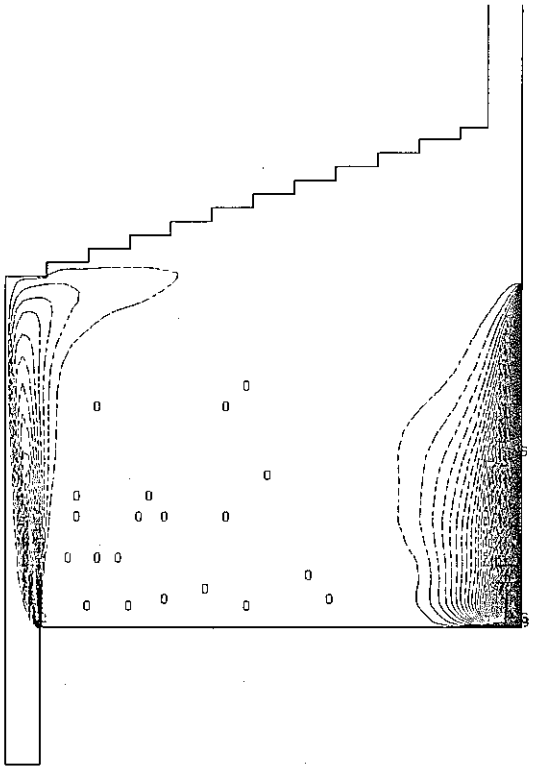

TIME: 7948.0 SEC. J = 1

(b) CASE 2

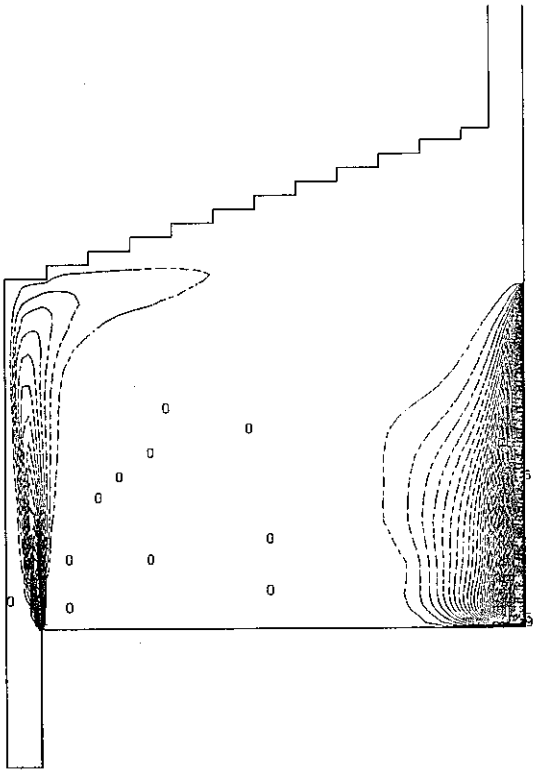

TIME: 4360.0 SEC. J = 1

(c) CASE 3

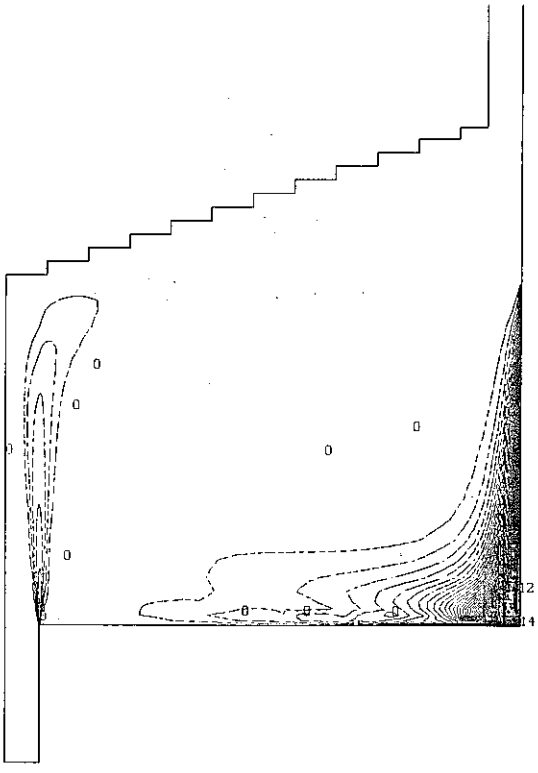

TIME: 6328.0 SEC. J = 1

(d) CASE 4

Fig. 30 Temperature fluctuation diagrams with default constants of the algebraic stress / flux model

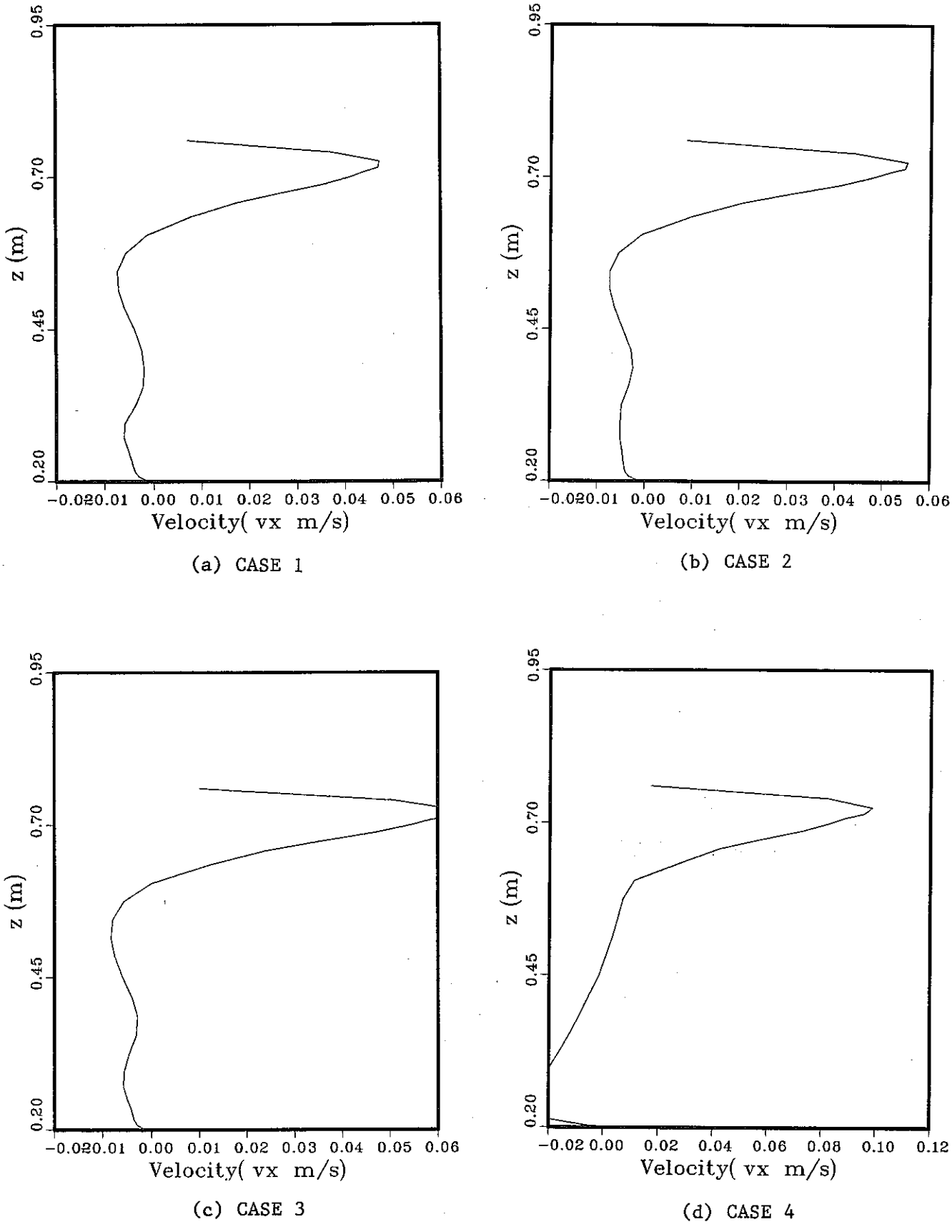

Fig. 31 Velocity distribution on P1 with default constants of the algebraic stress / flux model

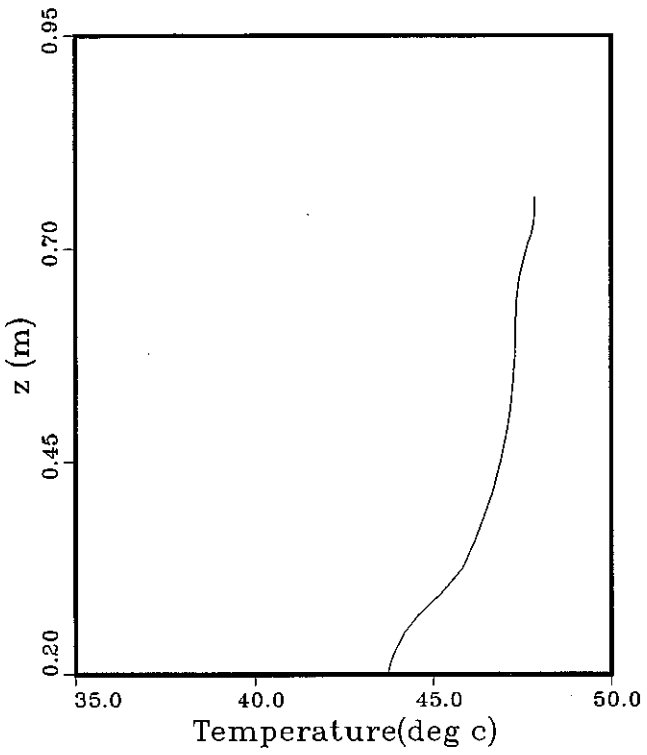

(a) CASE 1

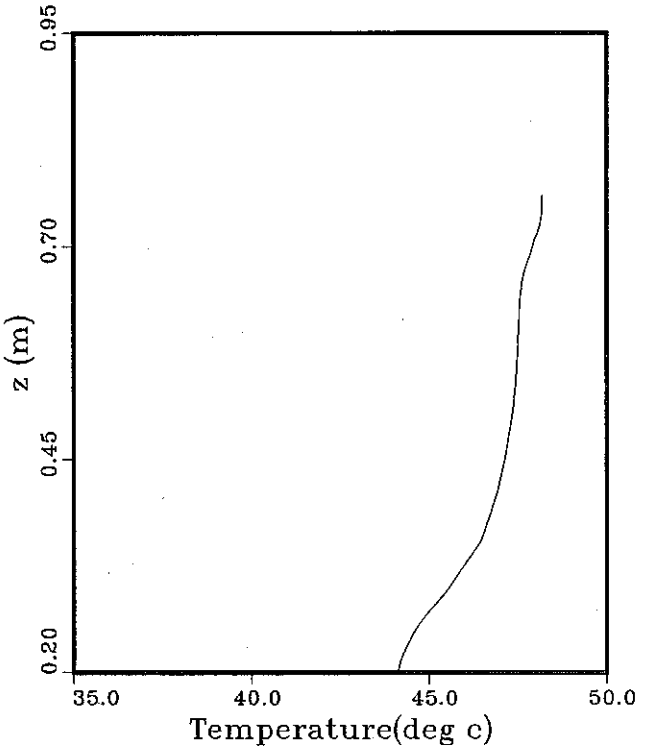

(b) CASE 2

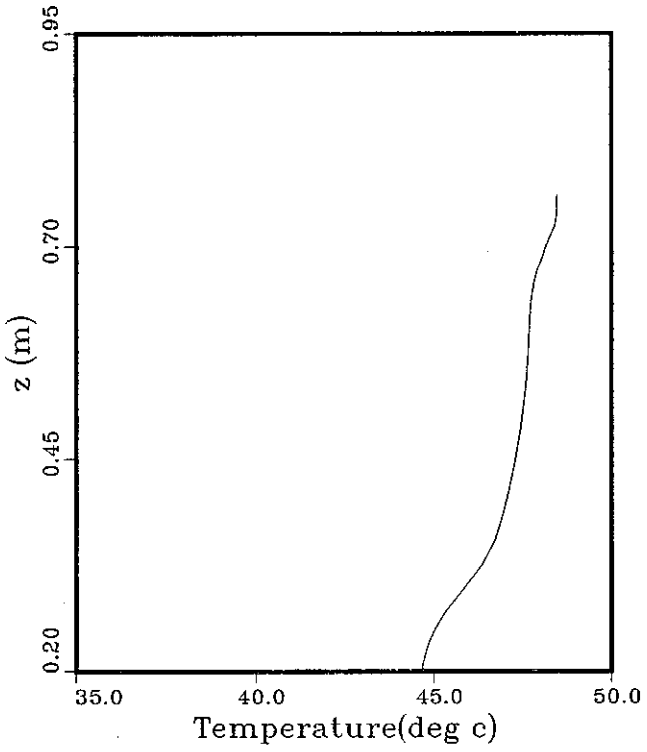

(c) CASE 3

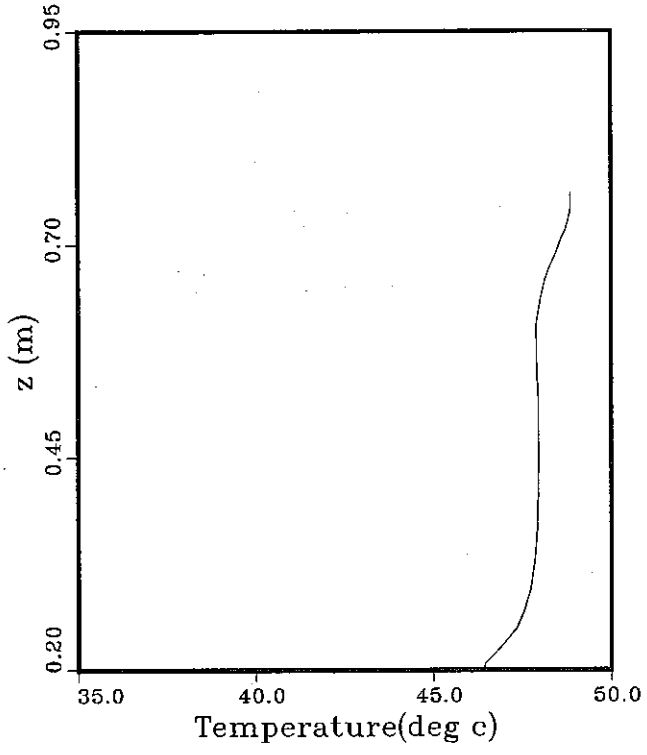

(d) CASE 4

Fig. 32 Temperature distribution on P1 with default constants of the algebraic stress / flux model

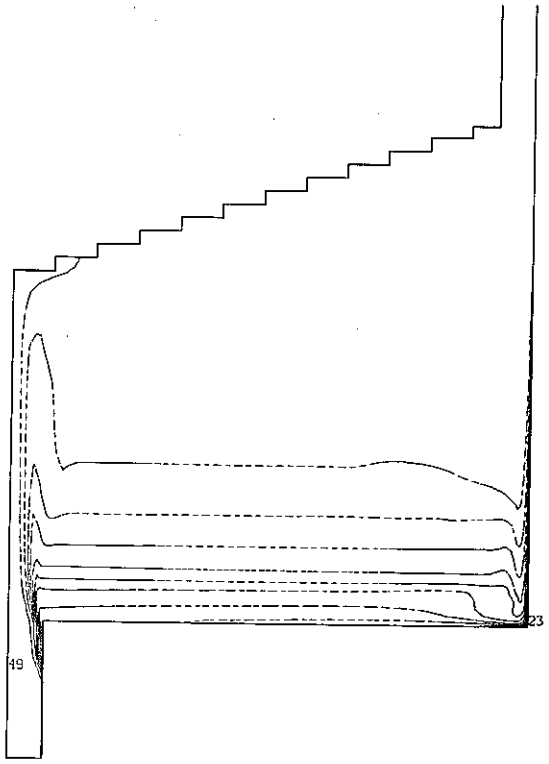

TIME: 4162.0 SEC. J = 1

(a) CASE 1

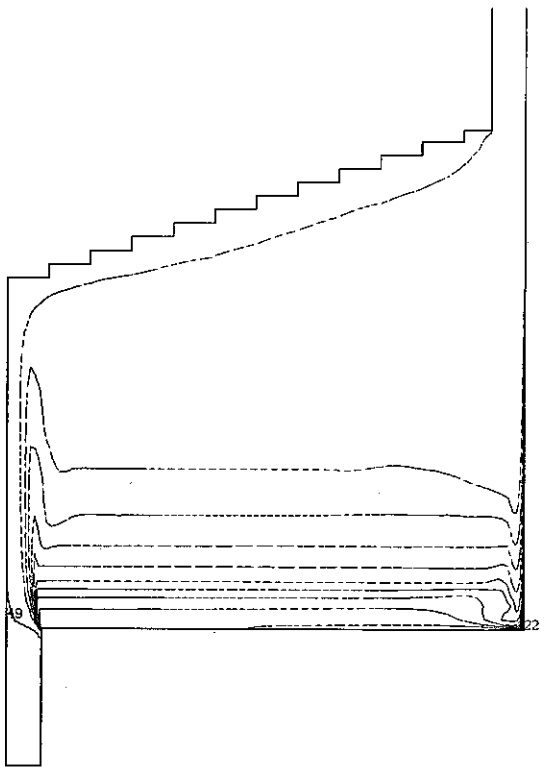

TIME: 6867.0 SEC. J = 1

(b) CASE 2

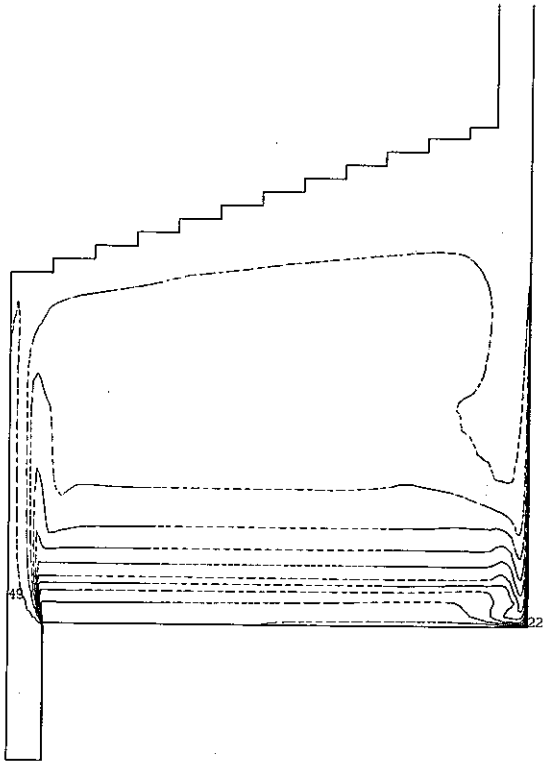

TIME: 7446.0 SEC. J = 1

(c) CASE 3

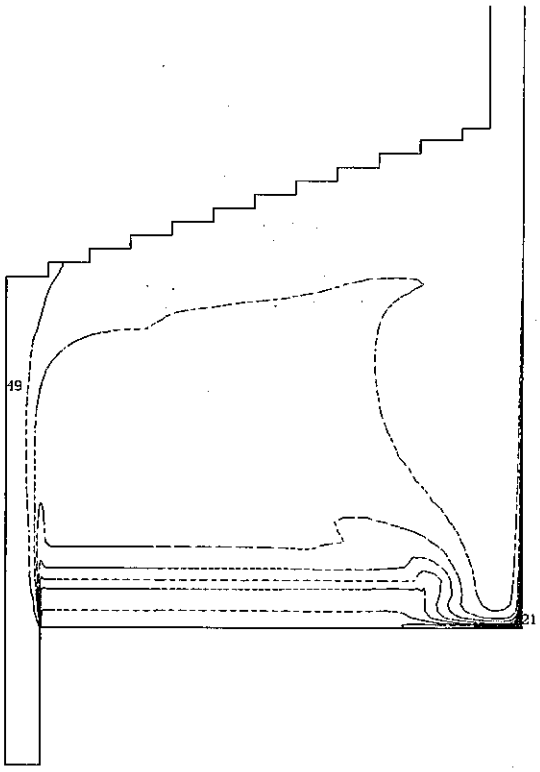

TIME: 6188.0 SEC. J = 1

(d) CASE 4

Fig. 33 Iso-temperature diagrams with C_1 = 1.656 of the k & ε two-equation model

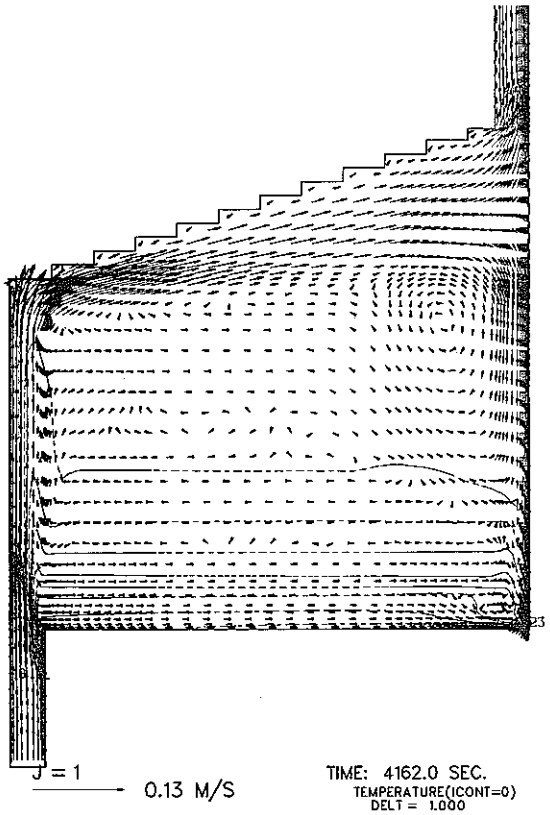

(a) CASE 1

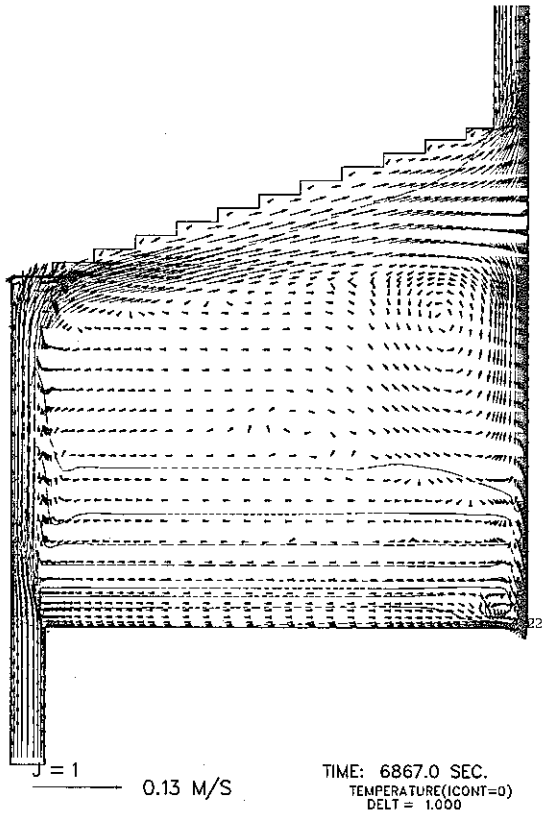

(b) CASE 2

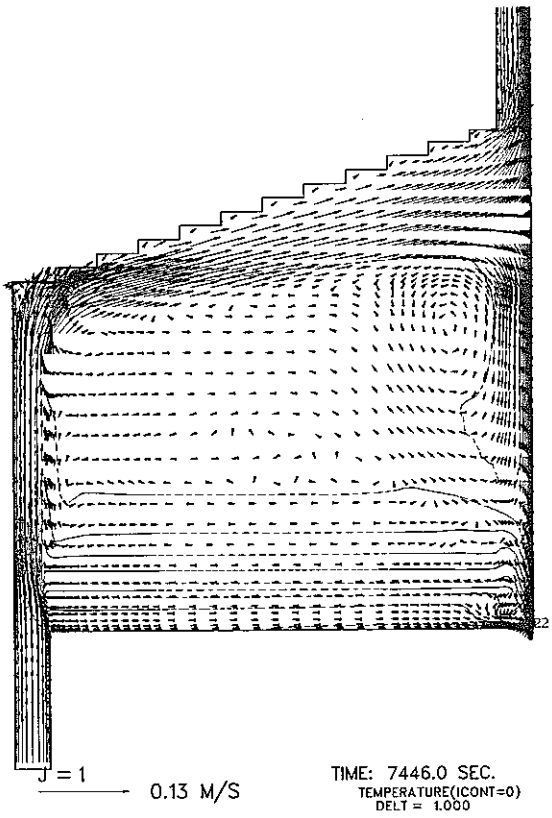

(c) CASE 3

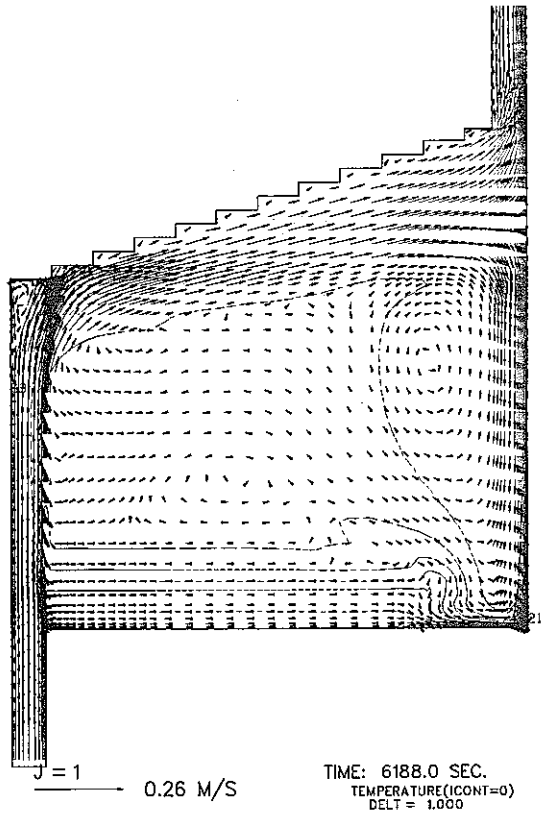

(d) CASE 4

Fig. 34 Iso-vector diagrams with C_1 = 1.656 of the k & ε two-equation model

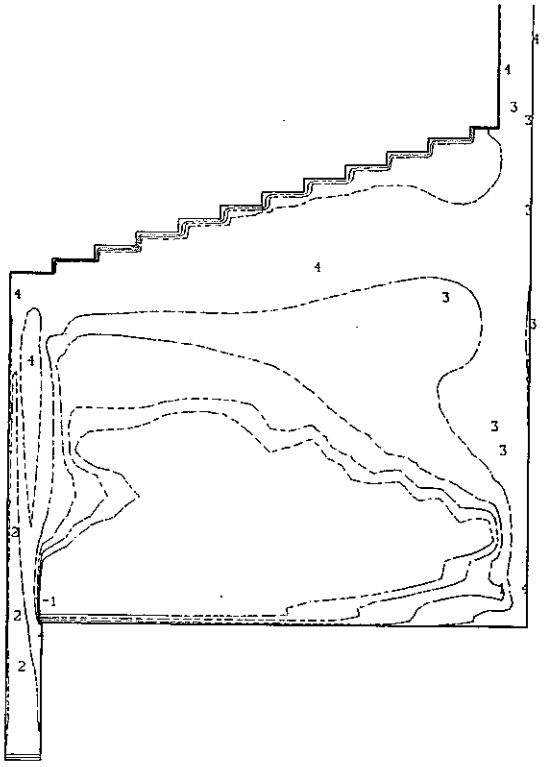

(a) CASE 1

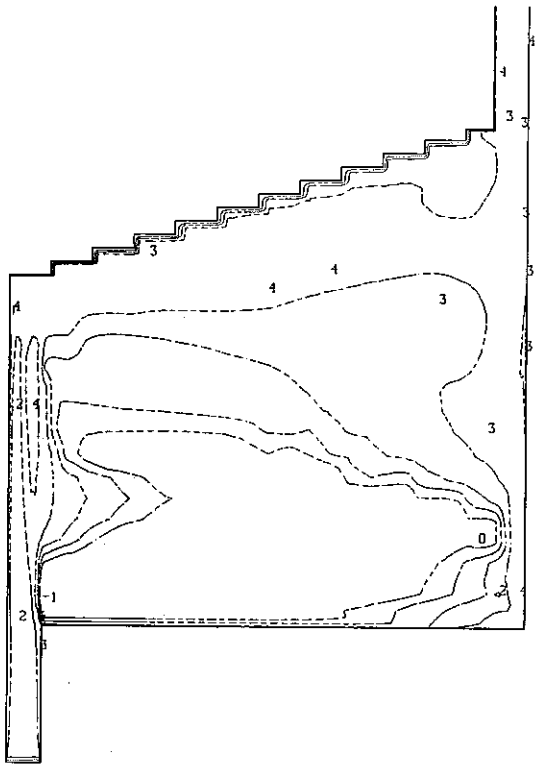

(b) CASE 2

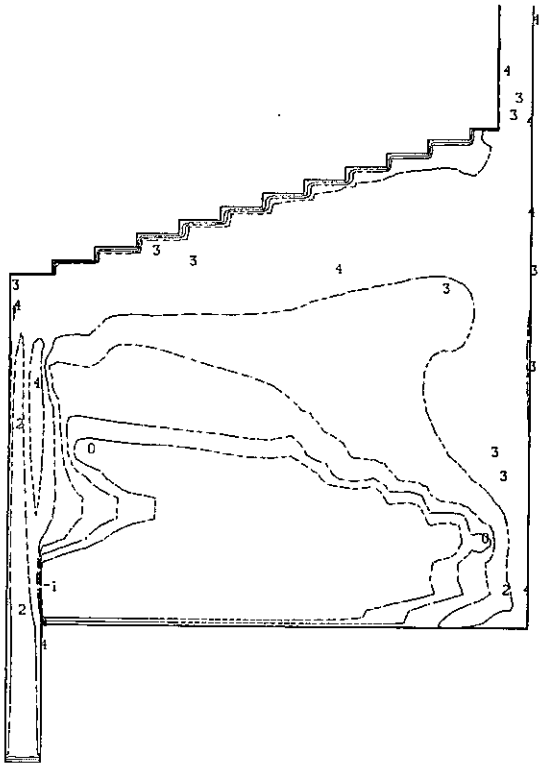

(c) CASE 3

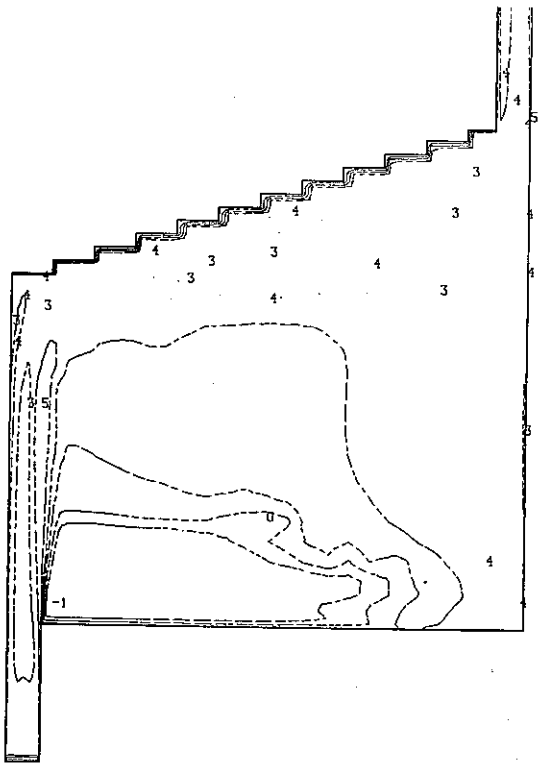

(d) CASE 4

Fig. 35 Iso-k diagrams with C_1 = 1.656 of the k & ε two-equation model

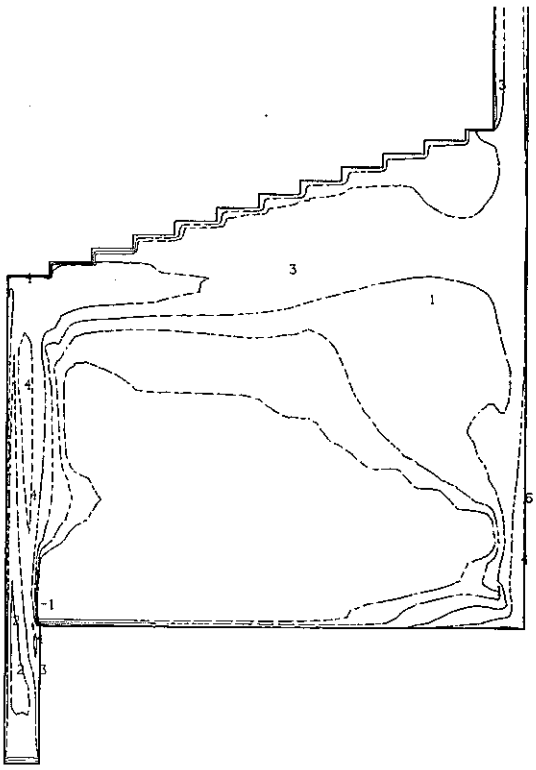

(a) CASE 1

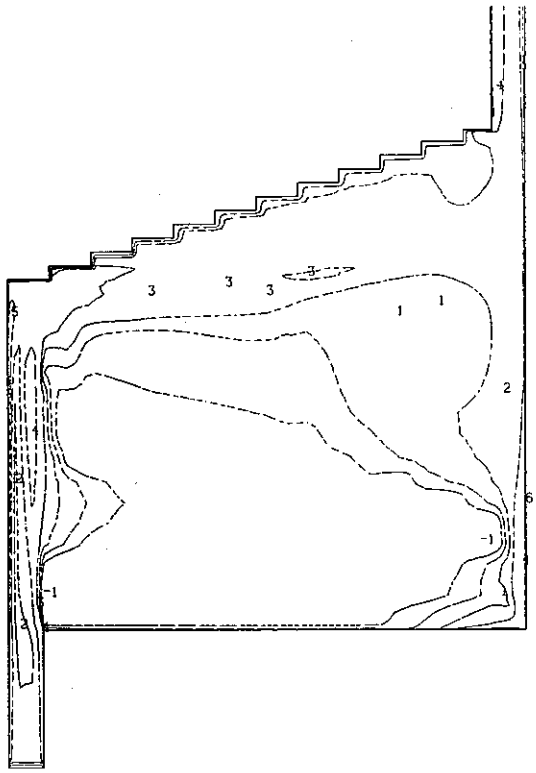

(b) CASE 2

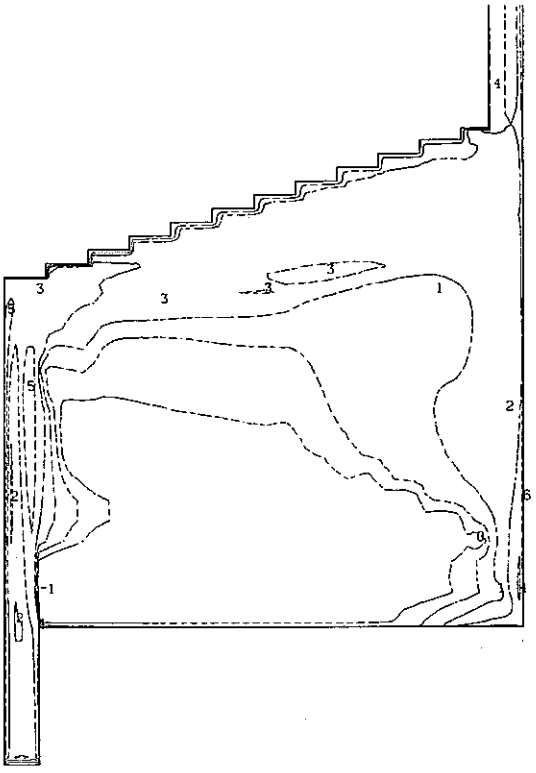

(c) CASE 3

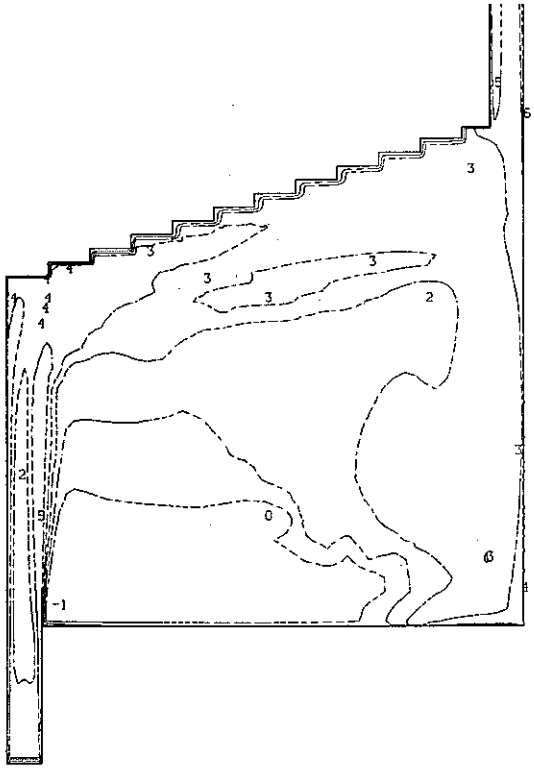

(d) CASE 4

Fig. 36 Iso-ε diagrams with C_1 = 1.656 of the k & ε two-equation model

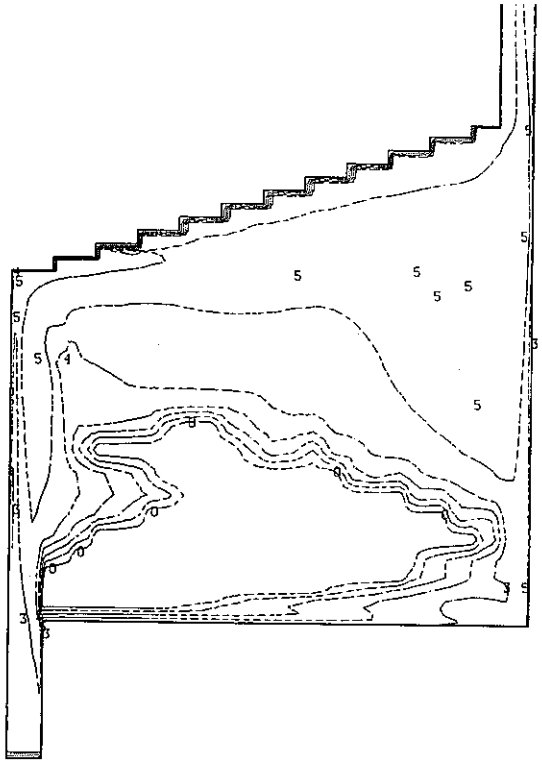

(a) CASE 1

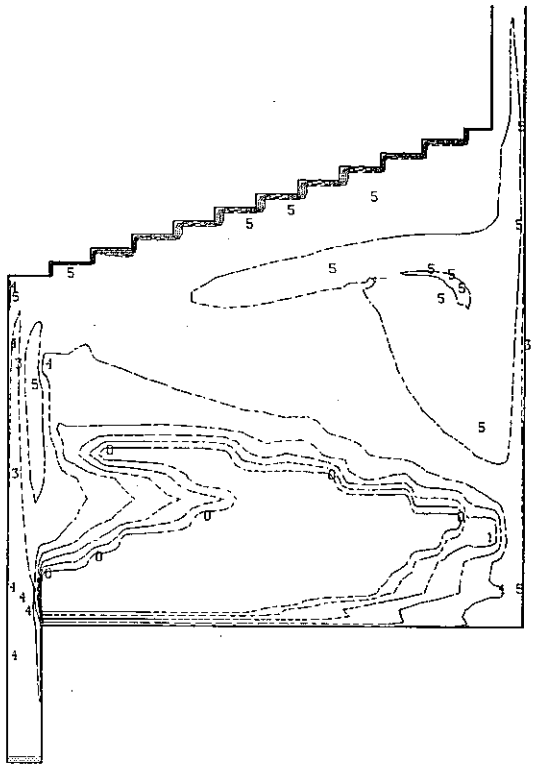

(b) CASE 2

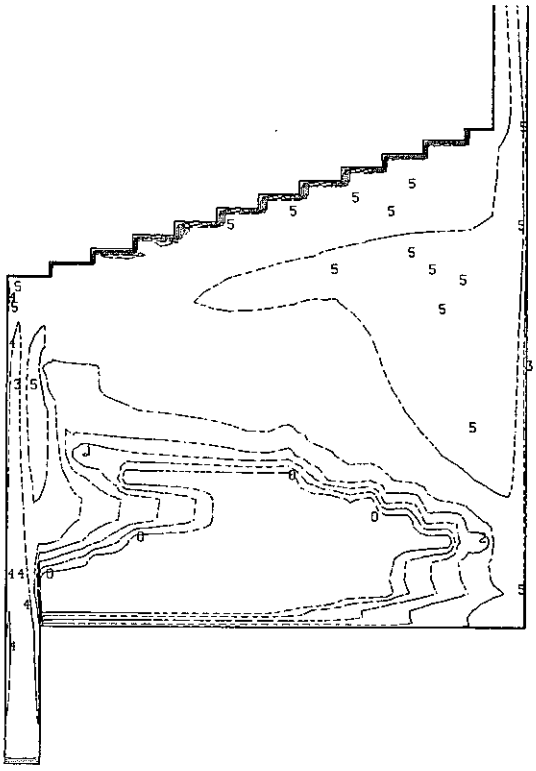

(c) CASE 3

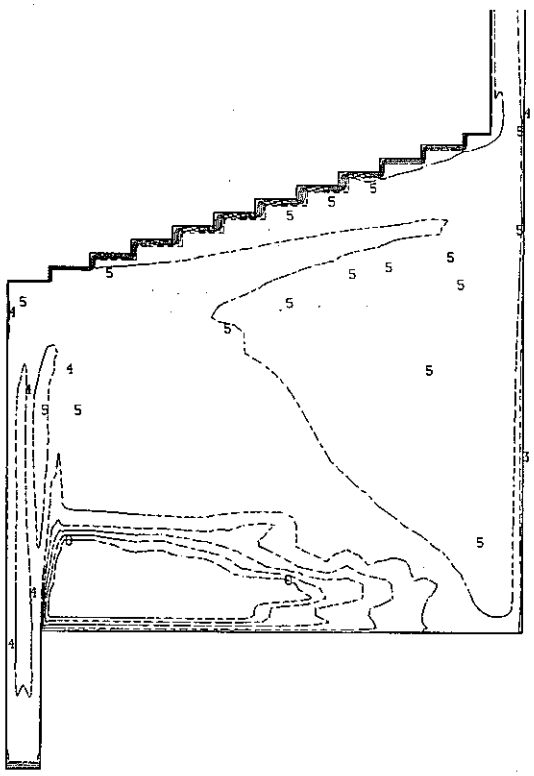

(d) CASE 4

Fig. 37 Iso-μ_t diagrams with C_1 = 1.656 of the k & ε two-equation model

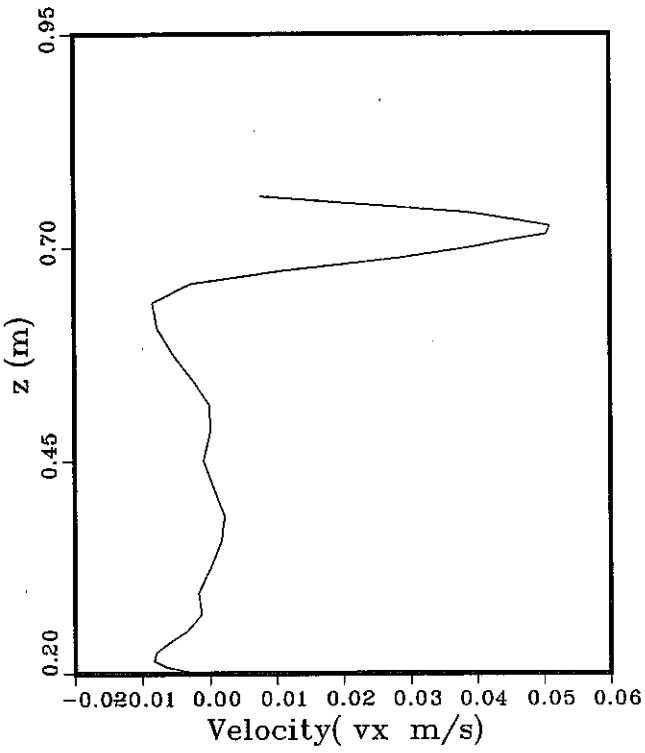

(a) CASE 1

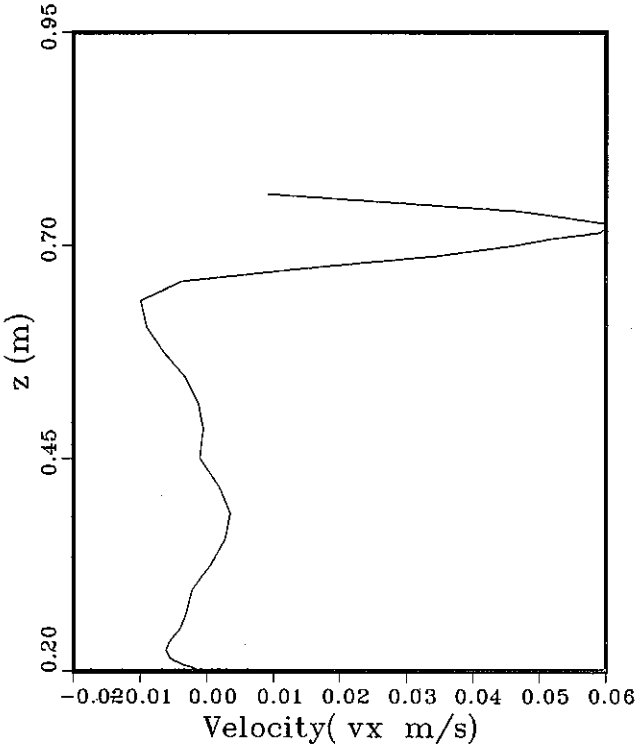

(b) CASE 2

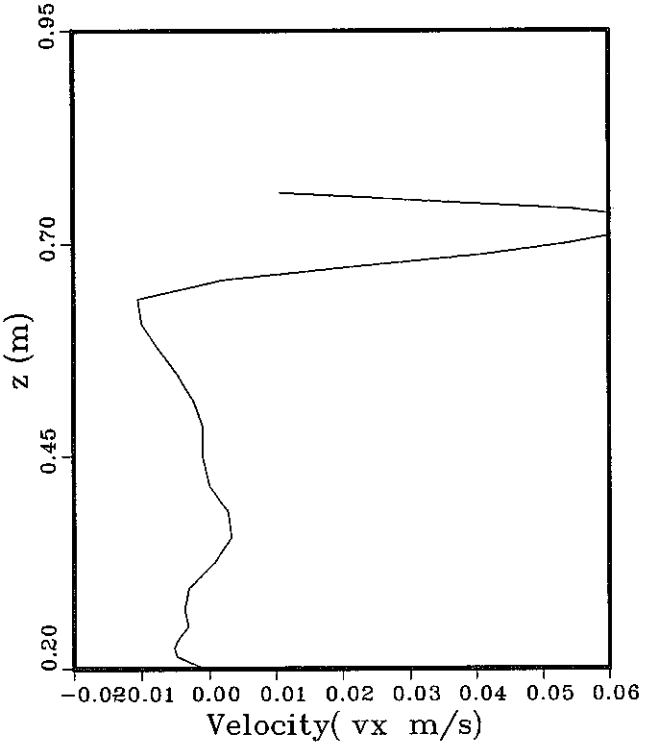

(c) CASE 3

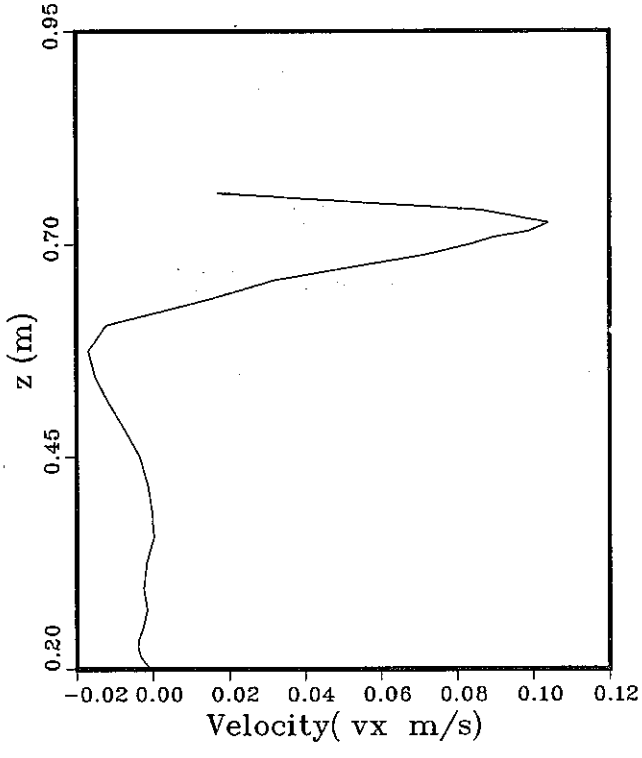

(d) CASE 4

Fig. 38 Velocity distribution on P1 with C_1 = 1.656 of the k & ε two-equation model

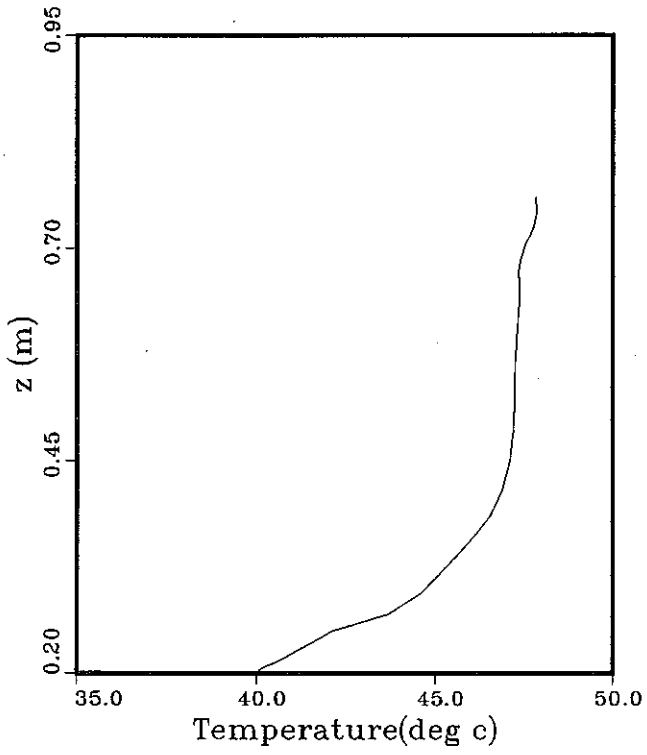

(a) CASE 1

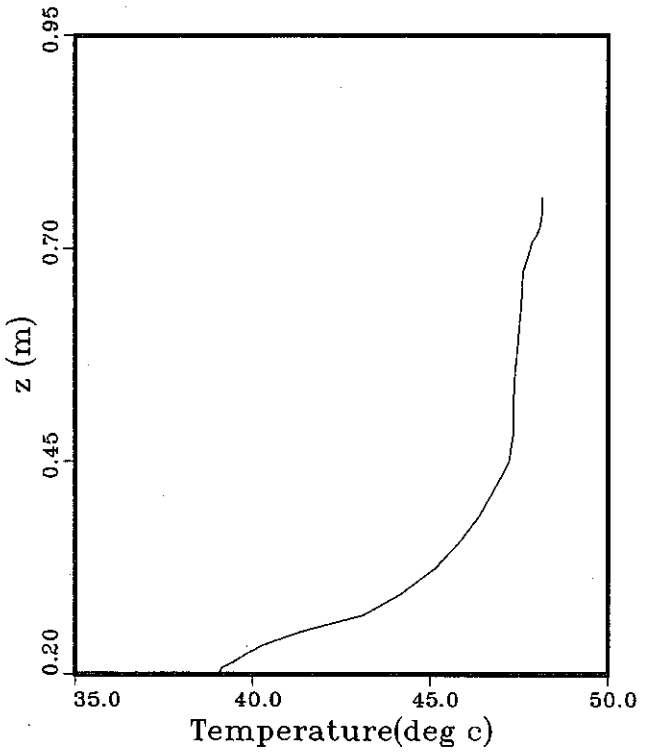

(b) CASE 2

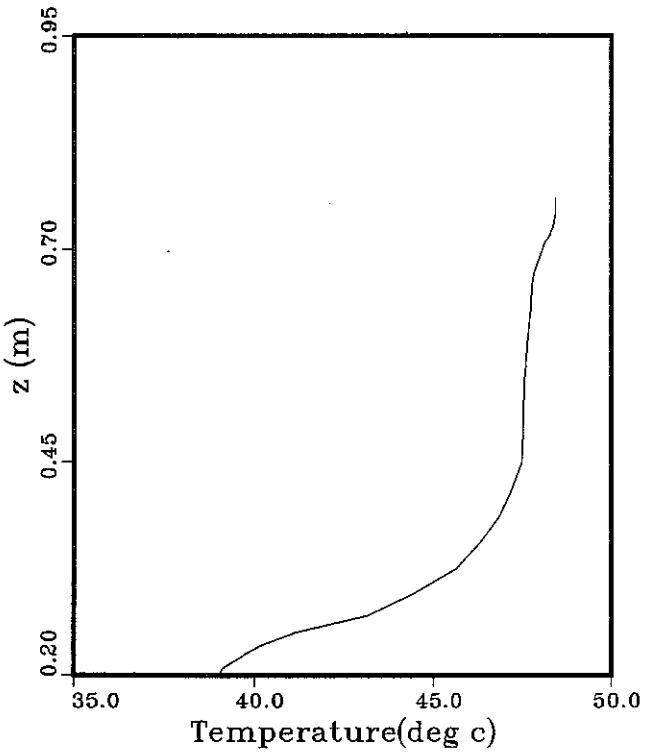

(c) CASE 3

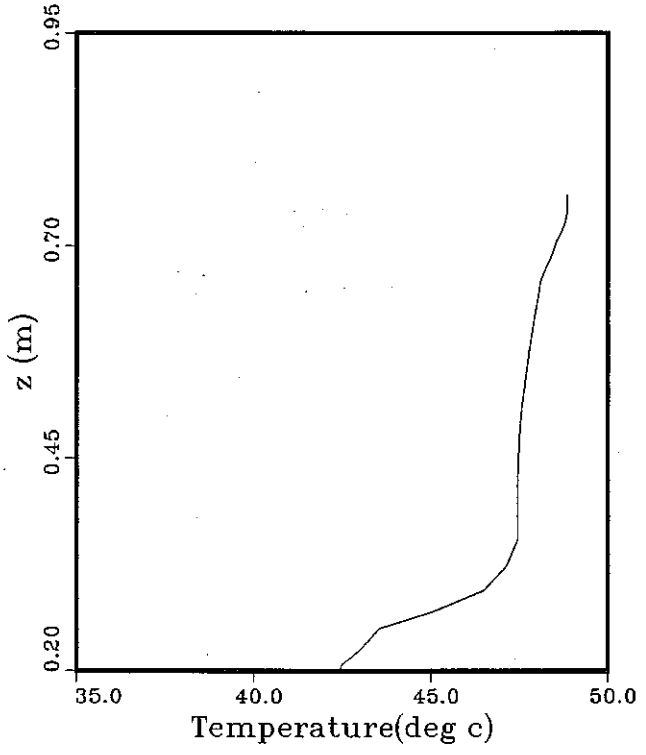

(d) CASE 4

Fig. 39 Temperature distribution on P1 with C_1 = 1.656 of the k & ε two-equation model

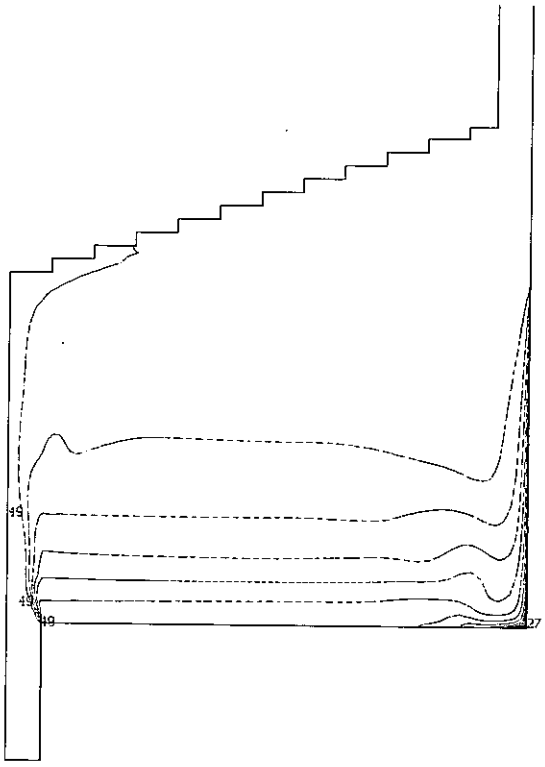

TIME: 9572.1 SEC. J = 1

(a) ISO-TEMP

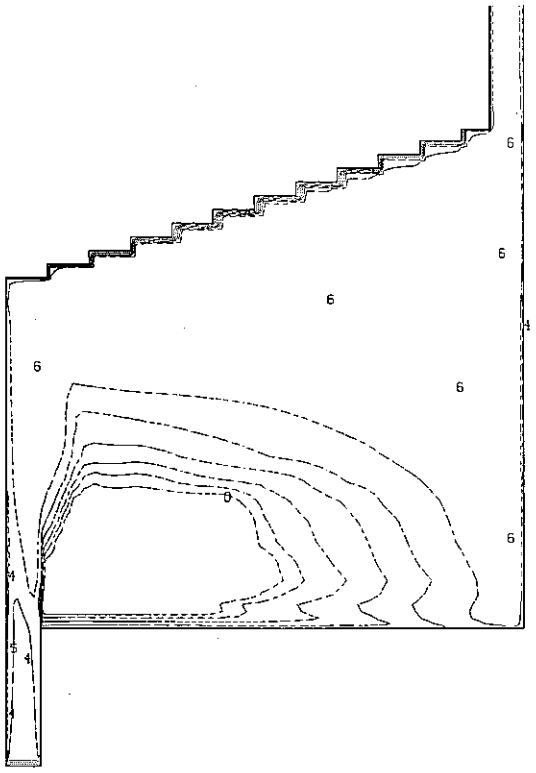

TIME: 9572.1 SEC. J = 1

(b) ISO-μt

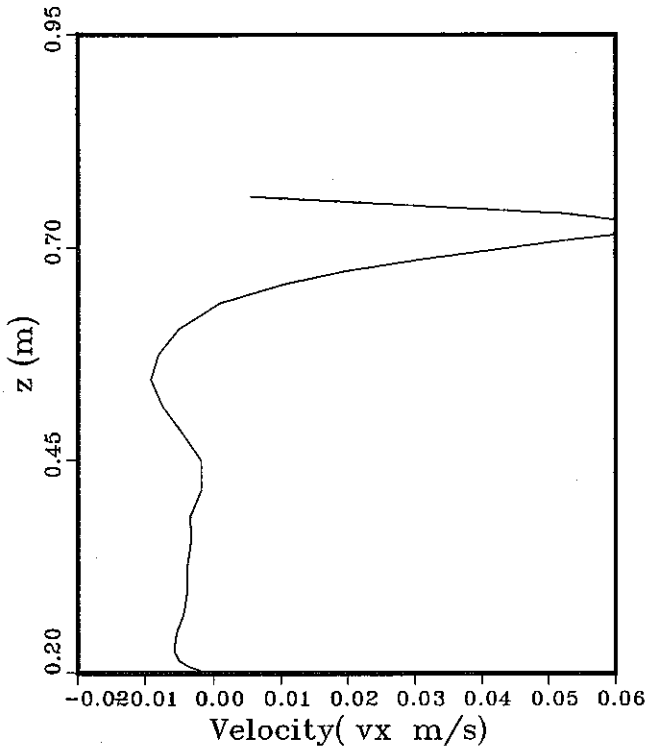

(c) VELOCITY P1

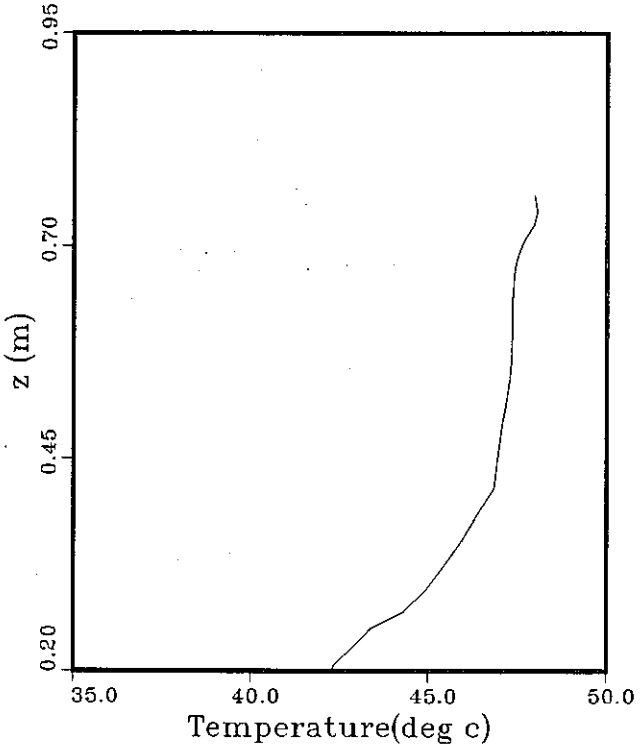

(d) TEMPERATURE P1

Fig. 40 Results of MICE for case 1 with AQUA default constants

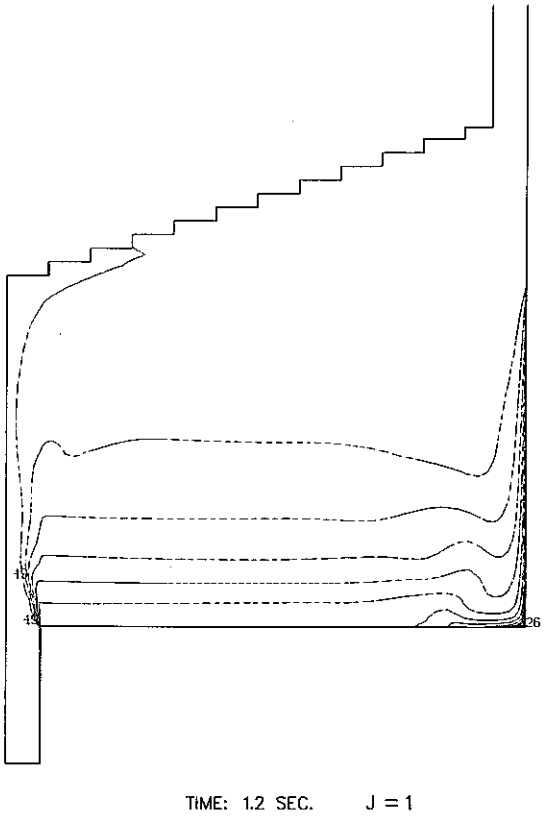

(a) ISO-TEMP

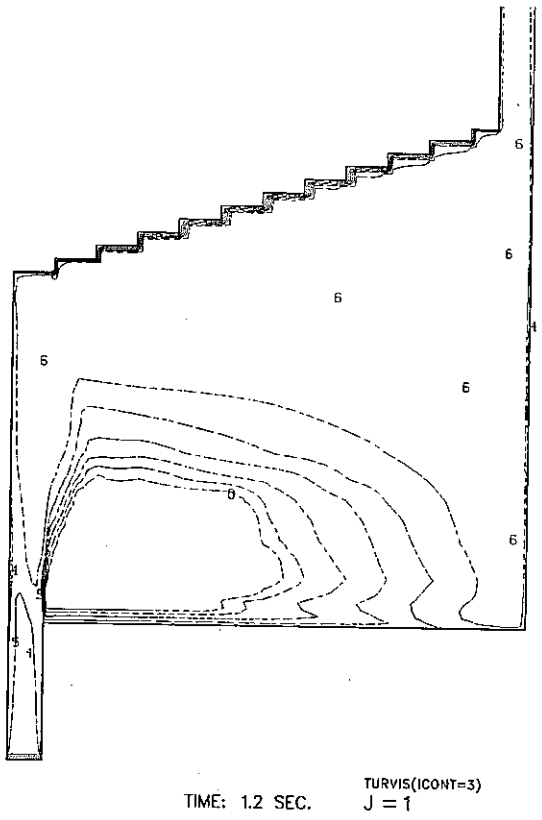

(b) ISO-μt

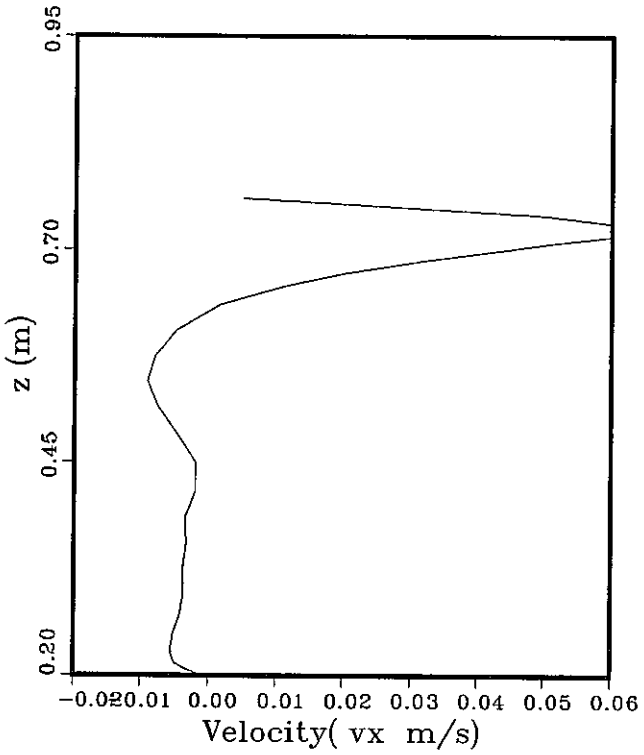

(c) VELOCITY P1

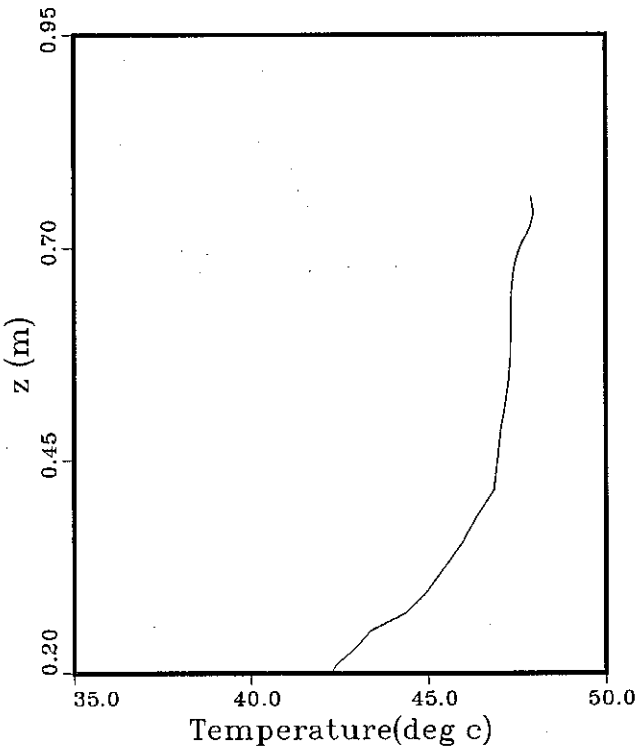

(d) TEMPERATURE P1

Fig. 41 Transient calculation results for case 1 with MICE and AQUA default constants

4.5 Discussion

The flows considered are not completely turbulent and no more laminar since we can find out that in certain limited regions the level of turbulence is significant but not the whole regions of the thermal cavity and also the plenum of the 7th IAHR benchmark problem. Usually these characteristics may be observed on the diagrams of the turbulent viscosity and the turbulent kinetic energy. In some sense it is the effect of buoyancy on the turbulence. The buoyance causes dissipation of turbulent kinetic energy where the stratification has been established. Thus in this region, there is a source of turbulent kinetic energy P, due to stress and a sink G, due to buoyancy. When the stratification is stable, generally the sum of P and G can be neglected and can even be negative. Therefore the molecular viscosity may be regarded as a dominant term in this region. On the other hand in the lower left corner of the thermal cavity, contrary to a dissipation role, the buoyance causes production of turbulent kinetic energy same as the stress. Thus it makes a flow as turbulent in this region.

In connection with the above discussion, Fig. 11(a), (b), and (c) show some variations of the effect of buoyance on turbulence with a modified model constant C_3. Actually it looks difficult to explain the role of buoyance in the lower left corner of the cavity using Fig. 11(c) which has been obtained with the value of $C_3 = 0.0$ suitable only for the near vertical boundary layer. However, Fig. 11(b) which has been obtained with the default value of AQUA, $C_3 = 0.7$, suitable only for the near horizontal boundary layer seems physically good same as Fig. 11(a) having a consistent value of the reference work.

When looking over the recirculation which can be explained by the important absolute value of P, it should be better to see the potential predictive capabilities of the standard k & ε two-equation models with the same set of empirical constants proposed first by Launder and Spalding. Generally its predicative capabilities for confined circulating flows such as the thermal cavity problem are well established, but for unconfined recirculating flows such as the IAHR benchmark problem it is also known that the agreement with experiments is found to be only moderate. Through analyses of the thermal cavity problem and the IAHR benchmark problem, I could confirm the above statements. In the thermal cavity problem, the second relative maximum value of the tur-

bulent viscosity in the top of the vertical boundary layer is closely related to the recirculation. And in the IAHR benchmark problem, we can see a large clockwise recirculating flow from the vector diagrams. As expected, both of the turbulence models in AQUA could not produce agreements without the modification of the empirical constants as shown on Fig. 19 through Fig. 32 because this is a problem of the unconfined recirculating flows. However it could produce agreements with simple adjustments of the empirical constants as shown on Fig. 33 through Fig. 39. Actually these results of C_1 = 1.656 could be selected as the best agreement among the results of the IAHR benchmark problem with modified model constants on the structure of the standard k & ε two-equation turbulence model in AQUA.

By the way it is necessary to have some descriptions about the difference of two turbulence models in AQUA, the k & ε turbulence models with or without the algebraic stress and flux relations. Comparing the results shown on Fig. 19 through Fig. 25 and Fig. 26 through Fig. 30, it may be said that higher levels of turbulence have been obtained on the same cases with the algebraic stress/flux model. However in the IAHR benchmark problem, the control results of experiment make a selection of model constants produce lower levels of the turbulence. Therefore a sensitivity study of the IAHR benchmark problem has focused only on the k & ε two-equation model without the algebraic stress and flux relations. The results of this sensitivity study show the same tendency of the thermal cavity problem and give some information how to modify the relevant model constants.

In this study, numerical techniques relied on the SIMPLEST-ANL method with the first order upwind difference scheme have been used extensively even though there are some problems on the accuracy of calculations and the convergence of turbulent quantities.

When referring to the accuracy with Fig. 10 of the calculated local Nusselt number profiles along the hot wall of the thermal cavity, we can find out that the calculation shows less than a half of the reference solution. In some sense, I think that it is possible to have some suspicion on the applied numerical method since the calculations have been established using the same mesh arrangements of the reference work. However when we see the temperature profiles of Figs. 17 and 40 in the IAHR benchmark problem, we can also think that it is more reasonable to have fine grids near the walls in AQUA to make a sharp

gradient of temperature.

On the other hand, I think that the difficulty to obtain the converged values of turbulent quantities k and ε in calculations is much more serious problem. Actually all cases of the IAHR benchmark problems except the case 4 having the default constants of standard k & ε two-equation model could not reach the convergence of the turbulent quantities and more could not show any signs of the convergence because relative variations of k and ε in time histories showed no changes. Though the MICE with much smaller value of time step size than the Courant limit can resolve the convergence problem, I think that it must be solved to ensure the calculations. This is the most troublesome aspects of this study and I just guess the reason of this difficulty as a consequence of some treatments which are focused on the physical meanings of the calculations. Anyway the calculations with the SIMPLEST-ANL method could be converged well for the velocity components and the energy within the simulation time of 300 CPU minutes or less in Fujitsu system. Of course we can obtain the accurate solutions with the required fine grids and the MICE having a second order difference scheme in AQUA and also we can solve the difficulty of convergence on turbulent quantities. However in this case, a problem arising from the limited small time step sizes must be overcome.

A sample transient calculations of Fig. 41 might be used to verify that the influence of the transient behavior on the temperature and velocity field in the plenum of the IAHR benchmark problem is negligible.

As a whole, the calculation results of the thermal cavity problem may be used to see the characteristics of the AQUA and as a verification example showing the applicability of the k & ε two-equation turbulence model to relatively slow buoyance driven confined recirculating flows. And the results of the IAHR benchmark problem can also be used to confirm the applicability of the k & ε two-equation models to relatively slow flows, particularly for unconfined recirculating flows with the buoyancy because it seems physically very good. Moreover having been obtained the empirical model constants of unconfined recirculating flows through the results of the experiment and the analysis of the IAHR benchmark problem, it may be tested to another unconfined recirculating flows regardless of the turbulence level.

4.6 Conclusions

To evaluate the applicability of the k & ε two-equation models to relatively slow flows, at first time a thermal cavity problem could be used to see the numerical features of AQUA. After obtaining some general information of numerical backgrounds, I could handle the turbulence models in AQUA numerically and theoretically.

Generally the predicative capabilities of the k & ε two-equation models have been well established with the same set of empirical constants for confined recirculating flows such as the thermal cavity problem. But it is also known that its predicative capabilities with the same set of constants are not so well for unconfined recirculating flows such as the 7th IAHR benchmark problem. Even though it is an eventual task of the turbulence models to set up reasonable model forms or to determine the proper values of the constants, this study requires a well developed turbulence model suitable for the IAHR benchmark problem. Therefore it has taken a lot of endeavors to simply adjust the empirical model constants of the ε equation in the IAHR benchmark problems. And I could match the calculations with the control results of the experiment. With respect to the thermal hydraulic phenomena occurring in the transition region, the application of the k & ε turbulence models in AQUA to buoyancy driven recirculating flows gives results which seem physically good regardless of the nature of confined or unconfined.

5. IMPRESSIONS

When I came to Japan on January 15, it was cold but it is very hot. As a mechanical engineer, I was very interested to the research subject of "Numerical analysis of three dimensional heat transfer behavior and experimental analysis using analytical codes". Through a specific study, I could understand many technical matters which are existing in the field of the numerical heat transfer and fluid dynamics. This achievement will encourage me to have more extensive and practical study in this field.

And of course I am very interested to the role of PNC in Japan's nuclear energy program. Now I can understand the concept of the nuclear fuel cycle and I could see many systematic approaches to complete the nuclear fuel cycle. Personally I also like the concept of a cycle because my original job area is entirely contributed to the Rankine cycle of the power plants and I could make an analogy between a practical cycle and a great conceptual cycle. Actually when we want to build an electric power plant, at first time we must make a conceptual cycle design to predict the whole effect on that power plant. I think PNC had already finished this phase of design. After that it is important how to well select the proper components of that cycle. On this phase, I think, PNC had a lot of improved technologies through the experimental FBR JOYO, the demonstrational ATR FUGEN, and etc. Next it is the time of the components design such as the construction of the demonstrational FBR MONJU. Next we are usually interested in the operation of the cycle. Also I think that PNC has already achieved on this stage through the reprocessing of the spent fuels in JOYO. However there are still many problems on the cycle how to improve the efficiency of that cycle. In my opinion it is the time of PNC to move into this stage on the nuclear fuel cycle. Of course the safety of the cycle must be considered as the first priority through the entire stages of a cycle.

While staying in the international house located in Oarai, I have taken a chance to meet many friends from Asian countries and it was a good opportunity to understand their countries. With all kinds of support from everyone, I could have a lot of fun in Japan. I also tried to know Japan not only the nuclear power industry but also the customs and language. Finally, I wish to express my deep appreciation for the kindness of people in Reactor Engineering Section, in Safety Engineer-

ing Division, in Oarai Engineering Center, in Power Reactor and Nuclear Fuel Development Corporation, and in Japan.

REFERENCES

1. Marie Pierre Fraiken, Jean J. Portier, and Christian J. Fraikin, "Application of a k-ε turbulence model to an enclosed buoyancy driven recirculating flow", Chemi. Eng. Commun. Vol.13, pp.289-314, (1982).
2. Wolfgang Kollmann von Karman Institute for fluid dynamics, "Prediction methods for turbulent flows (W. Rodi, Turbulence models for environmental problems)", Hemisphere Publishing Corporation,(1980).
3. H. Tennekes and J.L. Lumley, "A first course in turbulence", The MIT Press, 10th, (1985).
4. Suhas V. Patankar, "Numerical heat transfer and fluid flow", Hemishere Publishing Corporation, (1980).
5. H.M. Domanus, R.C. Schmitt, W.T. Sha, and V.L. Shah, "A new implicit numerical solution scheme in the COMMIX-1A computer program", Argonne National Laboratory, ANL-83-64, (1983).
6. I. Maekawa, T. Muramatsu, M. Matsumoto, H. Ninokata, and M. Bottoni, "Cooperation on the development of AQUA and COMMIX-KfK information exchange and numerical models discussions", Oarai Engineering Center of PNC, PNC SN9410 87-167, (1987).
7. T. Muramatsu and H. Ninokata, "Development of analytical model for evaluating coolant temperature fluctuation phenomena (I)", Oarai Engineering Center of PNC, PNC N9410 90-029, (1990).
8. I. Maekawa, T. Muramatsu, M. Matsumoto, and H. Ninokata, "Single phase multi-dimensional thermal hydraulic analysis code AQUA (Input manual, The description of the numerics, Program description)", Oarai Engineering Center of PNC, PNC N9520 87-011, PNC N9520 87-012, PNC N9520 87-013, (1987).
9. Letter from Y. Ieda dated January 30, 1991, "Benchmark problem description", Oarai Engineering Center of PNC (1991).